

COPY 2

WIND-TUNNEL STUDY
OF WESTILE BALLAST PAVER™

by

B. Bienkiewicz* and R.N. Meroney**



**FLUID MECHANICS AND
WIND ENGINEERING PROGRAM**

COLLEGE OF ENGINEERING

**COLORADO STATE UNIVERSITY
FORT COLLINS, COLORADO**

@ER85-86BB-RNM 13

WIND-TUNNEL STUDY
OF WESTILE BALLAST PAVER™

by

B. Bienkiewicz* and R.N. Meroney**

for

WESTILE, INC.
8311 West Carder Court
Littleton, CO 80125

Fluid Mechanics and Wind Engineering Program
Fluid Dynamics and Diffusion Laboratory
Civil Engineering Department
Colorado State University
Fort Collins, Colorado 80523

CSU Project 2-96460

November 1985

*Assistant Professor
**Professor

CER85-86BB-RNM13

ABSTRACT

This report is concerned with the wind-tunnel study and design considerations of Westile ballast pavers. Wind-tunnel tests employing model pavers were conducted to determine the effects of various parameters on the paver failure wind speed. Considered were different paver configurations, wind exposures and heights of a roof parapet.

The study showed that the paver configuration, the wind exposure and the parapet height affect the failure wind speed (speed at which pavers are dislodged) and the failure mode.

The experimental data was used in design considerations to establish maximum building heights recommended for the Westile pavers.

TABLE OF CONTENTS

| <u>Chapter</u> | | <u>Page</u> |
|----------------|--|-------------|
| | LIST OF TABLES | iv |
| | LIST OF FIGURES | v |
| 1.0 | INTRODUCTION | 1 |
| 2.0 | EXPERIMENTAL CONFIGURATION | 3 |
| | 2.1 Wind Tunnel | 3 |
| | 2.2 Model | 3 |
| | 2.3 Flow Conditions | 6 |
| | 2.4 Test Conditions | 6 |
| | 2.5 Test Procedure | 8 |
| 3.0 | RESULTS AND INTERPRETATION | 10 |
| | 3.1 Failure Wind Speed -- Original Configuration | 10 |
| | 3.2 Failure Wind Speed -- Modified Configuration | 11 |
| | 3.3 Interpretation of the Results | 11 |
| 4.0 | DESIGN CONSIDERATIONS | 13 |
| | 4.1 Methodology | 13 |
| | 4.2 Design Considerations Using Uniform Building Code (UBC [7]) | 14 |
| | 4.3 Design Considerations Using ANSI Standard (ANSI [8]) | 16 |
| | 4.4 Comparison of the Results Obtained Using UBC [7] and ANSI [8] | 17 |
| 5.0 | DISCUSSION | 18 |
| | 5.1 Failure Wind Speed | 18 |
| | 5.2 Failure Mode | 20 |
| | 5.3 Paver Failure and Pressure Distribution | 21 |
| | 5.4 Maximum Building Height | 23 |
| 6.0 | CONCLUSIONS AND RECOMMENDATIONS | 25 |
| | REFERENCES | 27 |
| | TABLES | 28 |
| | FIGURES | 37 |

LIST OF TABLES

| <u>Table</u> | | <u>Page</u> |
|--------------|--|-------------|
| 1 | Combined Height, Exposure and Gust Factor Coefficient Specified by UBC | 29 |
| 2 | Failure Wind Speed at Roof Height | 30 |
| 3 | Maximum Building Height (ft) Estimated Using UBC -- Original Configuration, Exposure C and B | 31 |
| 4 | Maximum Building Height (ft) Estimated Using UBC -- Modified Configuration, Exposure C and B | 32 |
| 5 | Wind Exposure Characteristics Specified by ANSI Standard | 33 |
| 6 | Maximum Building Height (ft) Estimated Using ANSI Standard -- Original Configuration, Exposure A, B and C | 34 |
| 7 | Maximum Building Height (ft) Estimated Using ANSI Standard -- Modified Configuration, Exposure A, B and C | 35 |
| 8 | Failure Wind Speed Ratio (Failure Wind Speed for Modified Configuration/Failure Wind Speed for Original Configuration) | 36 |

LIST OF FIGURES

| <u>Figure</u> | | <u>Page</u> |
|---------------|--|-------------|
| 1 | Fluid Dynamics and Diffusion Laboratory, Colorado State University | 38 |
| 2 | Industrial Aerodynamics Wind Tunnel | 39 |
| 3 | Westile Ballast Paver | 40 |
| 4 | Paver Model -- Details | 41 |
| 5 | Paver Model -- Overall View | 42 |
| 6 | Building Model | 43 |
| 7 | Building Model Placed in Wind Tunnel | 44 |
| 8 | Boundary Layer Generators | 45 |
| 9 | Mean Wind Speed and Turbulence Intensity Profiles -- Exposure C | 46 |
| 10 | Mean Wind Speed and Turbulence Intensity Profiles -- Exposure A | 47 |
| 11 | Tested Wind Direction | 48 |
| 12 | Experimental Configuration Tested | 49 |
| 13 | Original Paver Configuration | 50 |
| 14 | Details of Paver Layout -- Original Configuration | 51 |
| 15 | Failure Wind Speed at Roof Height -- Original Paver Configuration | 52 |
| 16 | Paver Failure -- Original Configuration With 0 in. Parapet | 53 |
| 17 | Paver Failure -- Original Configuration With 6 in. Parapet | 54 |
| 18 | Paver Failure -- Original Configuration With 12 in. Parapet | 55 |
| 19 | Modified Paver Configuraton | 56 |
| 20 | Details of Modified Paver Layout -- Modified Configuration | 57 |
| 21 | Failure Wind Speed at Roof Height -- Modified Paver Configuration | 58 |

| <u>Figure</u> | | <u>Page</u> |
|---------------|--|-------------|
| 22 | Paver Failure -- Modified Configuration With 0 in. Parapet | 59 |
| 23 | Paver Failure -- Modified Configuration With 12 in. Parapet | 60 |
| 24 | Main Parameters for Design Considerations | 61 |
| 25 | Maximum Building Height Estimated Using UBC -- Original Configuration With 0 in. Parapet, Exposure C and B . . . | 62 |
| 26 | Maximum Building Height Estimated Using UBC -- Original Configuration With 6 in. Parapet, Exposure C and B . . . | 63 |
| 27 | Maximum Building Height Estimated Using UBC -- Original Configuration With 12 in. Parapet, Exposure C and B . . | 64 |
| 28 | Maximum Building Height Estimated Using UBC -- Original Configuration With 18 in. Parapet, Exposure C and B . . | 65 |
| 29 | Maximum Building Height Estimated Using UBC -- Modified Configuration With 0 in. Parapet, Exposure C and B | 66 |
| 30 | Maximum Building Height Estimated Using UBC -- Modified Configuration With 6 in. Parapet, Exposure C and B | 67 |
| 31 | Maximum Building Height Estimated Using UBC -- Modified Configuration With 12 in. Parapet, Exposure C and B | 68 |
| 32 | Maximum Building Height Estimated Using UBC -- Modified Configuration With 18 in. Parapet, Exposure C and B | 69 |
| 33 | Maximum Building Height Estimated Using ANSI Standard -- Original Configuration With 0 in. Parapet, Exposure A, B and C | 70 |
| 34 | Maximum Building Height Estimated Using ANSI Standard -- Original Configuration With 6 in. Parapet, Exposure A, B and C | 71 |
| 35 | Maximum Building Height Estimated Using ANSI Standard -- Original Configuration With 12 in. Parapet, Exposure A, B and C | 72 |
| 36 | Maximum Building Height Estimated Using ANSI Standard -- Original Configuration With 18 in. Parapet, Exposure A, B and C | 73 |

| <u>Figure</u> | | <u>Page</u> |
|---------------|---|-------------|
| 37 | Maximum Building Height Estimated Using ANSI Standard -- Modified Configuration With 0 in. Parapet, Exposure A, B and C | 74 |
| 38 | Maximum Building Height Estimated Using ANSI Standard -- Modified Configuration With 6 in. Parapet, Exposure A, B and C | 75 |
| 39 | Maximum Building Height Estimated Using ANSI Standard -- Modified Configuration With 12 in. Parapet, Exposure A, B and C | 76 |
| 40 | Maximum Building Height Estimated Using ANSI Standard -- Modified Configuration With 18 in. Parapet, Exposure A, B and C | 77 |
| 41 | Maximum Building Height Estimated Using UBC and ANSI Standard -- Original Configuration With 12 in. Parapet, Exposure C | 78 |
| 42 | Maximum Building Height Estimated Using UBC and ANSI Standard -- Original Configuration With 12 in. Parapet, Exposure B | 79 |
| 43 | Maximum Building Height Estimated Using UBC and ANSI Standard -- Modified Configuration With 12 in. Parapet, Exposure C | 80 |
| 44 | Maximum Building Height Estimated Using UBC and ANSI Standard -- Modified Configuration With 12 in. Parapet, Exposure B | 81 |
| 45 | Failure Wind Speed at Roof Height, Exposure A: --⊙-- Original Configuration, ⊙ Modified Configuration | 82 |
| 46 | Failure Wind Speed at Roof Height, Exposure C: --△-- Original Configuration, △ Modified Configuration | 83 |
| 47 | Failure Wind Speed at Roof Height for Different Flow Conditions: --□-- Smooth Flow (n = 0.10); △ Open Country (n = 0.14); ⊙ Suburban Terrain (n = 0.30); ⊙ Built-Up Terrain (n = 0.37) | 84 |
| 48 | Mean Wind Speed and Turbulence Intensity Profiles -- Smooth Flow | 85 |
| 49 | Mean Wind Speed and Turbulence Intensity Profiles -- Suburban Terrain | 86 |
| 50 | Static-Pressure Coefficient, Parapet Height of 6 in. (Kind and Wardlaw [5]): a) Bare Roof Deck; b) Distribution Under Paver Array | 87 |

| <u>Figure</u> | | <u>Page</u> |
|---------------|--|-------------|
| 51 | Pressured Distribution Along a Paver (Kind and Wardlaw [4,5]): a) Low Uplift Force; b) High Uplift Force | 88 |
| 52 | Static-Pressure Coefficient on Roof Deck (Kind and Wardlaw [4]): a) 0 in. Parapet; b) 6 in. Parapet; c) 36 in. Parapet | 89 |
| 53 | Exterior (nonlinear) and Interior (linear) Static-Pressure Distribution over Paver (1,4) | 90 |

1.0 INTRODUCTION

The Westile roof paver is an extruded concrete loose-laid roofing product used to provide ballast over single-ply roofing membranes or as tiles for access walkways. The paver protects the underlying roof membrane from ultra-violet light, wear and abrasion. The Westile paver is designed with overlap joints along one edge to inhibit movement by rooftop winds. Wind effects on such systems are very important, since shifting or lofting of the tiles during windstorms could result in membrane damage or damage to surrounding structures. This report describes wind-tunnel experiments designed to determine Westile paver performance during high winds. Test results are used to prepare paver application design tables for different climatic winds, building exposures, and roof parapet heights.

Wind loading and wind-induced failure of roofing systems results from a complex interaction of wind environment, building shape and structure, and roofing system chosen. These systems cannot currently be analyzed reliably by any analytic or theoretical approach; hence, experiments are necessary to define product use envelopes. Almost no reliable field experiments exist concerning the behavior of full-size roofing systems. The cost of a full-scale roof system, as well as the lack of reliability of the atmosphere or large blowers or fans as a testing medium has limited such experience. Fortunately, fluid modeling in wind tunnels provides a powerful and cost-effective technique for the analysis of such wind engineering problems; hence, literature now exists which focuses on the behavior of roofing systems.

The most recent developments from experimental studies of wind effects on roofs and roof coverings have been summarized by Kramer [1]

Detailed mean and dynamic pressure measurements on flat top roofs has been published by Stathopoulos [2,3]. Experimental investigations of the failure mechanisms of loose-laid roof-insulation systems, including ballast pavers and gravel, were presented by Kind and Wardlaw [4,5,9]. Phalen [6] used mean pressure coefficient data to develop a wind design procedure for lightweight concrete ballast in loose-laid roof systems.

This study examined the modeled response of Westile pavers under different wind and roofing environments. Chapter 2 describes experimental configurations and procedures employed during the wind-tunnel study. The experimental results are presented and interpreted in Chapter 3, and the data are used to define design considerations for the paver in Chapter 4. Finally, the specific performance of the Westile paver, its failure mode, and design recommendations are presented in Chapter 5 and 6.

2.0 EXPERIMENTAL CONFIGURATION

2.1 Wind Tunnel

The study was conducted in the Industrial Aerodynamics Wind Tunnel located at the Fluid Dynamics and Diffusion Laboratory, Colorado State University. Location of the wind tunnel in the laboratory is shown in Figure 1. The wind tunnel is depicted in Figure 2. The wind tunnel is of recirculating type and the facility has a test section 6 ft wide and 60 ft long. Model blockage effects can be resolved with a test-section ceiling adjustable from 5 ft to 7 ft. Air flow in the tunnel is generated by a 16-blade axial fan driven by a single-speed induction 75 hp-motor. The air speed is controlled by varying the pitch of the fan blades. The speed range of the flow in the tunnel can be continuously adjusted in the range from 0 to approximately 80 fps. The flow enters the test section through a 4:1 contraction which produces uniform cross-section flow and background turbulence of low levels (turbulence intensity of approximately 0.5 percent). Simulated atmospheric boundary conditions are created by placing flow tripping devices at the entrance to the test section and a uniform fetch of roughness elements on the floor of the test section.

2.2 Model

A series of experiments involving model of the Westile Roof Paver was designed and conducted in the Industrial Aerodynamics Wind Tunnel. The experiments were to provide an information on the failure mode and the failure wind speed of the prototype pavers.

The prototype Westile Roof Paver is shown in Figure 3. A simplified model of the paver was used in the study. Most of the experiments were conducted using a 1:15 geometrical scale paver model shown

in Figures 4 and 5. The model was made of plexiglass. A few additional tests were performed using a 1:7.5 geometrical scale paver model. The larger model-pavers required a higher range of wind-tunnel speeds to produce failure; hence they could not be used to test the influence of taller roof parapets.

The wind-induced motion of the paver model must be dynamically similar to that of the prototype paver. This requires that the mass ratio (mass of air/mass of paver) must be the same for the model and for the prototype. If the paver geometry is properly scaled, this requirement states that the average mass density (mass per unit volume) of the prototype and the model pavers should be the same, or

$$\lambda_{\sigma} = 1 \quad (1)$$

where

$$\lambda_{\sigma} = \frac{\sigma_m}{\sigma_p} ,$$

σ_m = mass density of model paver, and

σ_p = mass density of prototype paver.

Sometimes it is difficult to match the mass density σ_m of the model and σ_p of the prototype. In such situations the paver thickness, t , is scaled at the geometrical scale λ_t which is slightly different from the geometrical scale λ_L assumed for the remaining dimensions of the paver. However, the mass per unit area is kept the same for the model and for the prototype. The similarity requirement (1) is then modified, as follows

$$\lambda_{\sigma} = \lambda_L \lambda_t^{-1} \quad (2)$$

where

$$\lambda_{()} = \frac{() \text{ model}}{() \text{ prototype}} ,$$

t = paver thickness, and

L = dimension in paver plane.

If the paver thickness is scaled at the same geometrical scale as the remaining dimensions of the paver ($\lambda_t = \lambda_L$), then Eq. 2 reduces to Eq. 1.

In the present study Eq. 2 was used to account for the slight deviation of the mass density of the prototype paver (dense extruded concrete) and the model paver (plexiglass). Thickness of the paver model was scaled using Eq. 2 and as a result the mass per unit area was the same for the model and for prototype paver. The geometrical scale λ_t for the paver thickness differed by approximately 30 percent from the scale λ_L assumed for the remaining dimensions of the paver model. In effect the paver model was approximately 30 percent thicker than a model which would result from uniform geometrical scaling.

Model pavers were placed in various configurations on a roof of a model building shown in Figure 6. The building shown was used to simulate flow conditions on a typical flat roof with ballast pavers. Only one building model of a square plan and a fixed height was employed in the study. The model represented a 15 ft tall prototype building with a 22 ft square flat roof. The size of the model was limited by the size of the wind-tunnel test section and by limitations caused by blockage effects. Flow blockage effects caused by the presence of the model were eliminated by adjustments of the wind-tunnel roof. The building model was configured with parapets of various heights. The building model with a typical parapet and model pavers is shown installed in the Industrial Aerodynamics Wind Tunnel in Figure 7.

2.3 Flow Conditions

The wind-tunnel study was conducted for various approach flows. Most of the results reported herein are for two representative approach flow configurations. One of the configurations represented conditions typical for flow over open or rural country (Uniform Building Code [7] -- Exposure C, ANSI A58.1-1982 [8] -- Exposure C). The other situation modeled flow over built-up or urban terrain (Uniform Building Code [7] -- Exposure A, ANSI A58.1-1982 [8] -- Exposure A).

The turbulent boundary layer was generated using flow tripping devices (spires and a barrier) placed at the entrance to the wind-tunnel test section combined with a uniform fetch of roughness elements located upstream of the model. The spires and the fetch of roughness elements are shown in Figure 8. A 40 inch deep boundary layer was generated for both the flow conditions.

The mean velocity and turbulence intensity profiles for the flow over open country -- Exposure C -- are shown in Figure 9. The corresponding profiles for the flow over built-up terrain -- Exposure A -- are depicted in Figure 10. Such velocity profiles are frequently described by an empirical power-law relationship, $U/U_{ref} = (Z/Z_{ref})^n$. The model power law coefficients n for the two cases are approximately 0.14 and 0.37 for the Exposures C and A, respectively.

2.4 Test Conditions

Wind-tunnel model tests must satisfy certain similarity criteria in order to be representative of prototype conditions. The model tested has to be dynamically similar to that of the prototype. Dynamic similarity considerations for the paver model were discussed in Section 2.2. The approach flow also needs to be dynamically scaled. This will be

achieved if the wind approaching the model has the same value for the main nondimensional flow parameters as the prototype flow. In the present study the main flow parameters are represented by

$$\text{Reynolds Number} = \frac{UL}{\nu} \quad , \quad \text{and} \quad (3)$$

$$\text{Froude Number} = \frac{U}{\sqrt{Lg}} \quad , \quad (4)$$

where

U = reference wind speed,

L = reference length,

ν = kinematic viscosity of air, and

g = gravitational acceleration.

The Reynolds number relates the relative ratio of inertial and viscous forces in the flow, whereas the Froude number relates the inertial lift forces of the air to the relative weight of the pavers. It is impossible to match both the Reynolds and Froude numbers in the present case. It is well established that flows over sharp edged objects are independent of Reynolds numbers, for moderately high Reynolds numbers. As a result, the Reynolds number similarity has been relaxed during the present study. The remaining similarity requirement (4) -- Froude Number -- is satisfied when the wind speed scale λ_U and the geometrical scale λ_L are related as follows

$$\lambda_V = \lambda_L^{1/2} \quad . \quad (5)$$

This relation can be used to compute the prototype wind speed corresponding to a given wind-tunnel speed.

Wind tunnel studies conducted in boundary-layer flows require proper scaling of the prototype boundary layer. At the 1:15 geometrical

scale used during the present study, proper scaling of the prototype boundary layer (more than a thousand feet deep) was impossible. Kind [4] and Kind and Wardlaw [5], indicated that the flow pattern over the upwind corner of the building rooftop is mainly dependent on the speed of the approaching wind at rooftop level. Hence, only the lower part of the boundary layer was modeled. It was assumed that characteristics of the flow at rooftop level were most dominant, with other parameters being of lesser importance. Since the boundary layer depth was not properly scaled in the study the wind-tunnel flow was expected to be lacking low frequency (large scale) gusts. This lack of large-scale, low-frequency gusts was not expected to influence the aerodynamics of the relatively small pavers.

Earlier studies by Kind and Wardlaw [4] established that most paver failures occur near the upwind corner of a roof, and that the most critical wind direction for such failures is along the bisector of the upwind corner, as indicated in Figure 11. This critical wind direction was examined in the present study, and the model was tested in the configuration shown in Figure 12.

2.5 Test Procedure

The wind-tunnel experiments were conducted according to the following procedure. The pavers were placed on the roof of a building model in a desired arrangement. Wind speed in the tunnel was gradually increased, and the behavior of the pavers was observed. Wind speed was measured by a pitot-static tube mounted in the tunnel at rooftop level of the model building. The tube was connected to an electronic manometer, and the transducer output voltage was monitored by a minicomputer

on line. When a paver failure (dislocation) was observed, the wind-tunnel speed was maintained constant and the mean wind speed was recorded. The prototype wind speed, corresponding to the measured mean wind speed is called throughout this report the failure wind speed at roof height, and it is denoted V_D . The paver failure wind speed, V_D , was measured for various flow conditions, paver configurations, and parapet heights.

3.0 RESULTS AND INTERPRETATION

3.1 Failure Wind Speed -- Original Configuration

The original configuration of the Westile paver model studied is shown in Figure 13. Details of the locking system are shown in Figure 14. The failure wind speed at rooftop is plotted in Figure 15 as a function of the parapet height. The data is presented for two representative approach flow conditions: open country -- Exposure C, and built-up terrain -- Exposure A. The failure speed is higher for the Exposure C. This means that an increase in turbulence level results in a decrease in the mean wind speed associated with the paver failure.

The effects of the parapet height were similar for both the flow conditions. A relatively low height parapet (up to approximately 6 inches) causes a decrease in the failure velocity, V_D . A parapet of moderate height (larger than approximately 6 inches) results in an increase in the wind speed, V_D , at which paver failure occurs. These parapet height effects are consistent with pressure data reported recently by Stathopoulos [2]. The author observed that peak pressure coefficients near roof corners increase when parapets of low heights are added. As the parapet height is increased, the peak pressure coefficients are reduced. These peaks seem to initiate the paver failure. The failure mode of the pavers is schematically shown in Figures 16 through 18 for three cases: roof without parapet, roof with parapet of low height, and roof with parapet of moderate height. The failure was usually initiated by one or two pavers being dislodged first. Other pavers were subsequently dislodged until the situation indicated in Figures 16 through 18 has been reached.

3.2 Failure Wind Speed -- Modified Configuration

A modified configuration of the paver layout was also investigated. The pavers were arranged in a staggered pattern as shown in Figures 19 and 20. The outer pavers along roof edge AB were connected together by circular adhesive paper tabs attached to the upper and lower surfaces of the two adjacent pavers (see Figures 19 and 20). The adhesive tabs modeled the presence of metal clips between the outer pavers. The failure of pavers was investigated applying the same experimental procedure as for the original paver configuration. The results are presented in Figures 21 through 23. The prototype failure wind speed plotted versus the parapet height is shown in Figure 21. The failure mode of the pavers for two presentative parapet heights (without a parapet and a parapet of moderate height) are shown in Figures 22 and 23. Paver failure occurred at higher wind speed for the modified configuration than for the original configuration. This is indicated in Figures 45 and 46, which compare both the paver configurations (original and modified) for a given wind exposure. The character of the failure of pavers arranged in the modified configuration differed from the failure of pavers arranged in the original configuration. It was more sudden, and more pavers were dislodged simultaneously.

3.3 Interpretation of the Results

The failure wind speed, V_D , is the rooftop mean wind speed at which pavers initially dislodged. The wind approaching the building model is turbulent. The wind-tunnel experiments lead to the conclusion that the failure wind speed, V_D , is also dependent on the turbulence intensity present in the flow. Gustiness of the flow affects the paver failure. Actual failure (dislodging of a paver or several pavers) is initiated by

peak velocity of spatial distribution and temporal duration sufficient to cause the paver or pavers uplift. The mean failure wind speed, V_D , is thus substantially lower than the peak wind velocity, and it should be viewed as a conservative measure of the wind velocity associated with paver failure. The failure wind speed can be used to establish rough design criteria for the use of the pavers on roofs of typical low-rise buildings located within uniform surroundings, which are defined in codes and standards.

4.0 DESIGN CONSIDERATIONS

4.1 Methodology

The failure wind speed, V_D , has been defined as the mean wind speed at the rooftop level at which paver failure occurs. The design wind speed, V_m , is specified by codes and standards as the mean wind speed at a height of 30 ft (approximately 10 m) above the ground, as shown in Figure 24. The peak wind speed, V_H , at height H (see Figure 24) is related to the design wind speed V_m

$$V_H = C_H V_m \quad (6)$$

where

C_H = a correction factor for variation in the mean wind speed and gustiness with height.

It is proposed that the condition for the paver failure be expressed as follows

$$V_H = V_D \quad (7)$$

The condition (7) requires that the peak velocity, V_H , at rooftop height, H , be equal to the failure velocity, V_D (the mean velocity at rooftop height during paver failure). Such an approach involves a reasonable level of safety margin which was discussed in Sec. 3.3. Combination of Eqs. (6) and (7) leads to

$$V_D = C_H V_m \quad (8)$$

where

V_D = failure wind speed (from wind tunnel testing)

V_m = design wind speed defined for a given site (from codes/standards)

C_H = correction factor for variation in the mean wind speed and gustiness with height, evaluated at height H .

Equation (8) can be used to compute the upper bound for the height H of a building for which the use of Westile pavers is appropriate.

Application of the described methodology using the Uniform Building Code specification for standard wind environment is described next.

4.2 Design Considerations Using Uniform Building Code (UBC [7])

The design wind pressure, p , is defined by UBC [7] as follows

$$p = C_e C_q C_s I \quad (9)$$

where

p = design wind pressure,

C_e = combined height, exposure and gust factor coefficient (Tab. No. 23-G, UBC [7]),

C_q = pressure coefficient,

C_s = wind stagnation pressure at 30 ft, and

I = importance factor.

The recommended combined height, exposure and gust factor coefficient C_e is quoted (from UBC [7]) in Table 1. It can be approximated as follows

$$C_e(z) = \begin{cases} a z^2 + bz + c & z \leq 120 \text{ ft} \\ dz + e & z > 120 \text{ ft} \end{cases} \quad (10)$$

where

z = height (ft), and

a, b, c, d, e = constants.

A curve fit of the data in Table 1 and Eq. 10 leads to the following relations

18 In Eq. (10) replace $dz + e$ by $e + dz$

Exposure C

$$C_e(z) = \begin{cases} -1.11 * 10^{-5} z^2 + 6.33 * 10^{-3} z + 1.078 & z \leq 120 \text{ ft} \\ 1.433 + 2.22 * 10^{-3} z & z > 120 \text{ ft} \end{cases} \quad (11)$$

Exposure B

$$C_e(z) = \begin{cases} -1.11 * 10^{-5} z^2 + 6.33 * 10^{-3} z + 0.558 & z \leq 120 \text{ ft} \\ 0.983 + 2.22 * 10^{-3} z & z > 120 \text{ ft} \end{cases} \quad (12)$$

The paver failure condition expressed in Eq. 8 can be stipulated by using information on the effects of height, exposure and gustiness, expressed by coefficient C_e .

$$V_D^2 = C_e(H) V_m^2 \quad (13)$$

where

$$C_e(H) \equiv C_e(z = H) = C_H^2$$

Equation (13) can be solved for C_e

$$C_e(H) = \left(\frac{V_D}{V_m} \right)^2 \quad (14)$$

The maximum permissible building height, H , can be then computed using Eqs. 14, and 10.

15

17

In Eq. (15) replace top terms

$$\text{line} \quad H = \frac{-b \pm \sqrt{b^2 - 4a[c - (\frac{V_D}{V_m})^2]}}{2a} \quad H \leq 120$$

by

$$H = \frac{-b \pm \sqrt{b^2 - 4a[c - (\frac{V_D}{V_m})^2]}}{2a} \quad H \leq 120$$

of the design wind speed, V_m , and failure wind speed, V_D , for different parapet heights. The failure speed, V_D , read from Figures 15 and 21 for

the original and modified paver configurations, respectively, are provided as Table 2. The results of computations are summarized in Tables 3 and 4, and in Figures 25 through 32.

4.3 Design Considerations Using ANSI Standard (ANSI [8])

The paver failure condition Eq. 8 can also be written in terms of the wind/load parameters specified by ANSI [8].

$$V_D^2 = K_z(z = H) G_z(z = H) V_m^2 \quad (16)$$

where

K_z = pressure exposure coefficient,

G_z = gust response factor,

V_D = failure wind speed, and

V_m = design wind speed at 30 ft.

The pressure coefficient factor K_z and the gust response factor G_z are defined in ANSI [8]

$$K_z = \begin{cases} 2.58 \left(\frac{z}{z_g}\right)^{2/\alpha} & \text{for } z \geq 15 \text{ ft} \\ 2.58 \left(\frac{15}{z_g}\right)^{2/\alpha} & \text{for } z < 15 \text{ ft} \end{cases} \quad (17)$$

where

z = height (ft),

z_g = gradient height (ft),

α = power law coefficient,

and

$$G_z = 0.65 + 0.35 T_z \quad (18)$$

where

$$T_z = \frac{2.35 (D_o)^{1/2}}{(z/30)^{1/\alpha}}, \quad \text{and} \quad (19)$$

D_o = surface drag coefficient.

The gradient height, z_g , the power law coefficient, α , and the surface drag coefficient, D_o , are specified by ANSI [8], and are summarized in Table 5. Substitution of Eqs. 17 through 19 into Eq. 16 leads to the following expression for the maximum building height

$$H = 30 \left\{ \frac{-13.5(D_o)^{1/2} + \sqrt{174 D_o + 2.4 \left(\frac{z_g}{30}\right)^{2/\alpha} \left(\frac{V_D}{V_m}\right)^2}}{2} \right\}^\alpha \quad (20)$$

The numerical values of maximum permissible building height, ft, were computed for two paver configurations and different values of the design wind speed V_m , five parapet heights, and three wind exposures A, B and C (Tables 6 and 7). The failure wind speed, V_m , is specified in Table 2, discussed in Section 4.2. The results are plotted in Figures 33 through 36 for the original paver configuration, and in Figures 37 through 40 for the modified paver configuration.

4.4 Comparison of the Results Obtained Using UBC [7] and ANSI [8]

The maximum building height for a 12 in. parapet computed using UBC (Section 4.2) and ANSI (Section 4.3) is compared for the wind exposures C and B in Figures 41 and 42 for the original configuration and in Figures 43 and 44 for the modified configuration. It can be seen that the maximum building heights, computed using the two approaches, are similar for the wind exposure C, Figures 41 and 43. The use of the UBC code leads to more conservative results for the wind Exposure B, Figures 42 and 44.

5.0 DISCUSSION

5.1 Failure Wind Speed

The paver failure wind speed is summarized in Table 2 for three wind exposures, two paver configurations and five parapet heights. It can be seen that the failure wind speed depends on the paver configuration. It is higher for the modified configuration (staggered pavers with locks, Figures 19 and 20) than for the original configuration (unstaggered pavers without locks, Figures 13 and 14) by the percentage indicated in Table 8. The difference between the failure wind speed for the two configurations decreases as the parapet height increases, see Table 8 and Figures 45 and 46. The failure wind speed reaches approximately the same magnitude for the two configurations when the parapet height is equal to 18 inches.

The failure wind speed depends also on wind exposure. It is higher for Exposure C (open country) than for Exposure A (built-up terrain), as shown in Figures 15 and 21. To investigate the sensitivity of the failure wind speed to the changes in the approach flow additional measurements were taken for the modified configuration. The results are presented in Figure 47. Four wind exposures, ranging from approximately smooth flow (power law exponent $n = 0.10$) to Exposure A (built-up terrain, power law exposure $n = 0.37$) were considered. The approach flow conditions are shown in Figure 9 ($n = 0.14$ -- open country), Figure 10 ($n = 0.37$ -- built-up terrain), Figure 48 ($n = 0.10$ -- smooth flow), and in Figure 49 ($n = 0.30$ -- suburban terrain). The turbulence intensity, I_u , at rooftop height was

$I_u = 4.1$ percent for smooth flow -- $n = 0.10$,

$I_u = 9.1$ percent for open country -- $n = 0.14$,

$I_u = 13.3$ percent for suburban terrain -- $n = 0.30$, and

$I_u = 17.5$ percent for built-up terrain -- $n = 0.37$.

The results in Figure 47 indicate that the failure wind speed is dependent on the gustiness of the approach flow and wind variations over the rooftop. This dependence is proportional to the level of turbulence at the rooftop height and it is also augmented by separation over the parapet. An experimental study of failure of several roofing systems, reported by Kind and Wardlaw [4,5], showed that an array of 2 ft x 2 ft (15 psf) paving slabs in upwind corner (wind direction 45°, 6 in. parapet height) failed at 60 mph rooftop wind speed (turbulence intensity at rooftop $I_u \cong 11$ percent). The comparable failure wind speed obtained in the present study (Westile ballast paver of approximately 12 psf) (Exposure C, open country -- $n = 0.14$, $I_u = 9.1$ percent, original configuration, parapet height 6 in., see Figure 15) was 70 mph. The two wind speeds are in the same range. The difference between them is not unexpected since pavers had different geometry and weight and were tested in different experimental configurations.

Phalen [10] reported full-scale studies of tapered interlocking ballast blocks which weighted 11.2 psf. The pavers were also interlocked with a tapered edgestrip fastened to the roof. The blocks, tested with and without a 12 in. parapet, did not fail for the wind speeds below 120 mph. Westile pavers tested in the present study failed for similar flow conditions (modified configuration) at a wind speed of approximately 120 mph (Figure 47, smooth flow, 12 in. parapet). The failure wind speed for the Westile paver is expected to be higher than

120 mph if the pavers were attached to the parapet or the roof, as was done in the study reported by Phalen [10].

5.2 Failure Mode

The failure mode of the pavers is shown in Figures 16 through 18 for the original configuration (Figure 13) and in Figures 22 and 23 for the modified configuration (Figure 20). The failure modes for three realizations of each experiment are sketched. It can be seen that the failure mode for a given experimental configuration exhibits elements of randomness superimposed on features that do not change from realization to realization.

Failure mode for the original configuration involves smaller number of dislodged pavers. The parapet height also affects the failure mode. The presence of a parapet of low height (6 inches) results in a failure of a smaller number of pavers (Figure 17) than for the case without a parapet (Figure 16) or with a parapet of moderate height (Figure 18). It was observed in Section 3.1 that introduction of a parapet of a low height is associated with reduction in the failure wind speed, Figures 15 and 21. It follows that the paver failure at lower wind speed involves a smaller number of pavers than the failure at higher wind speeds. Paver failure at higher wind speeds is also more sudden than the failure at lower wind speeds.

The paver failure was usually initiated by first dislodging paver (1,4). Adjacent pavers were dislodged next. Similar failure sequences were observed by Kind and Wardlaw [4,5].

Wind-tunnel experiments performed with pavers without interlock indicated that the first pavers to be dislodged were (1,4) or (4,1). The paver edge adjacent to the parapet tended to remain on the rooftop,

while the opposite edge lifted upwards, so that the paver tilted towards the parapet and was then blown a small distance downwind. Next, at about the same wind speed, pavers (1,5) or (5,1) and (sometimes) also pavers (1,3) and or (3,1) were dislodged. Based on this observation a configuration for Westile pavers with interlocks, shown in Figure 14, was proposed and tested. This configuration was then modified to obtain the paver arrangement shown in Figure 20.

5.3 Paver Failure and Pressure Distribution

Uplift of paver systems occurs because a substantial pressure difference develops underneath and above the system. At failure, the pressure difference is sufficiently large to lift the pavers into the wind flow and the flow displaces them further downstream.

Recent studies by Kind and Wardlaw [5] which follow their earlier study, Kind and Wardlaw [4], included pressure measurements on a roof deck with and without pavers. The pressure patterns underneath the paver were roughly similar to the patterns on the exterior surface of the pavers. It was concluded that there is sufficient permeability even for closely spaced pavers, such that the exterior pressure perturbations are transmitted almost instantly to the underside of the system. However, the pressure distributions on the two surfaces of a paver are not identical and in some portions of the roof an uplifting pressure difference will prevail.

For sufficiently high wind speed this pressure difference is sufficiently large to cause dislodging of a paver. Kind and Wardlaw [5] concluded that 60 percent of the effective uplift force acting on a paver is due to the time-average component, and the remaining 40 percent of the uplift force is due to the fluctuating component.

The Kind and Wardlaw data also shows the maximum suction levels and pressure gradients are higher on the exterior surface. The data from Ref. 5 is shown in Figure 50. The static-pressure on the exterior surface of the paver system can be assumed similar to the pressure distribution on a bare roof. Kind and Wardlaw [5] concluded that for a given paver the static pressure underneath the paver should vary approximately linearly between the values at the edges of the paver. Thus, the more the external pressure departs from a linear distribution, the greater the pressure differences across the element, and the higher the uplift force, see Figure 51.

The present study confirm observations made by Kind and Wardlaw [4,5]. The failure wind speed was dependent on wind exposure and associated turbulence intensity. The paver failure occurred at lower wind speeds for appropriate flows of higher turbulence level. It is postulated that higher level turbulence caused the instantaneous static pressure distributions over the pavers were of the form shown in Figure 51b. The resulting uplift force would be higher at lower wind speed, and this force causes an earlier paver failure. It is apparently inappropriate to analyze paver failure using only time-averaged pressure data.

The effects of the parapet height on the failure wind speed, discussed earlier in Section 5.1, can be explained by using the reasoning developed above. The paver failure is strongly dependent on the linearity of the gradient of pressure distribution along the external surface of a paver. Pressure distribution on the external surface of a paver system can be approximated by pressure distribution on a roof without pavers. Kind and Wardlaw [4] published the results of pressure

measurement on a roof without a parapet and with parapets 6 in. and 36 in. high. The data from Ref. 4 is summarized in Figure 52. The failure of the system in Figure 52 was initiated by dislodging paver (1,4). Based on the data in Figure 52, the mean and RMS pressure gradients for the paver (1,4) were estimated along direction A-B in Figure 52 perpendicular to the roof edge, and they are shown in Figure 53. The direction perpendicular to the roof edge was chosen because the experimental study showed that the paver first rotated about the roof edge. Note in Figure 53 that the mean and RMS pressure distribution over the paver is the most nonlinear for the 6 in. parapet height. It follows from the previous discussion that the lowest failure wind speed will correspond to the 6 in. parapet height. The results shown in Figures 15 and 21 confirm this prediction.

5.4 Maximum Building Height

The experimental failure wind speed data was used to compute the maximum building height, as described in Section 4.1. Two approaches (one employing the UBC Code and the other employing the ANSI Standard) were applied, Sections 4.2 and 4.3. The results are compared in Section 4.4. The experimental failure wind speed data is discussed in Sections 3.3 and 5.1. In Section 3.1 the manner in which the failure speed was established was addressed, and it was concluded that the method used to incorporate failure wind speed in the proposed design procedure is conservative.

The failure wind speed was used to compute maximum building heights, which are considered to be conservative. The maximum building heights are presented in Tables 3 and 4, and in Tables 6 and 7 and they are plotted in Figures 25 through 44. The upper limit for the maximum

height was arbitrarily selected to be 300 ft. Taller buildings would be surrounded by other tall buildings and they would create flow conditions not tested in the present study. The plotted maximum building heights should be treated as rough design guidelines, appropriate for typical low-rise buildings placed in uniform environments which would create typical wind exposures, specified in the UBC Code and/or the ANSI standard.

6.0 CONCLUSIONS AND RECOMMENDATIONS

The results of the study indicate that wind effects on and failure of ballast paver are of complicated nature; hence further investigations are needed. However, based on the presented study several observations and conclusions can be formulated.

- A. The failure wind speed (the mean rooftop wind speed corresponding to paver failure) is affected by wind exposure and parapet height.
- B. As the level of turbulence in the approach wind increases, the failure wind speed decreases.
- C. Low height parapets (up to approximately 6 in.) cause reduction in the failure wind speed (when compared with the failure speed for the roof 0 in. parapet).
- D. Moderate height parapets (higher than 6 in.) result in an increase in the failure wind speed.
- E. Two paver configurations were tested. The failure wind speed was higher for the modified configuration (staggered pavers with locks) than for the original configuration (unstaggered pavers without locks).
- F. The effects of wind exposure on the failure wind speed were more pronounced at lower values of the parapet height. They were also more significant for the modified configuration.
- G. The effects of parapet height on the failure wind speed were similar for the two paver configurations.
- H. The procedure used to determine the failure wind speed ensured conservative values for the failure wind speed.

- I. Design considerations resulted in estimates of conservative values for the maximum heights of buildings employing Westile pavers.
- J. The maximum building heights specified should be treated as guidelines for application of Westile pavers for low-rise buildings located in aerodynamically uniform surrounding.
- K. The results of the present study are in agreement with the results of studies conducted by other researchers.

REFERENCES

- [1] Kramer, C., "Wind Effects on Roofs and Roof Coverings", Proc. Fifth U.S. National Conference on Wind Engineering, November 6-8, 1985, Texas Tech. University, Lubbock, Texas.
- [2] Stathopoulos, T., and Baskaran, A., "The Effects of Parapets on Wind-Induced Roof Pressure Coefficients", Proc. Fifth U.S. National Conference on Wind Engineering, November 6-8, 1985, Texas Tech. University, Lubbock, Texas.
- [3] Stathopoulos, T., "Wind Pressures on Low Buildings with Parapets", JI. of the Structural Division, Proc. ASCE, Vol. 108, No. St12, December, 1982.
- [4] Kind, R. J., and Wardlaw, R. L., "Failure Mechanism of Loose-Laid Roof Insulation Systems", JI. of Wind Engineering and Industrial Aerodynamics, Vol. 9, 1982, pp. 325-341.
- [5] Kind, R. J., and Wardlaw, R. L., "Model Studies of the Wind Resistance of Two Loose-Laid Roof-Insulation Systems", Laboratory Technical Report, LTR-LA-234, National Aeronautical Establishment, National Research Council of Canada, Ottawa, Canada, May 1979.
- [6] Phalen, T., Jr., "Wind Design Considerations for Lightweight Concrete Ballast in Loose Laid Roof Systems—A Simplified Approach", Technical Report Number 1, Roofblock Limited, 1983.
- [7] Uniform Building Code, International Conference of Building Officials, Whittier, California, 1982.
- [8] Minimum Design Loads for Buildings and Other Structures, ANSI A58.1-1982, American National Standards Institute, Inc., New York, NY, 1982.
- [9] Kind, R. J., "Further Wind Tunnel Tests on Building Models to Measure Wind Speeds at Which Gravel is Blown Off Rooftops", Laboratory Technical Report, LTR-LA-189, National Aeronautical Establishment, National Research Council of Canada, Ottawa, Canada, August 1977.
- [10] Phalen, T., Jr., "Full Scale Wind Tests on Conventional Stone and Lightweight Concrete Tapered Ballast Blocks for Looselaid Roof Systems", Technical Report Number 2, Roofblock Limited, 1983.

TABLES

Table 1. Combined Height, Exposure and Gust Factor Coefficient Specified by UBC

| Height Above Average Level of Adjoining Ground (ft) | Exposure C | Exposure B |
|---|------------|------------|
| 0-20 | 1.2 | 0.7 |
| 20-40 | 1.3 | 0.8 |
| 40-60 | 1.5 | 1.0 |
| 60-100 | 1.6 | 1.1 |
| 100-150 | 1.8 | 1.3 |
| 150-200 | 1.9 | 1.4 |
| 200-300 | 2.1 | 1.6 |
| 300-400 | 2.2 | 1.8 |

Table 2. Failure Wind Speed at Roof Height

ORIGINAL CONFIGURATION

| Wind | Parapet Height (in.) | | | | |
|----------|----------------------|------|------|------|-------|
| Exposure | 0 | 2 | 6 | 12 | 18 |
| A* | 70 | 65.7 | 66 | 82.1 | 108.4 |
| B** | 72 | 67.9 | 67.7 | 87.9 | 122.2 |
| C* | 74 | 70 | 69.3 | 93.6 | 136 |

MODIFIED CONFIGURATION

| Wind | Parapet Height (in.) | | | | |
|----------|----------------------|-------|-------|-------|-------|
| Exposure | 0 | 2 | 6 | 12 | 18 |
| A* | 98.9 | 88.2 | 82.4 | 87.2 | 101.2 |
| B** | 107.4 | 96.3 | 93.1 | 100.8 | 117.6 |
| C* | 115.8 | 104.3 | 103.7 | 114.4 | 133.9 |

* Measured in Wind Tunnel

** Interpolated between values for Exposures A and C

Table 3. Maximum Building Height (ft) Estimated Using UBC --
Original Configuration, Exposure C and B

| Exposure | C | | | | | B | | | | |
|--|----------------------|----|----|-----|------|----------------------|----|----|-----|------|
| | Parapet Height (in.) | | | | | Parapet Height (in.) | | | | |
| Basic Wind Speed U _m (mph) | 0 | 2 | 6 | 12 | 18 | 0 | 2 | 6 | 12 | 18 |
| 60 | 82 | 49 | 44 | 451 | 1669 | 64 | 34 | 33 | 653 | 1872 |
| 70 | 0 | 0 | 0 | 160 | 1055 | 0 | 0 | 0 | 94 | 1258 |
| 80 | 0 | 0 | 0 | 50 | 656 | 0 | 0 | 0 | 21 | 859 |
| 90 | 0 | 0 | 0 | 0 | 383 | 0 | 0 | 0 | 0 | 586 |
| 100 | 0 | 0 | 0 | 0 | 177 | 0 | 0 | 0 | 0 | 76 |
| 110 | 0 | 0 | 0 | 0 | 83 | 0 | 0 | 0 | 0 | 26 |
| 120 | 0 | 0 | 0 | 0 | 35 | 0 | 0 | 0 | 0 | 0 |

Table 4. Maximum Building Height (ft) Estimated Using UBC --
Modified Configuration, Exposure C and B

| Exposure | C | | | | | B | | | | |
|--|----------------------|-----|-----|-----|------|----------------------|-----|-----|------|------|
| | Parapet Height (in.) | | | | | Parapet Height (in.) | | | | |
| Basic Wind Speed U _m (mph) | 0 | 2 | 6 | 12 | 18 | 0 | 2 | 6 | 12 | 18 |
| 60 | 1032 | 716 | 700 | 992 | 1598 | 1235 | 918 | 903 | 1195 | 1801 |
| 70 | 587 | 355 | 343 | 558 | 1003 | 790 | 557 | 546 | 760 | 1205 |
| 80 | 298 | 126 | 121 | 276 | 616 | 501 | 66 | 48 | 97 | 819 |
| 90 | 114 | 45 | 43 | 104 | 352 | 61 | 11 | 0 | 29 | 554 |
| 100 | 45 | 0 | 0 | 39 | 155 | 12 | 0 | 0 | 0 | 53 |
| 110 | 0 | 0 | 0 | 0 | 73 | 0 | 0 | 0 | 0 | 10 |
| 120 | 0 | 0 | 0 | 0 | 28 | 0 | 0 | 0 | 0 | 0 |

Table 5. Wind Exposure Characteristics Specified by ANSI Standard

| Exposure | Power Law Exponent α | Gradient Height z_g (ft) | Surface Drag Coefficient D_o |
|----------|-----------------------------|----------------------------|--------------------------------|
| A | 3 | 1500 | 0.025 |
| B | 4.5 | 1200 | 0.010 |
| C | 7 | 900 | 0.005 |
| D | 10 | 700 | 0.003 |

Table 6. Maximum Building Height (ft) Estimated Using ANSI Standard --
Original Configuration, Exposure A, B and C

| Exposure | C | | | | | B | | | | | A | | | | |
|--|----------------------|----|----|-----|-------|----------------------|-----|-----|-----|------|----------------------|-----|-----|------|------|
| | Parapet Height (in.) | | | | | Parapet Height (in.) | | | | | Parapet Height (in.) | | | | |
| Basic Wind Speed U _m (mph) | 0 | 2 | 6 | 12 | 18 | 0 | 2 | 6 | 12 | 18 | 0 | 2 | 6 | 12 | 18 |
| 60 | 82 | 50 | 45 | 651 | 14809 | 216 | 153 | 150 | 677 | 4092 | 489 | 389 | 385 | 1044 | 3446 |
| 70 | 20 | 12 | 11 | 169 | 4172 | 86 | 60 | 59 | 281 | 1786 | 267 | 210 | 208 | 583 | 1987 |
| 80 | 0 | 0 | 0 | 51 | 1359 | 38 | 26 | 26 | 128 | 856 | 155 | 121 | 120 | 347 | 1220 |
| 90 | 0 | 0 | 0 | 17 | 495 | 18 | 12 | 12 | 63 | 441 | 95 | 74 | 73 | 216 | 785 |
| 100 | 0 | 0 | 0 | 6 | 197 | 0 | 0 | 0 | 33 | 240 | 60 | 46 | 46 | 140 | 525 |
| 110 | 0 | 0 | 0 | 3 | 84 | 0 | 0 | 0 | 18 | 137 | 39 | 30 | 30 | 94 | 362 |
| 120 | 0 | 0 | 0 | 1 | 38 | 0 | 0 | 0 | 10 | 81 | 27 | 20 | 20 | 65 | 256 |

Table 7. Maximum Building Height (ft) Estimated Using ANSI Standard --
Modified Configuration, Exposure A, B and C

| Exposure | C | | | | | B | | | | | A | | | | |
|--|----------------------|------|------|------|--------|----------------------|------|-----|------|------|----------------------|------|------|------|------|
| | Parapet Height (in.) | | | | | Parapet Height (in.) | | | | | Parapet Height (in.) | | | | |
| Basic Wind Speed U _m (mph) | 0 | 2 | 6 | 12 | 18 | 0 | 2 | 6 | 12 | 18 | 0 | 2 | 6 | 12 | 18 |
| 60 | 3947 | 1641 | 1563 | 3567 | 113047 | 2046 | 1126 | 934 | 1448 | 3335 | 2175 | 1463 | 1292 | 1729 | 3008 |
| 70 | 1077 | 438 | 416 | 971 | 3665 | 877 | 475 | 391 | 615 | 1448 | 1240 | 825 | 726 | 979 | 1729 |
| 80 | 340 | 135 | 128 | 306 | 1190 | 413 | 220 | 180 | 287 | 690 | 752 | 495 | 434 | 591 | 1058 |
| 90 | 120 | 47 | 44 | 108 | 432 | 209 | 110 | 89 | 144 | 354 | 479 | 312 | 273 | 374 | 679 |
| 100 | 46 | 18 | 17 | 41 | 171 | 112 | 58 | 47 | 76 | 192 | 317 | 204 | 178 | 246 | 452 |
| 110 | 19 | 0 | 0 | 17 | 73 | 63 | 32 | 26 | 43 | 109 | 216 | 138 | 120 | 167 | 311 |
| 120 | 0 | 0 | 0 | 0 | 33 | 37 | 18 | 15 | 25 | 64 | 151 | 96 | 83 | 116 | 219 |

Table 8. Failure Wind Speed Ratio (Failure Wind Speed for Modified Configuration/Failure Wind Speed for Original Configuration)

| Wind Exposure | Parapet Height (in.) | | | | |
|---------------|----------------------|------|------|------|------|
| | 0 | 2 | 6 | 12 | 18 |
| A | 1.42 | 1.34 | 1.25 | 1.06 | 0.93 |
| B | 1.49 | 1.42 | 1.38 | 1.15 | 0.96 |
| C | 1.56 | 1.49 | 1.50 | 1.22 | 0.98 |

FIGURES

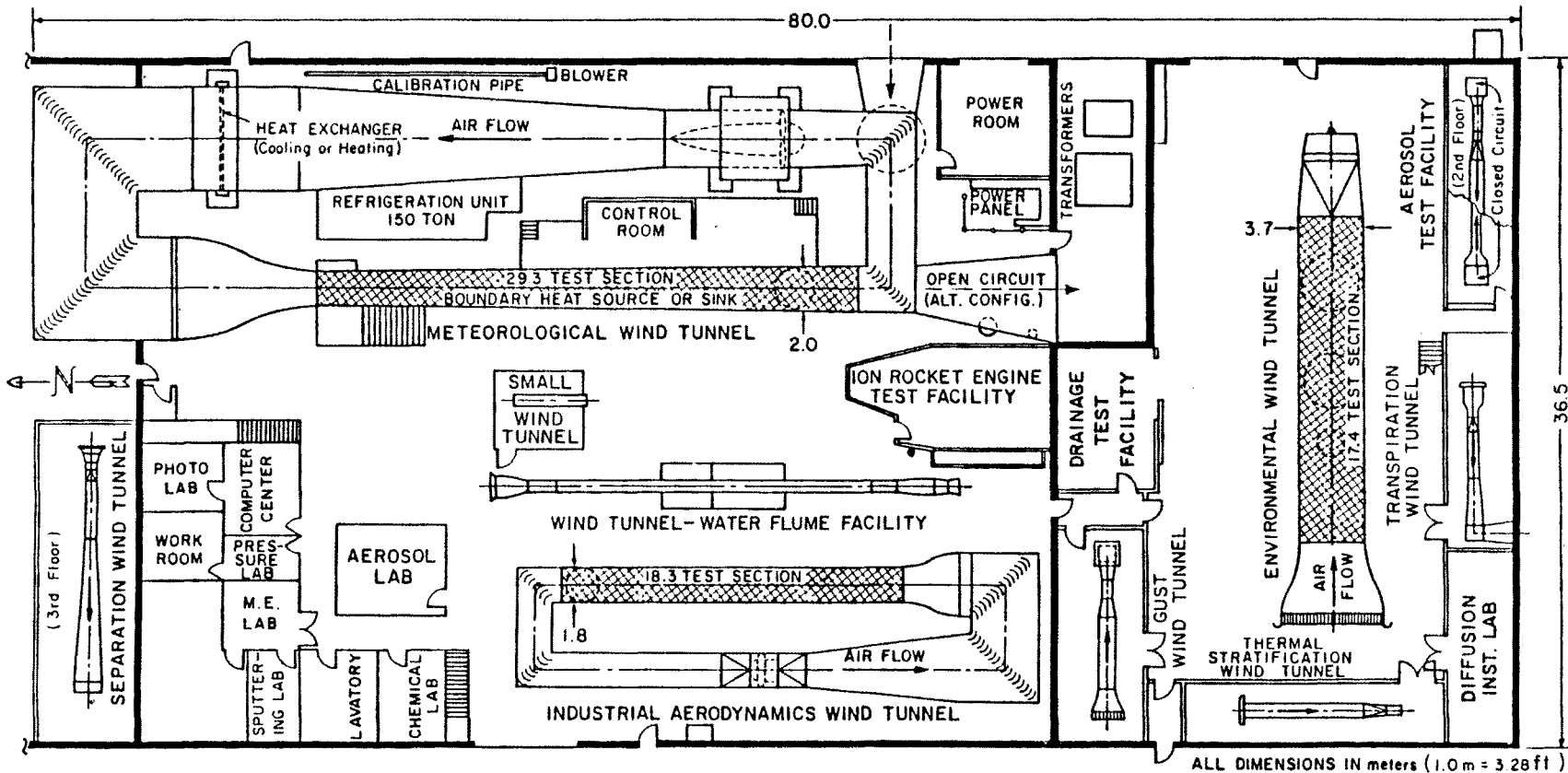
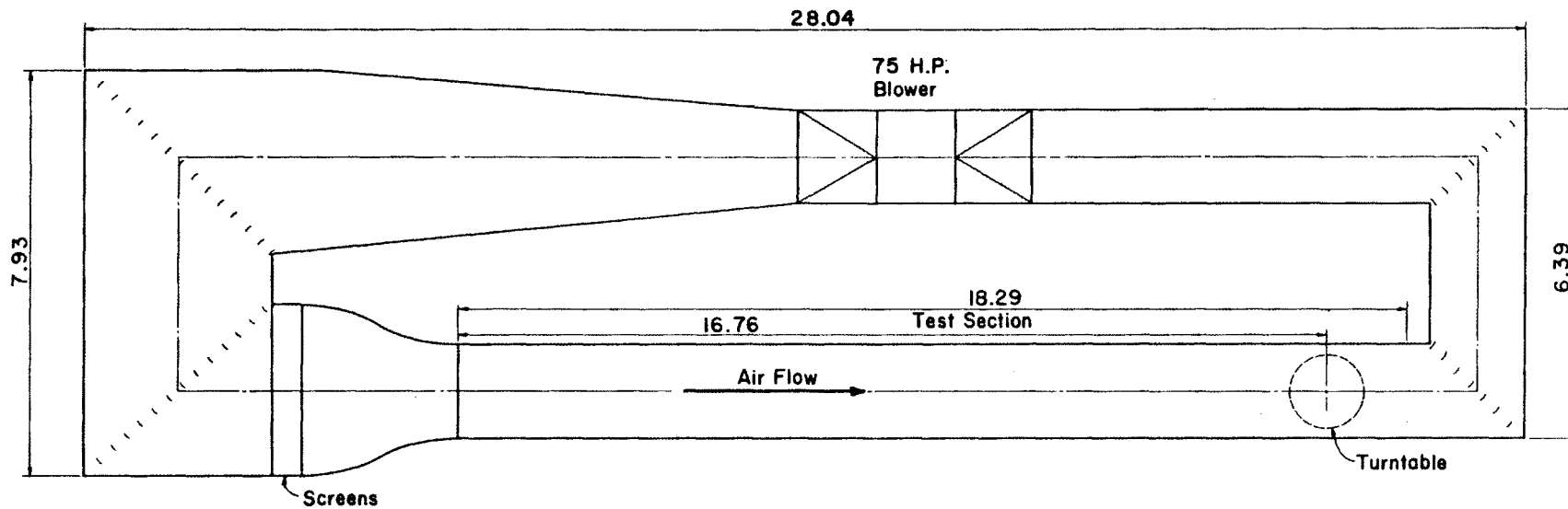
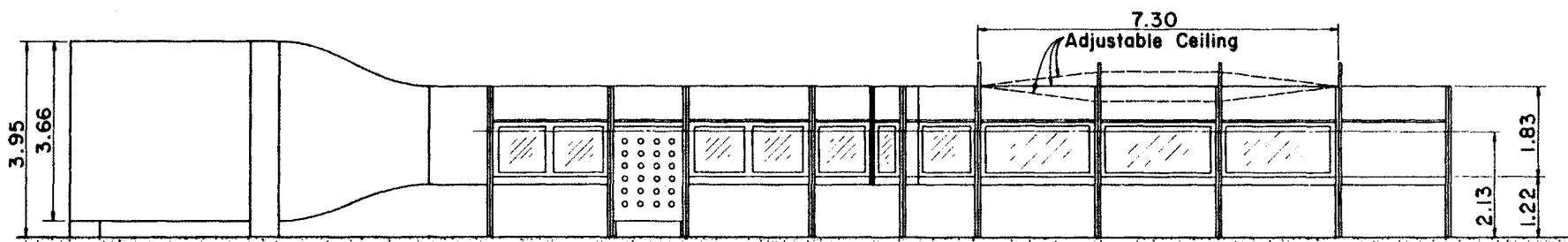
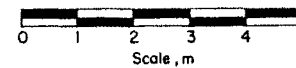


FIG. 1. FLUID DYNAMICS AND DIFFUSION LABORATORY
 ENGINEERING RESEARCH CENTER
 COLORADO STATE UNIVERSITY

Figure 1. Fluid Dynamics and Diffusion Laboratory, Colorado State University



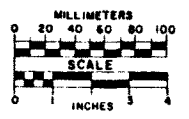
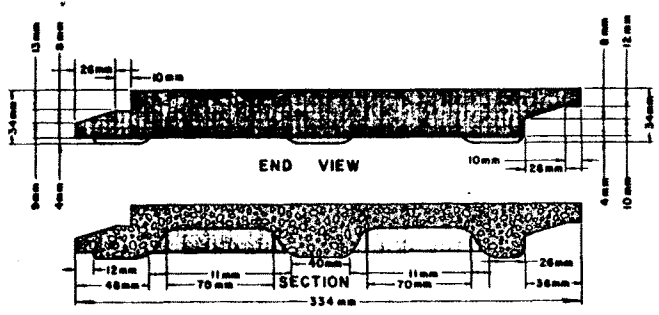
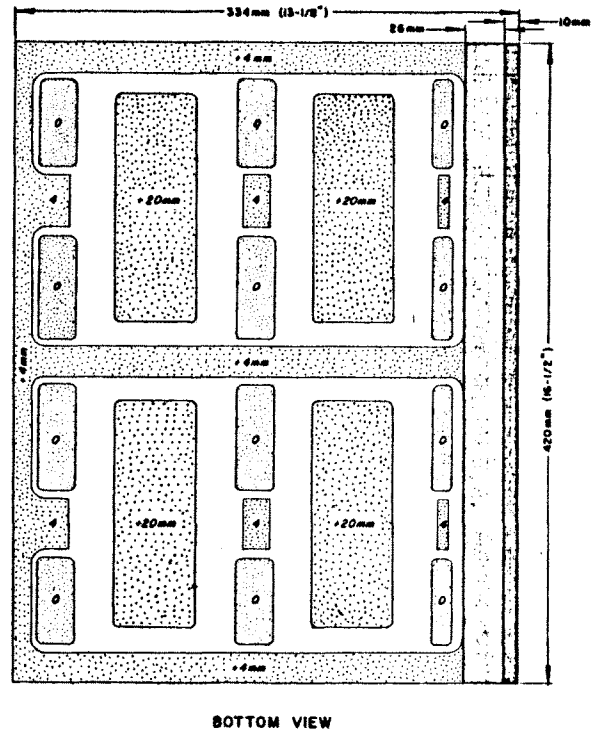
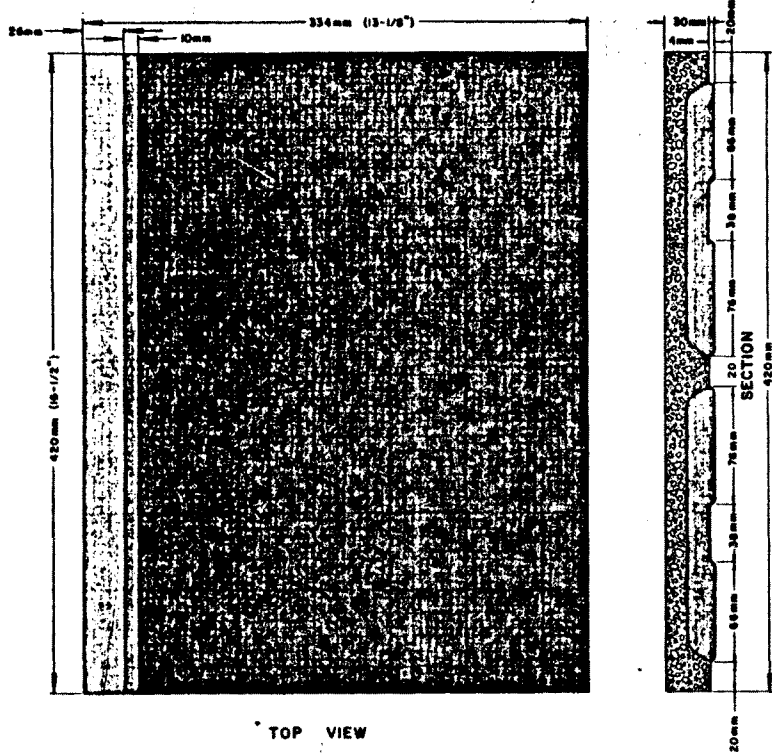
PLAN



All Dimensions in m

ELEVATION

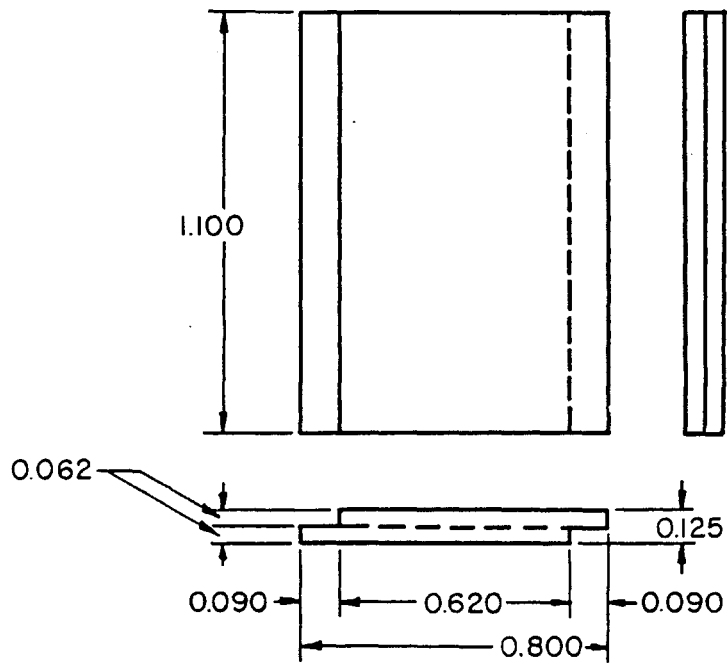
Figure 2. Industrial Aerodynamics Wind Tunnel.



O = CONTACT AREA • FOOTPRINT
 • Xmm = DISTANCE ABOVE CONTACT SURFACE

Figure 3. Westile Ballast Paver

Paver Model



All dimensions in inches

Figure 4. Paver Model -- Details

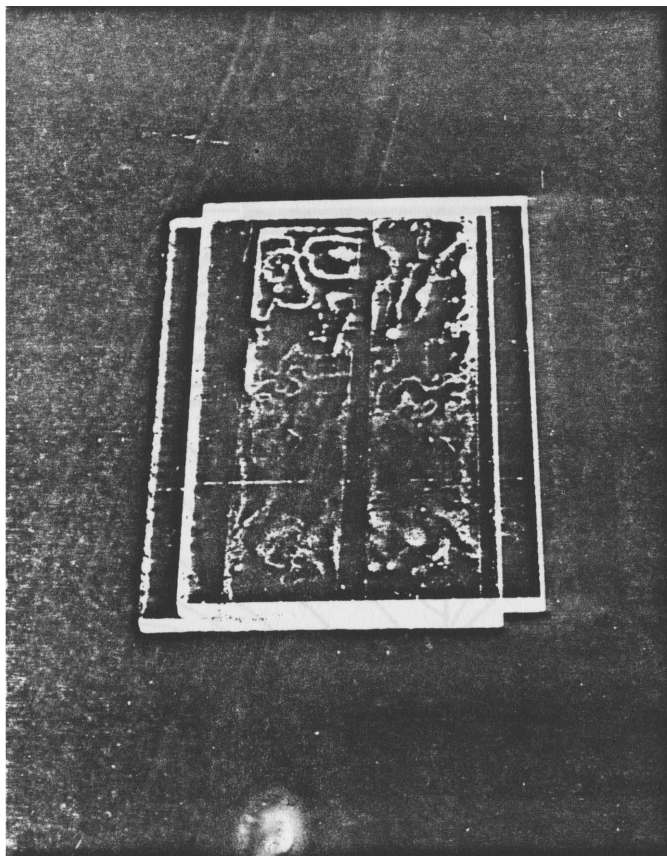


Figure 5. Paver Model -- Overall View

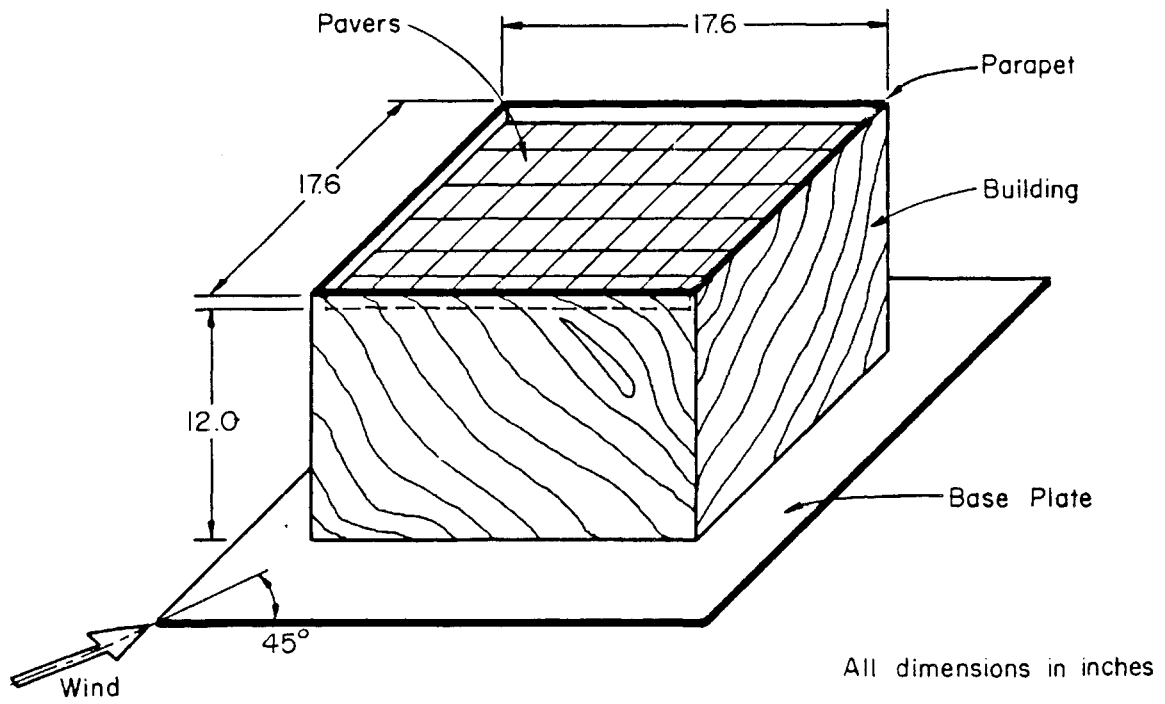


Figure 6. Building Model

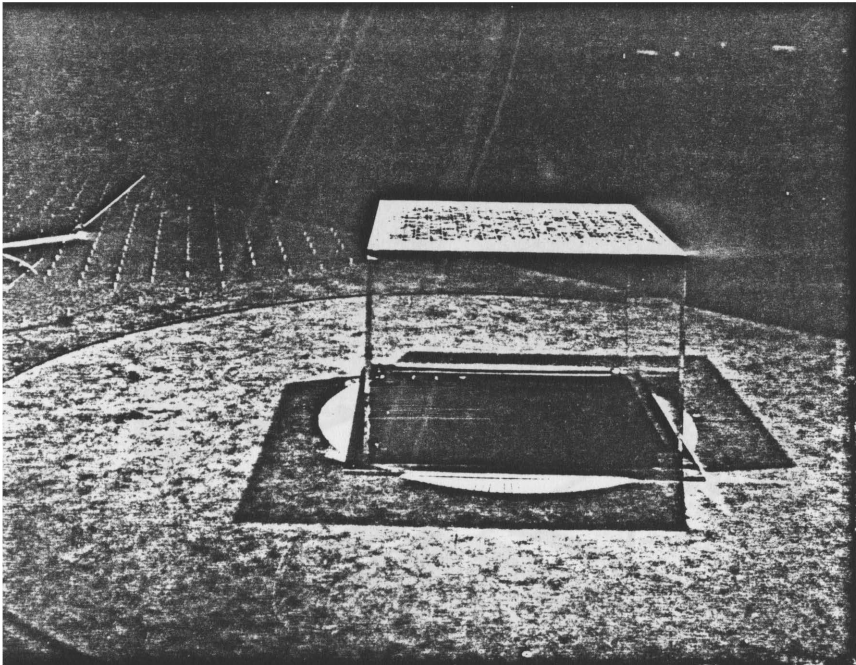


Figure 7. Building Model Placed in Wind Tunnel

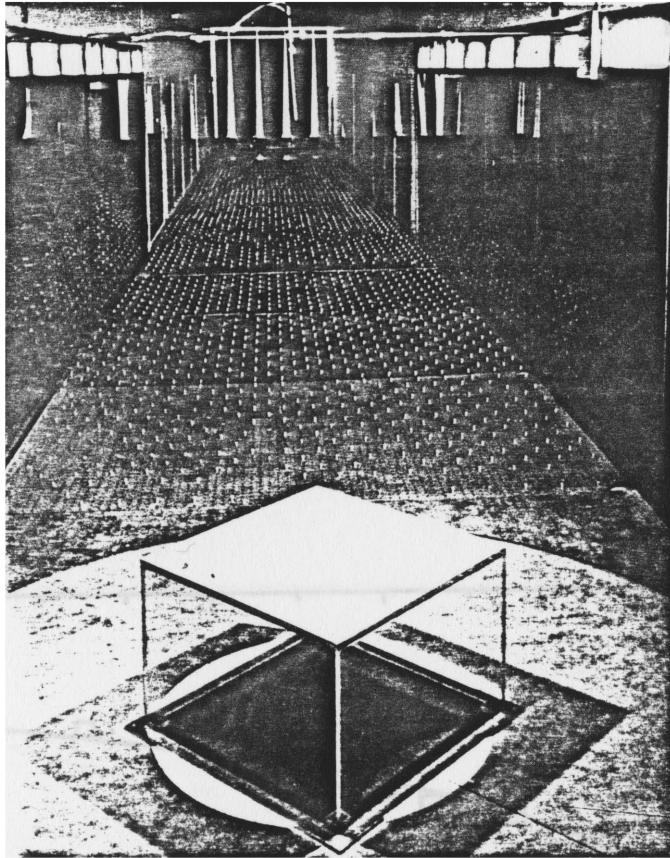


Figure 8. Boundary Layer Generators

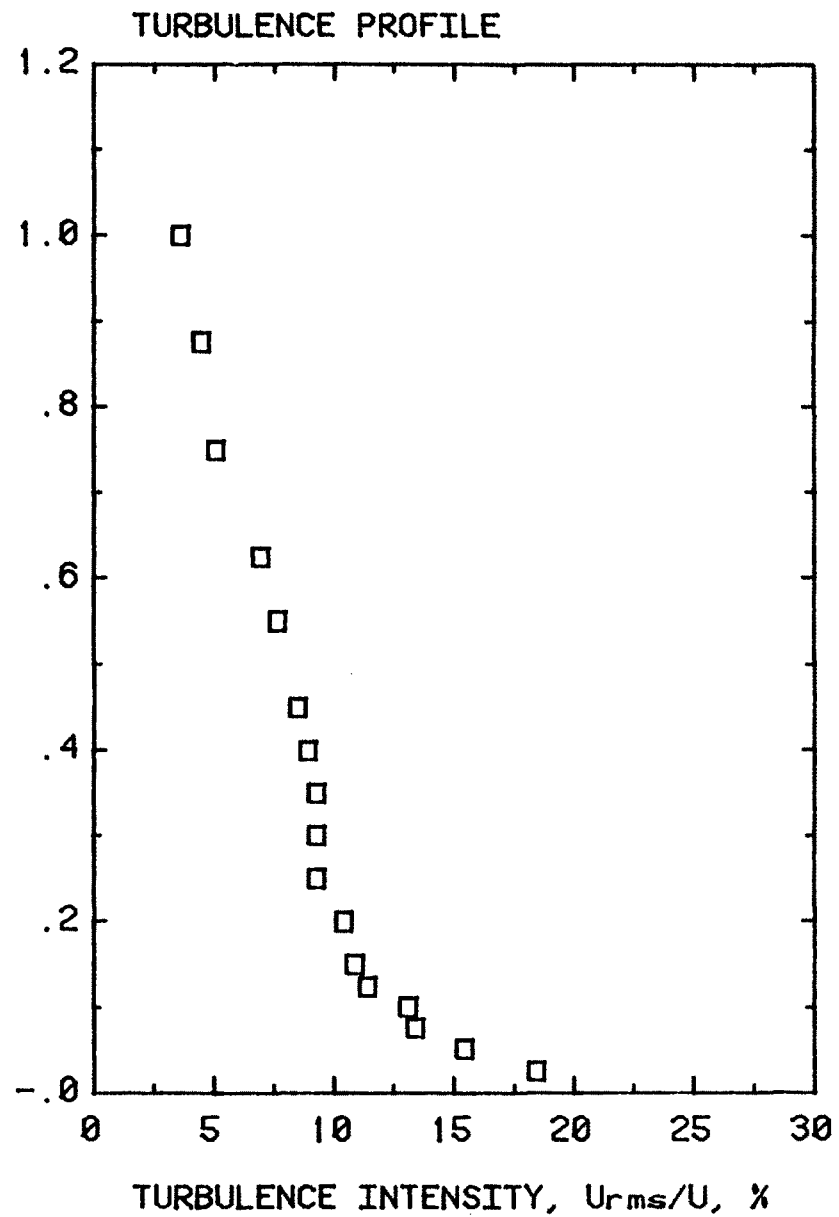
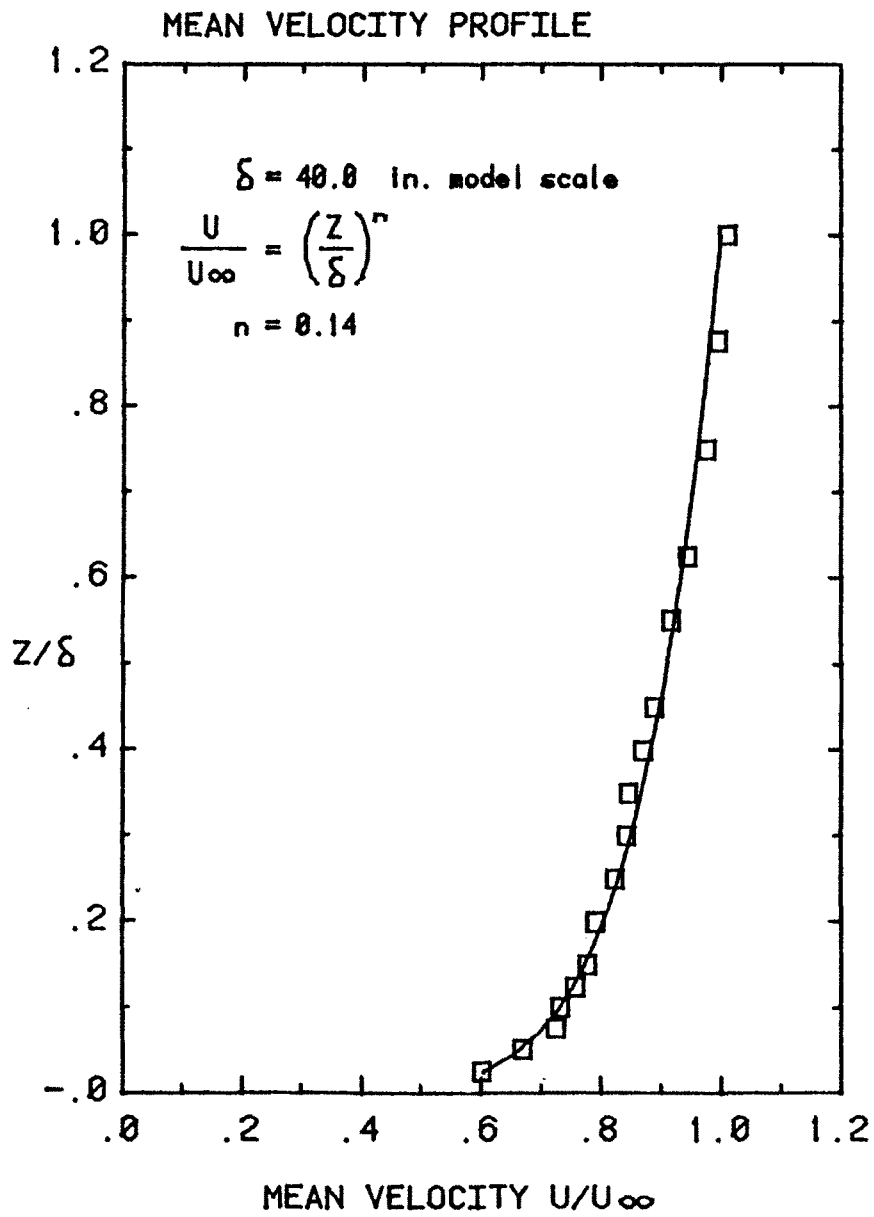


Figure 9. Mean Wind Speed and Turbulence Intensity Profiles -- Exposure C

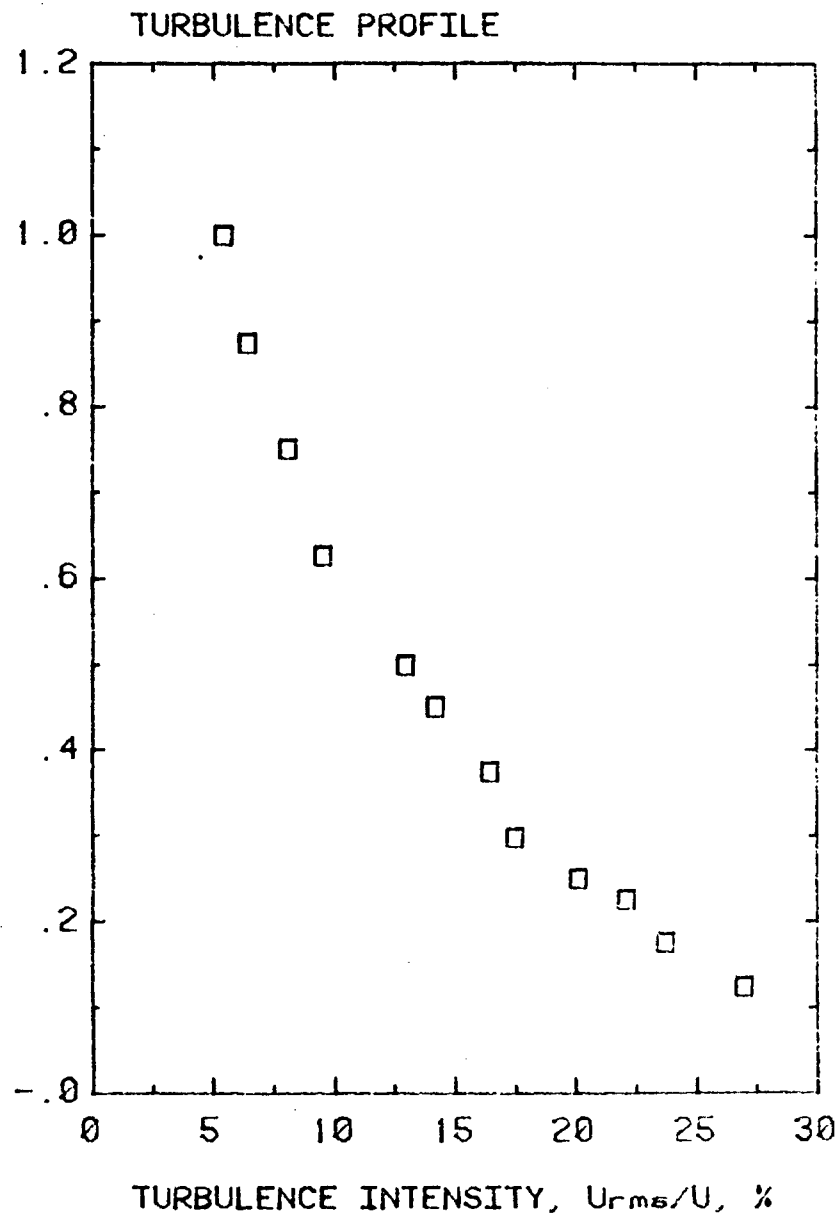
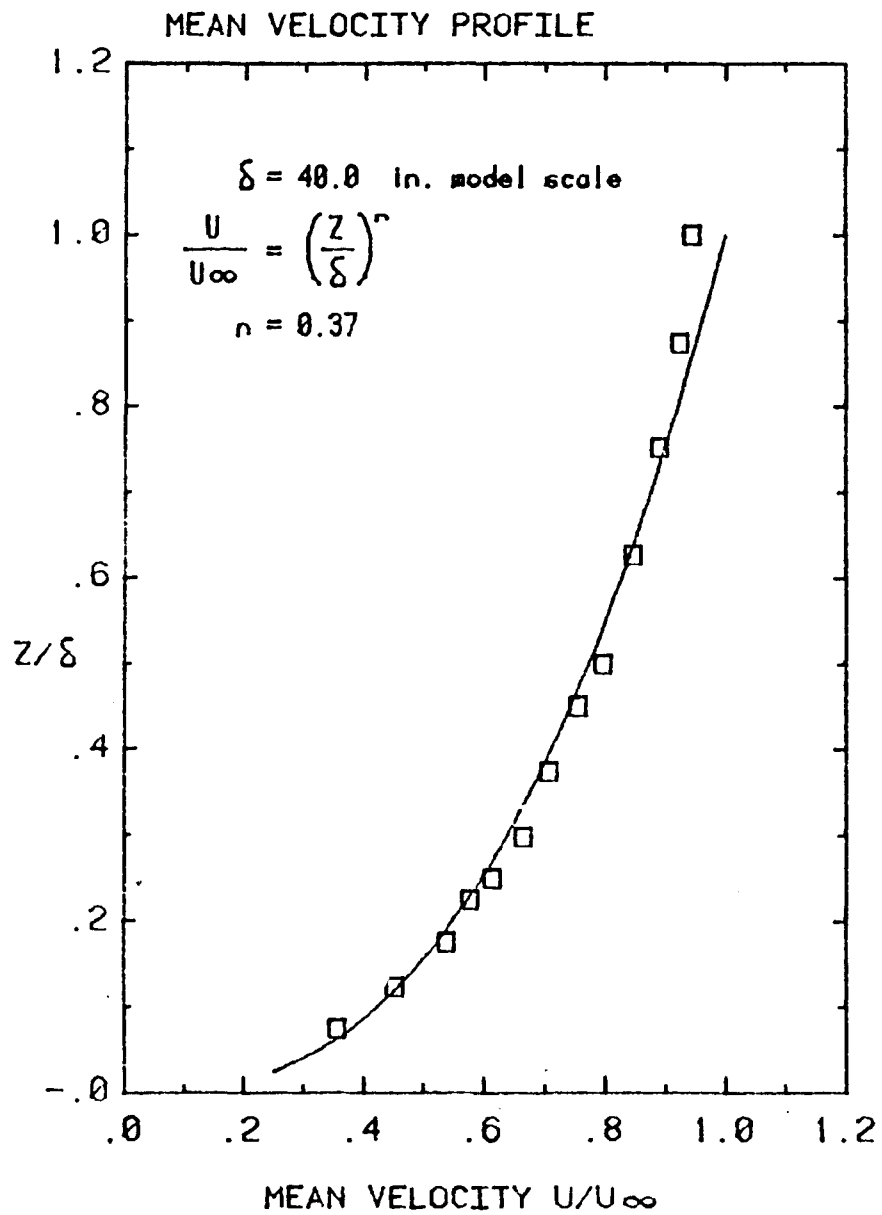


Figure 10. Mean Wind Speed and Turbulence Intensity Profiles -- Exposure A

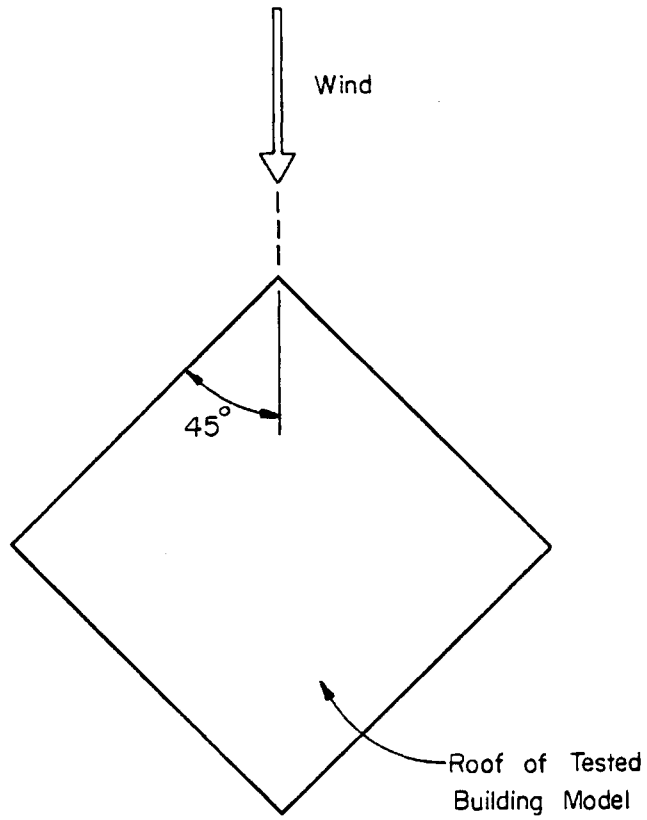


Figure 11. Tested Wind Direction

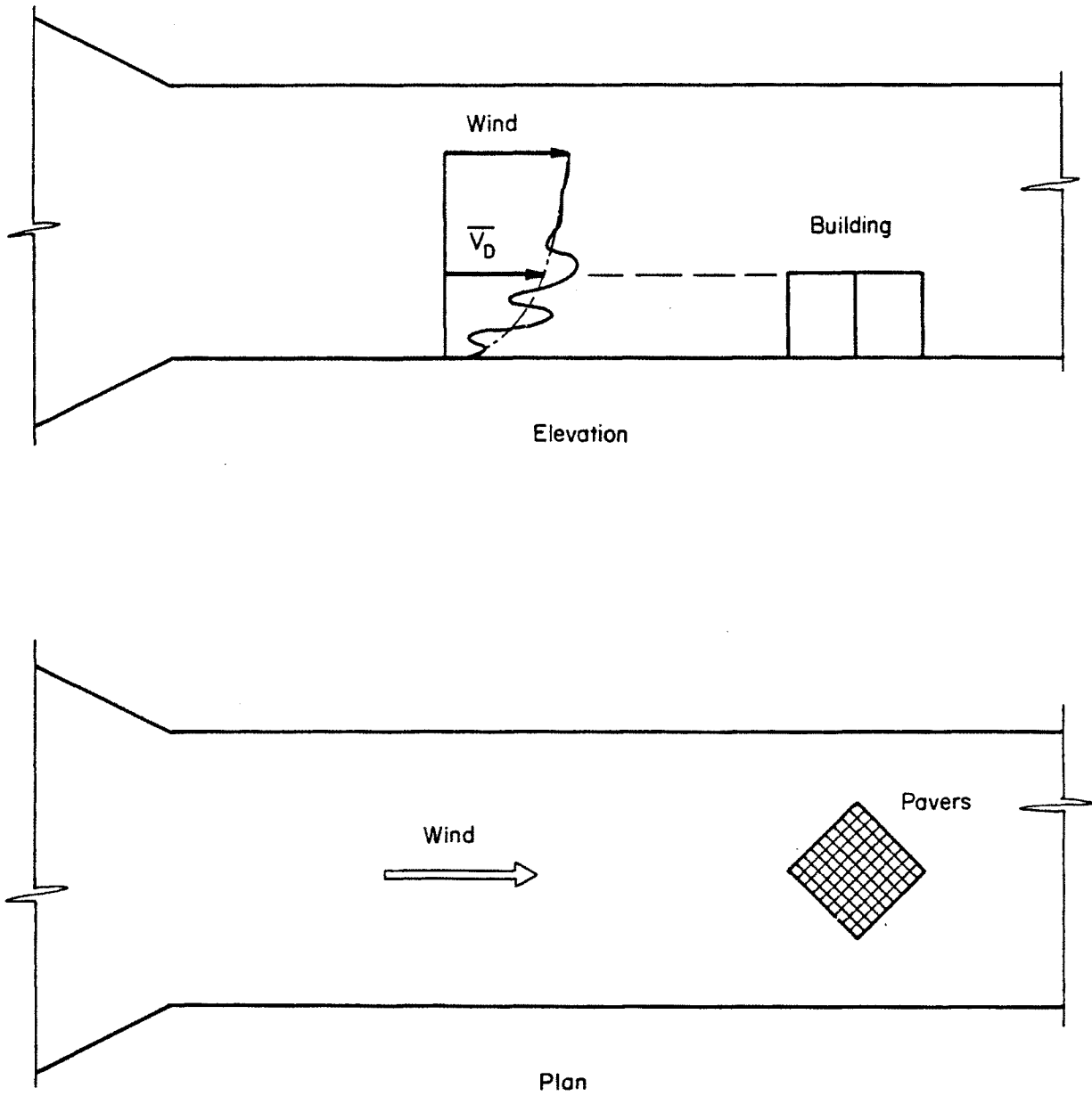


Figure 12. Experimental Configuration Tested

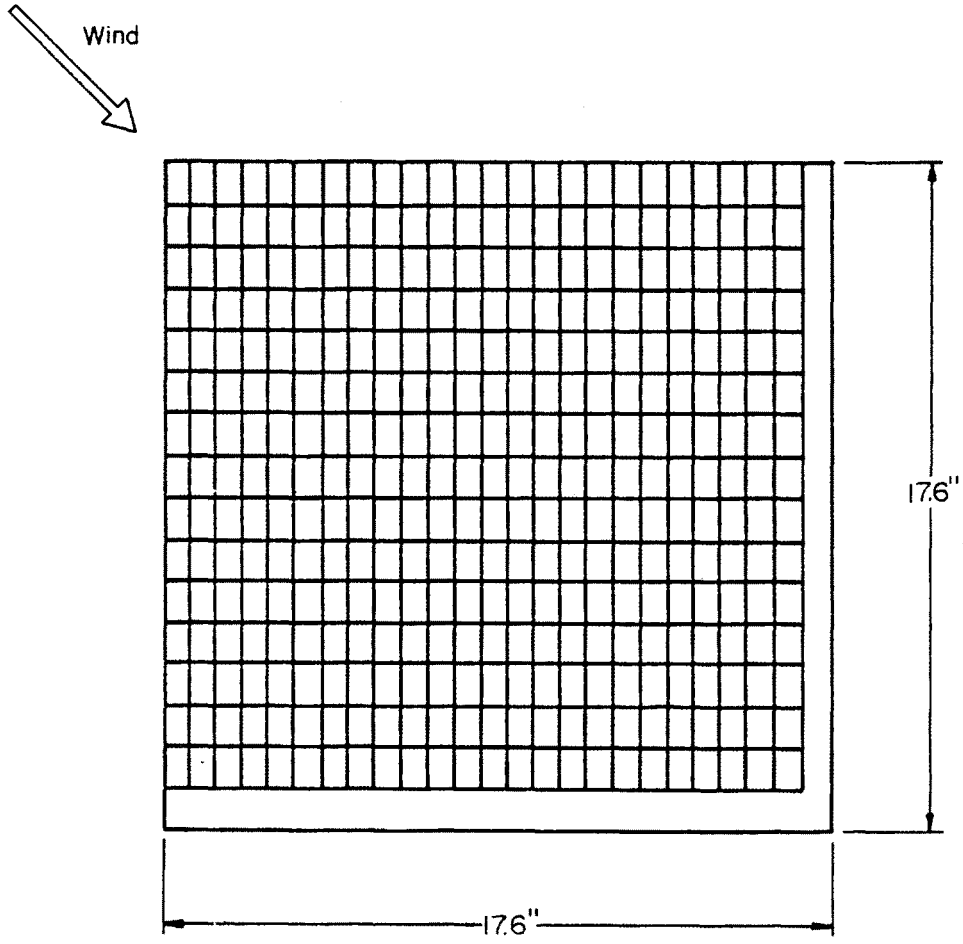


Figure 13. Original Paver Configuration

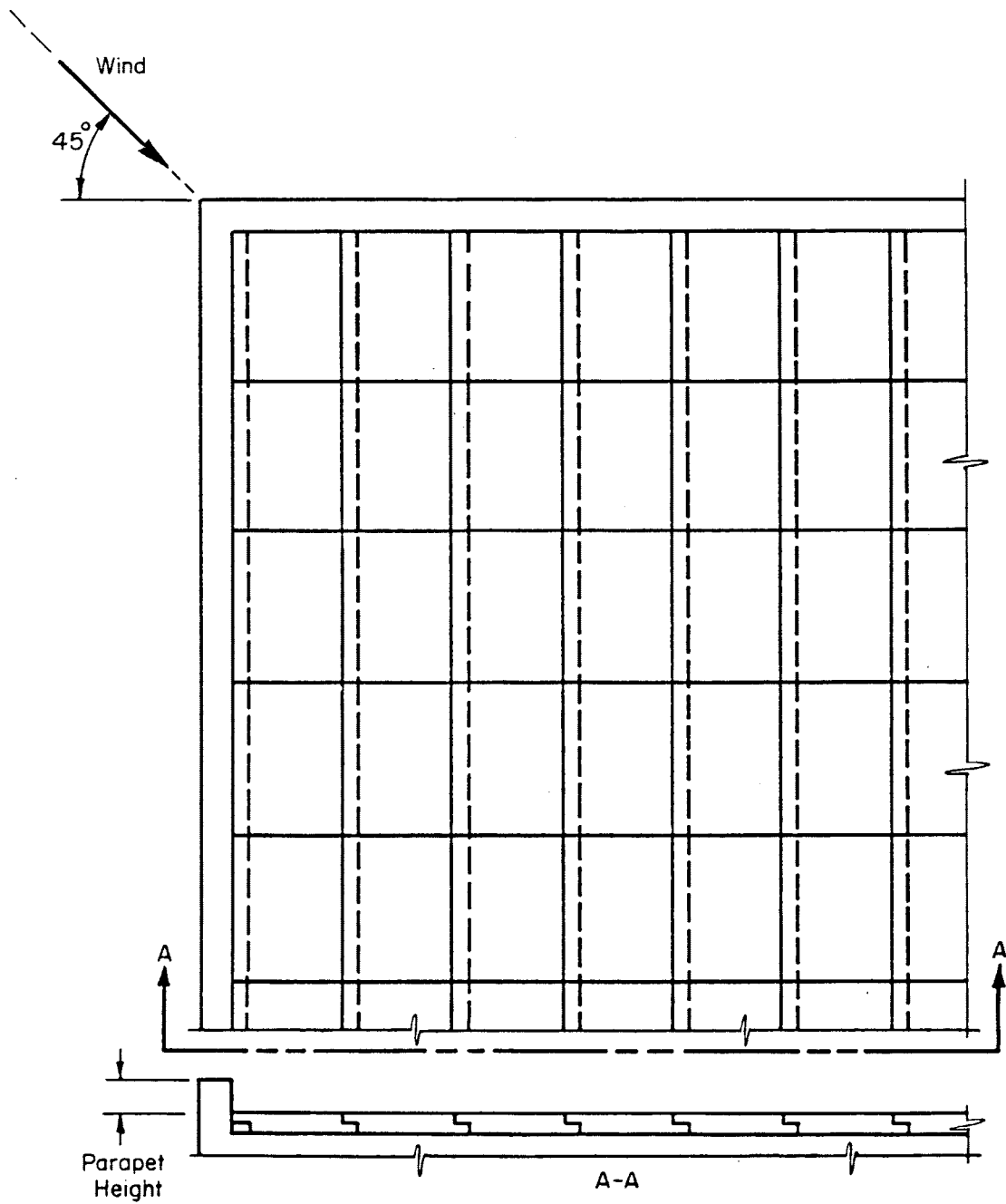


Figure 14. Details of Paver Layout -- Original Configuration

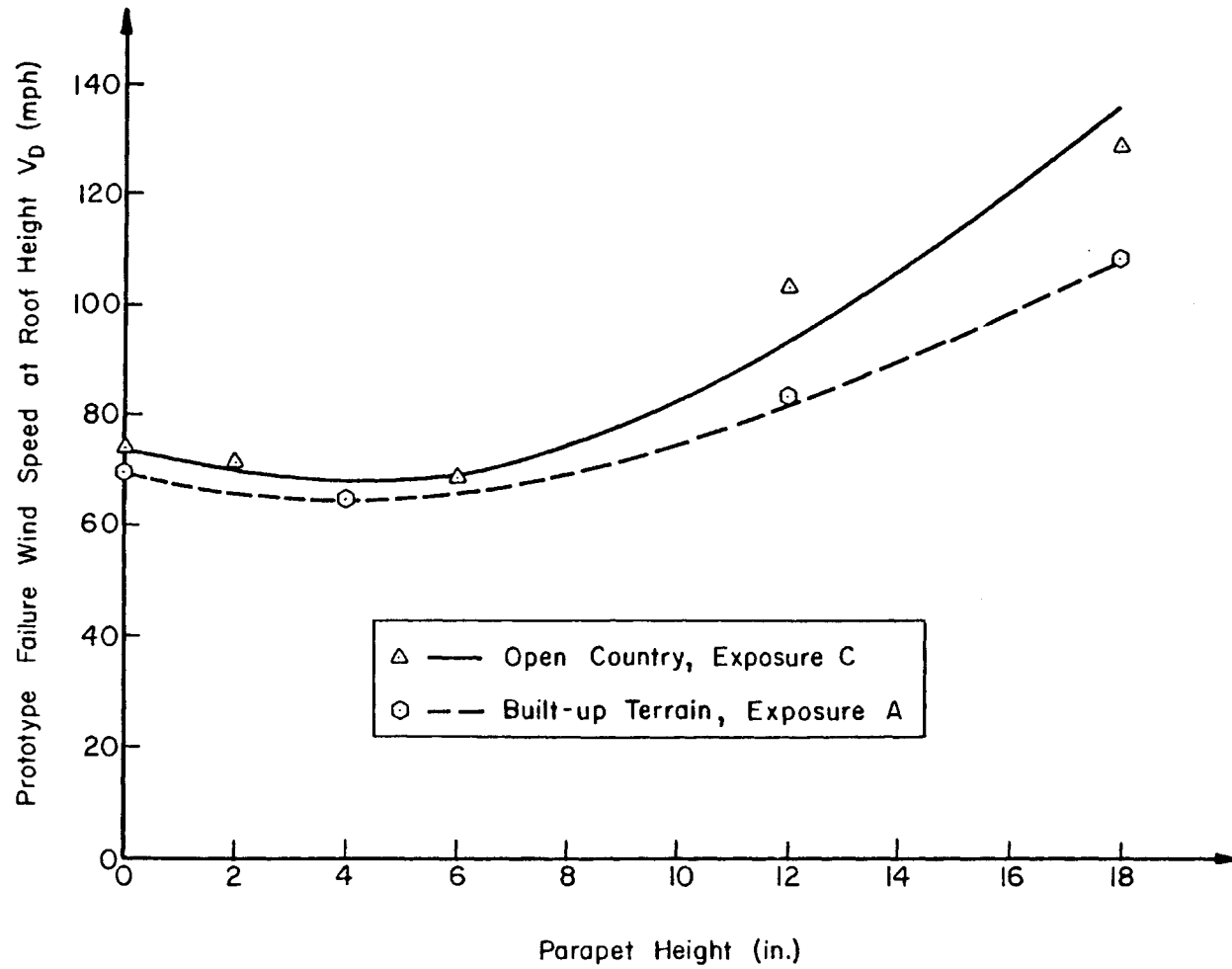
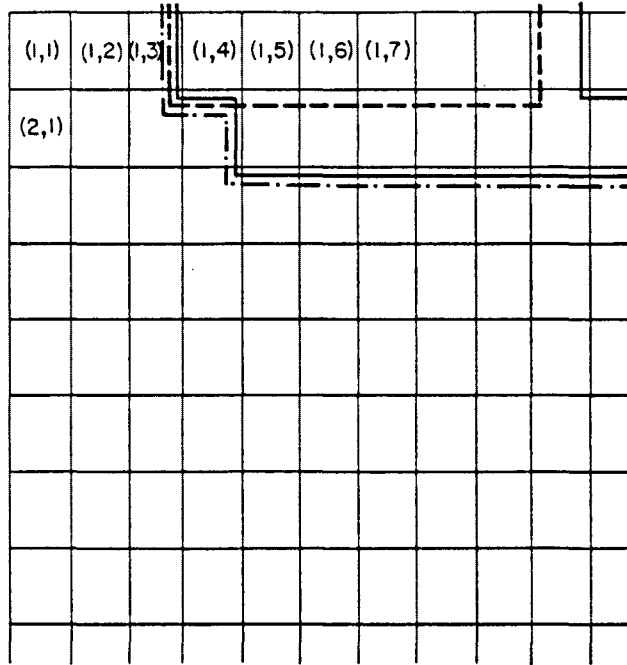
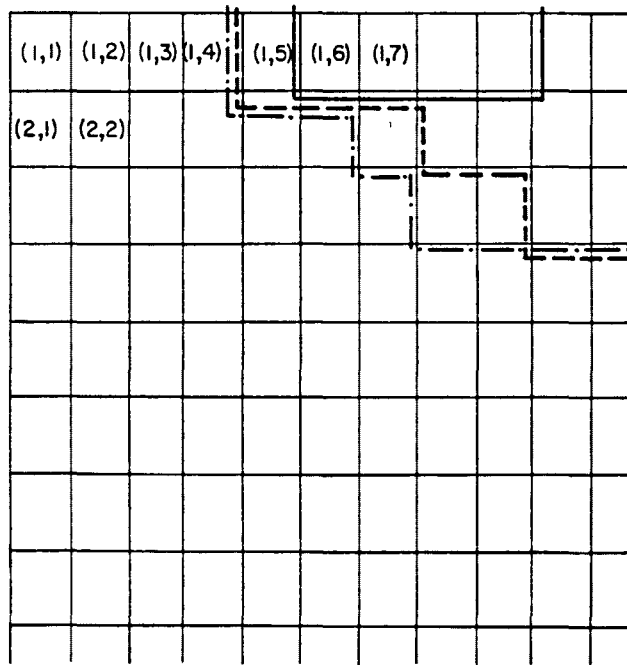


Figure 15. Failure Wind Speed at Roof Height -- Original Paver Configuration

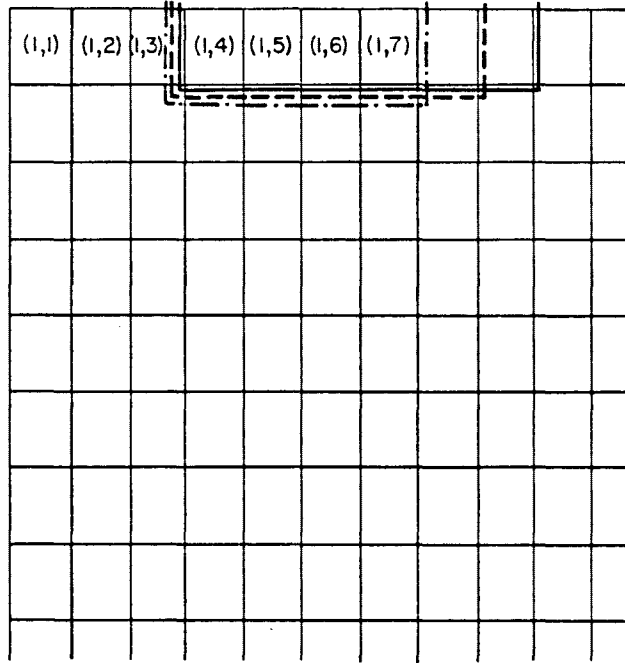


Exposure C

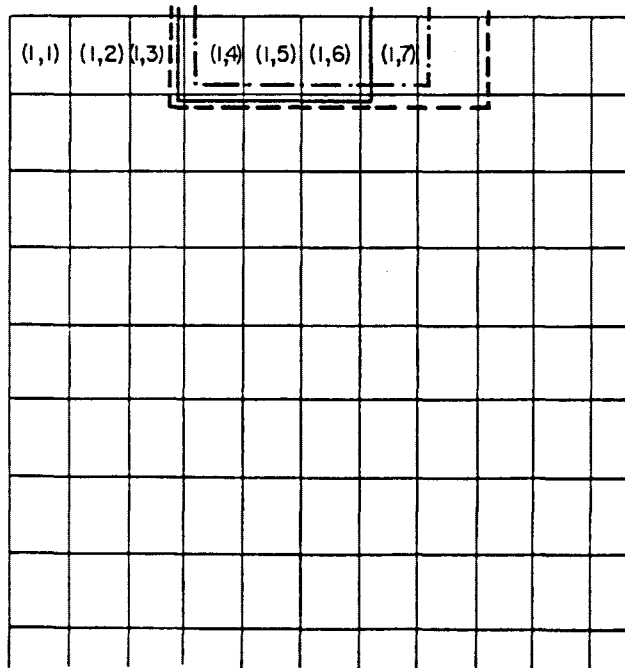


Exposure A

Figure 16. Paver Failure -- Original Configuration With 0 in. Parapet

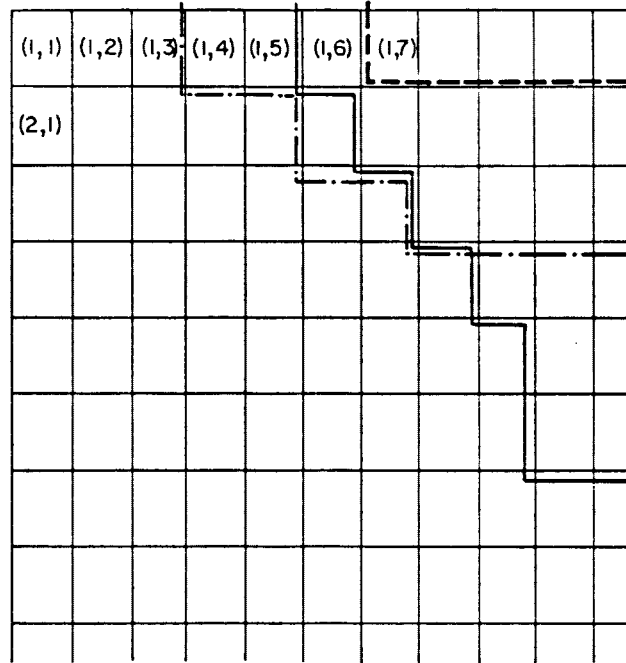


Exposure C

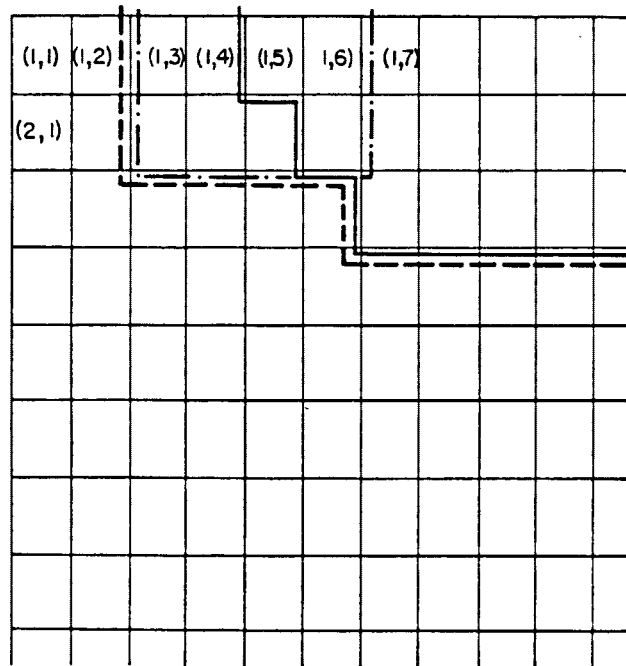


Exposure A

Figure 17. Paver Failure -- Original Configuration With 6 in. Parapet



Exposure C



Exposure A

Figure 18. Paver Failure -- Original Configuration With 12 in. Parapet

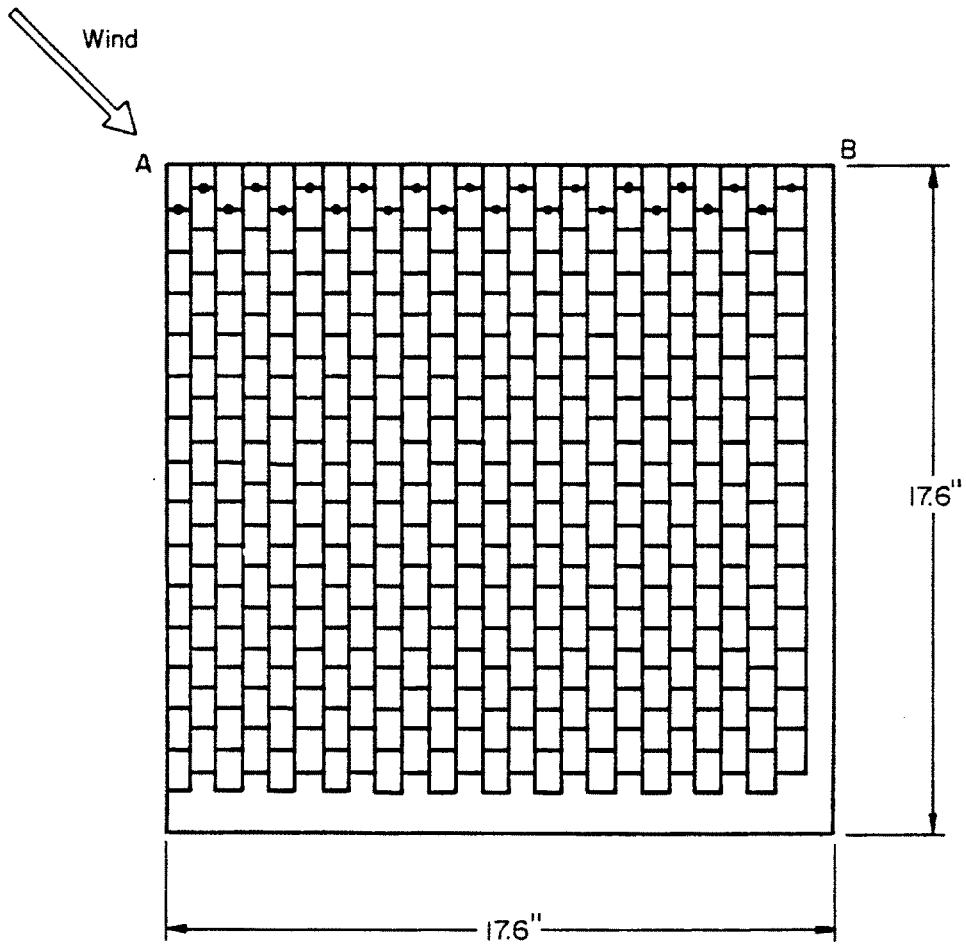


Figure 19. Modified Paver Configuraton

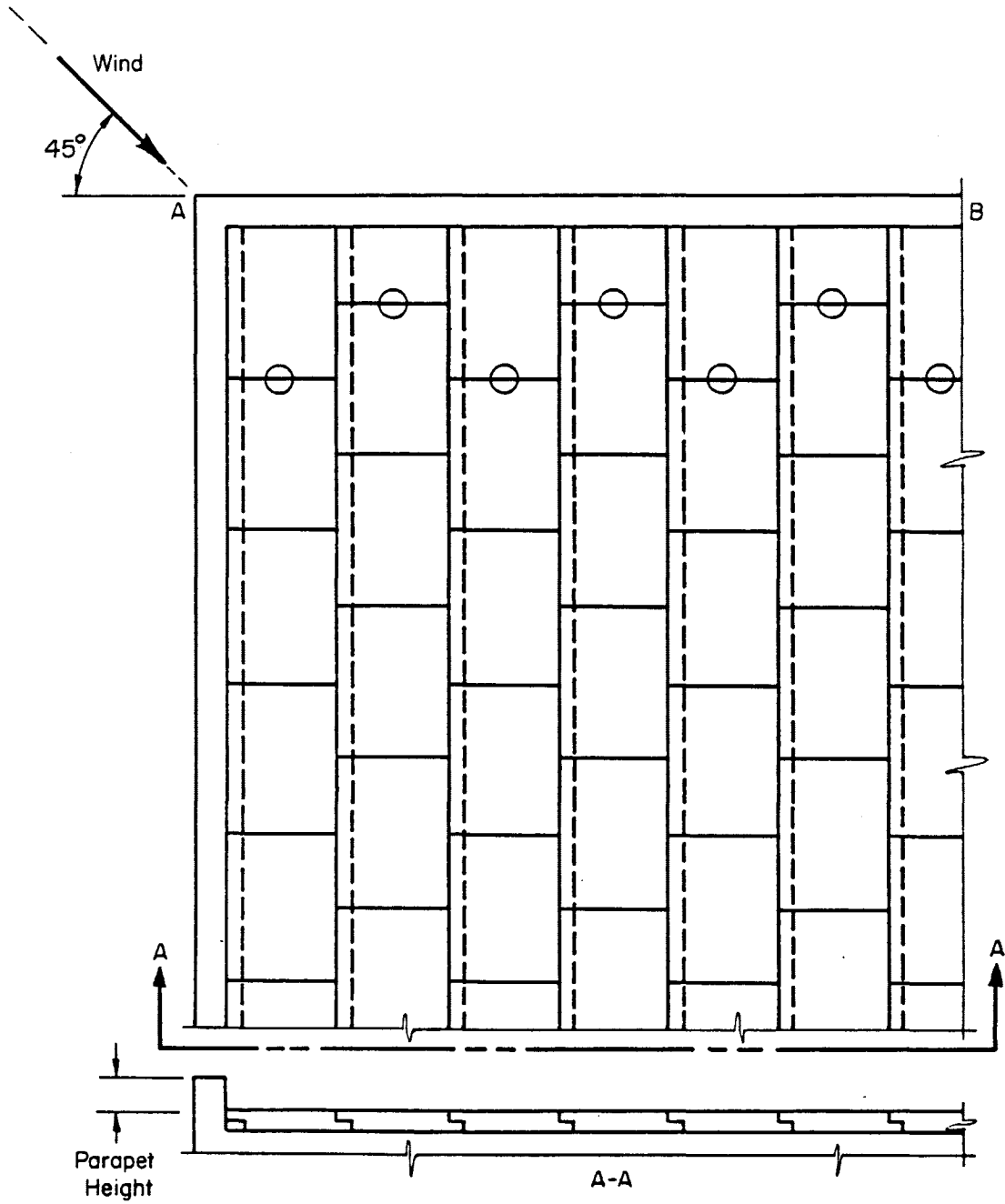


Figure 20. Details of Modified Paver Layout -- Modified Configuration

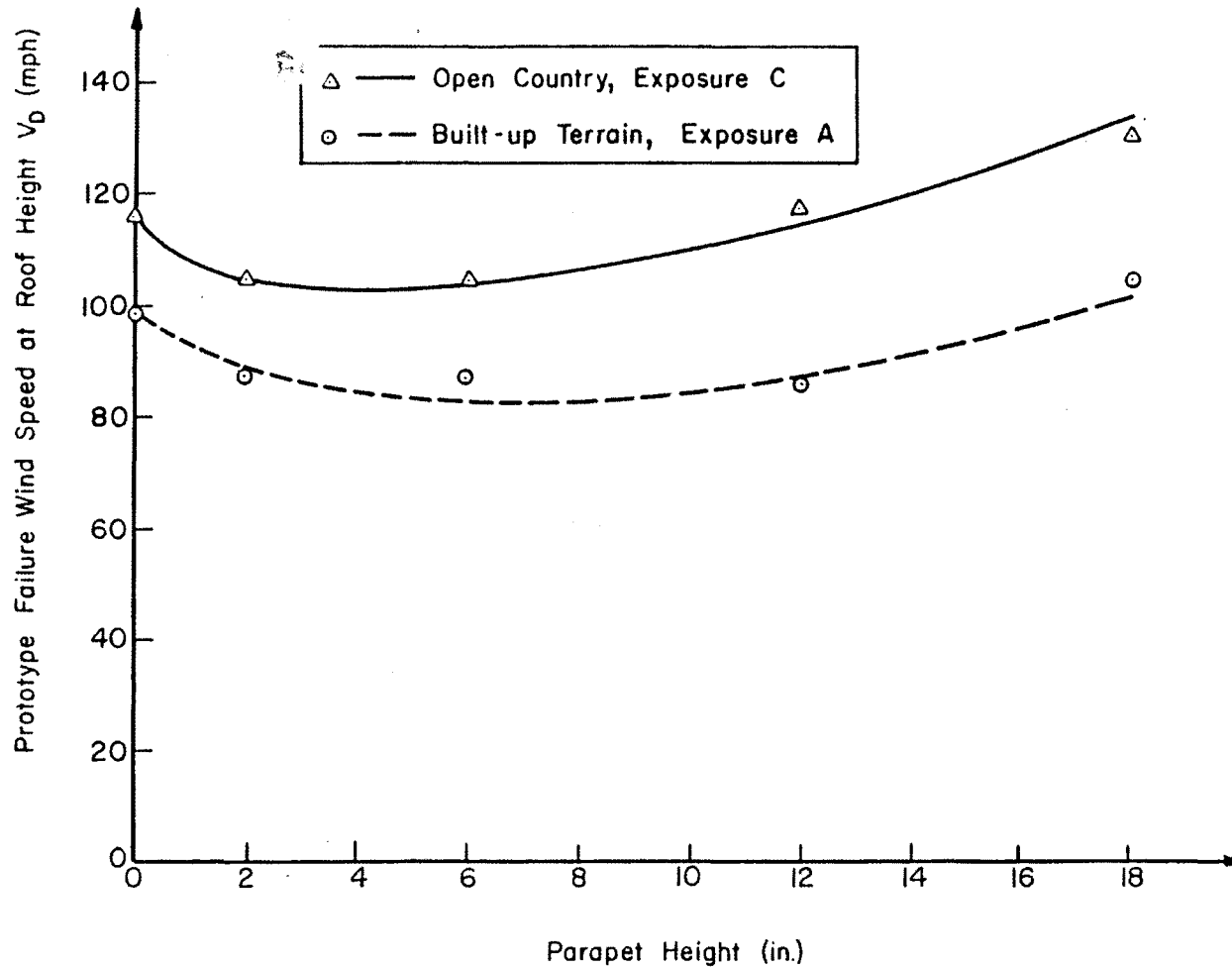
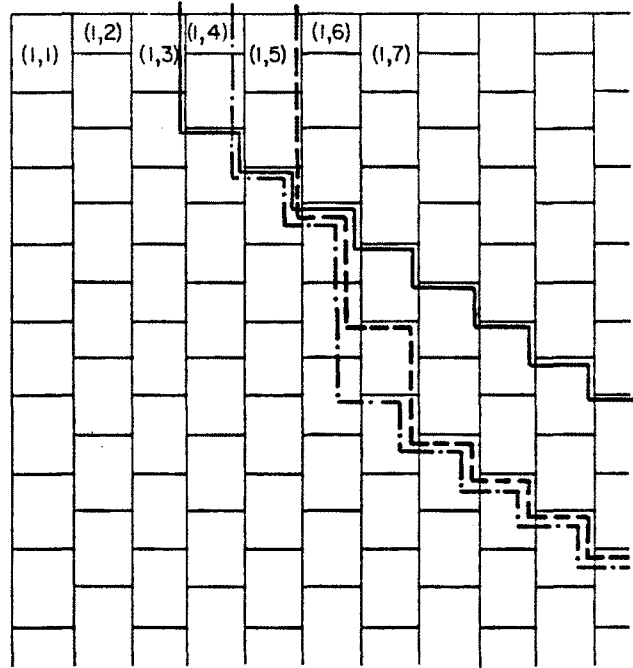
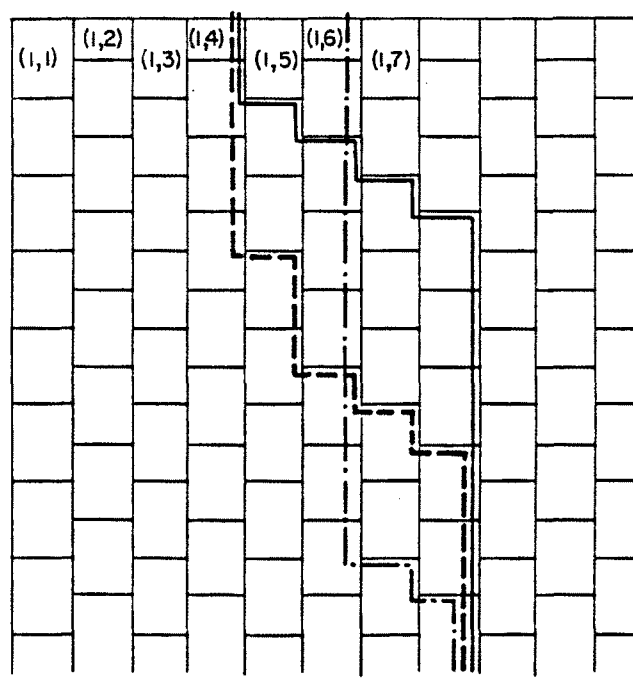


Figure 21. Failure Wind Speed at Roof Height -- Modified Paver Configuration



Exposure C



Exposure A

Figure 22. Paver Failure -- Modified Configuration With 0 in. Parapet

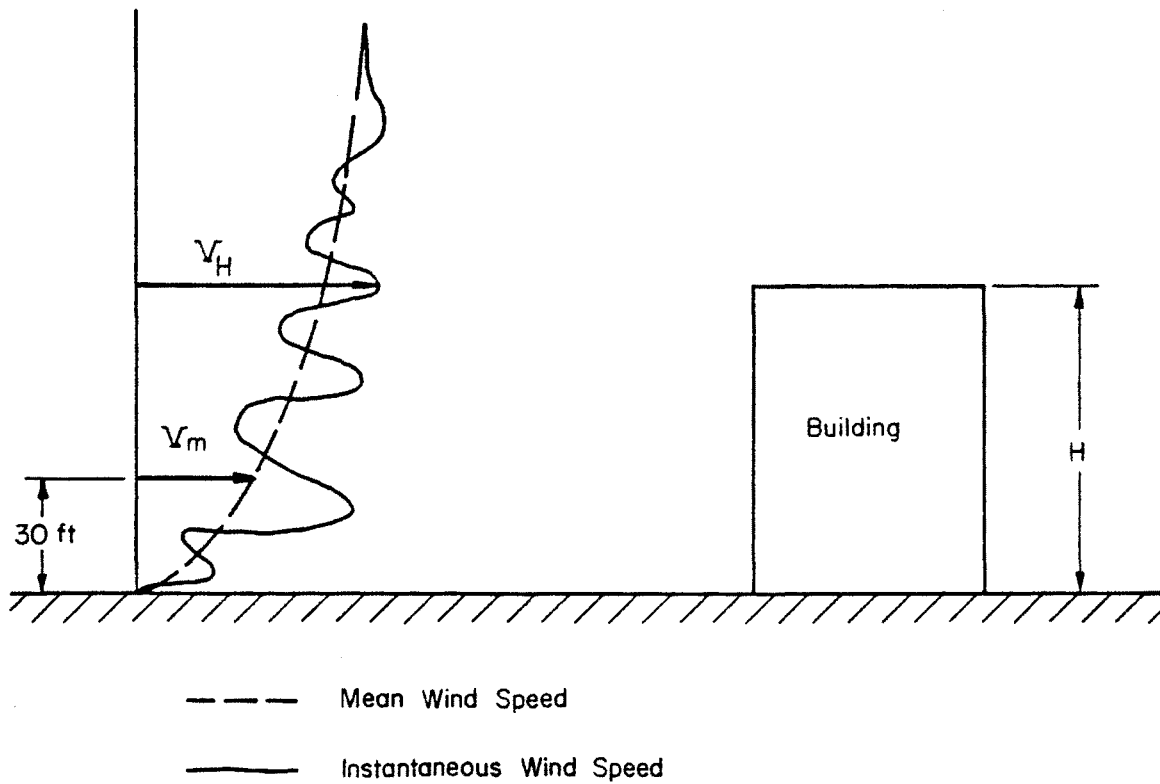


Figure 24. Main Parameters for Design Considerations

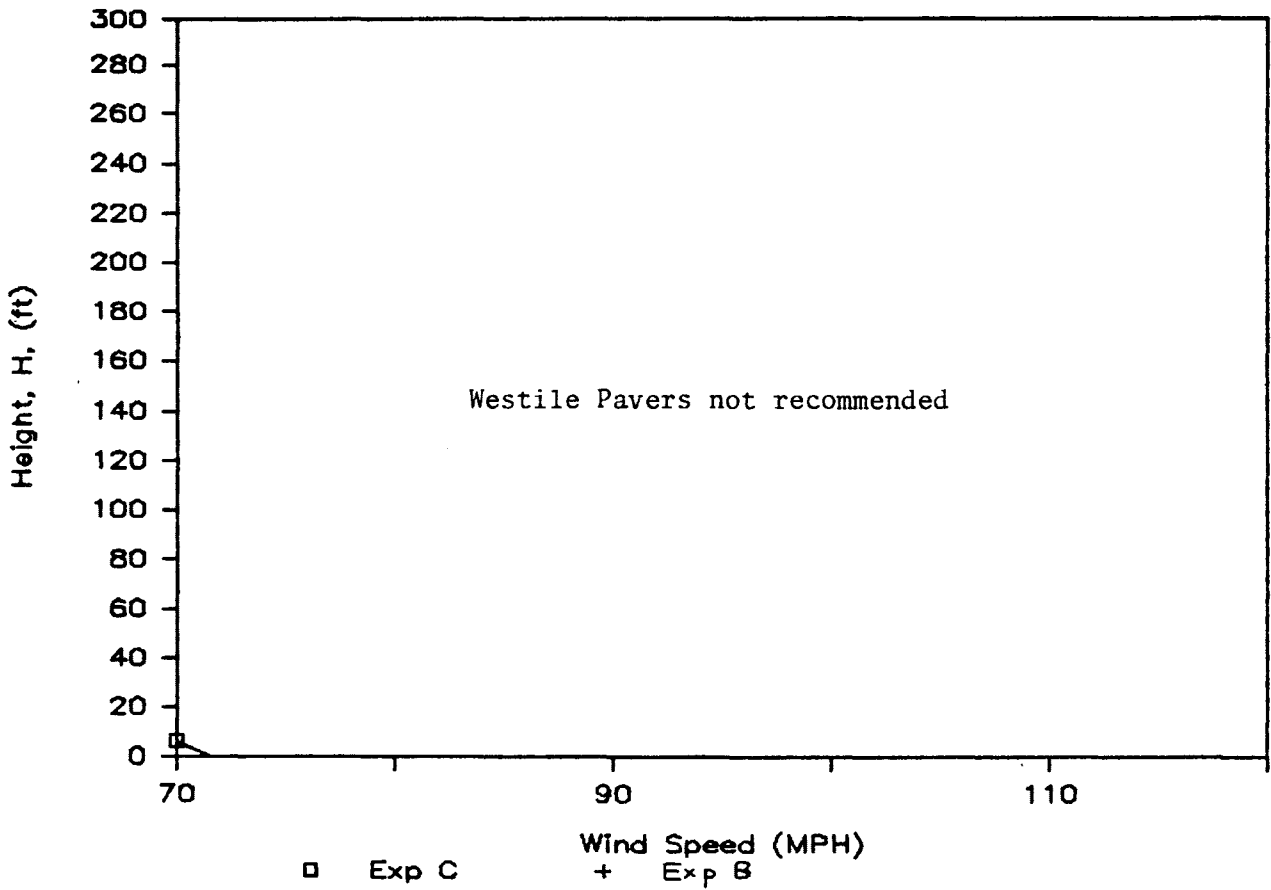


Figure 25. Maximum Building Height Estimated Using UBC -- Original Configuration With 0 in. Parapet, Exposure C and B

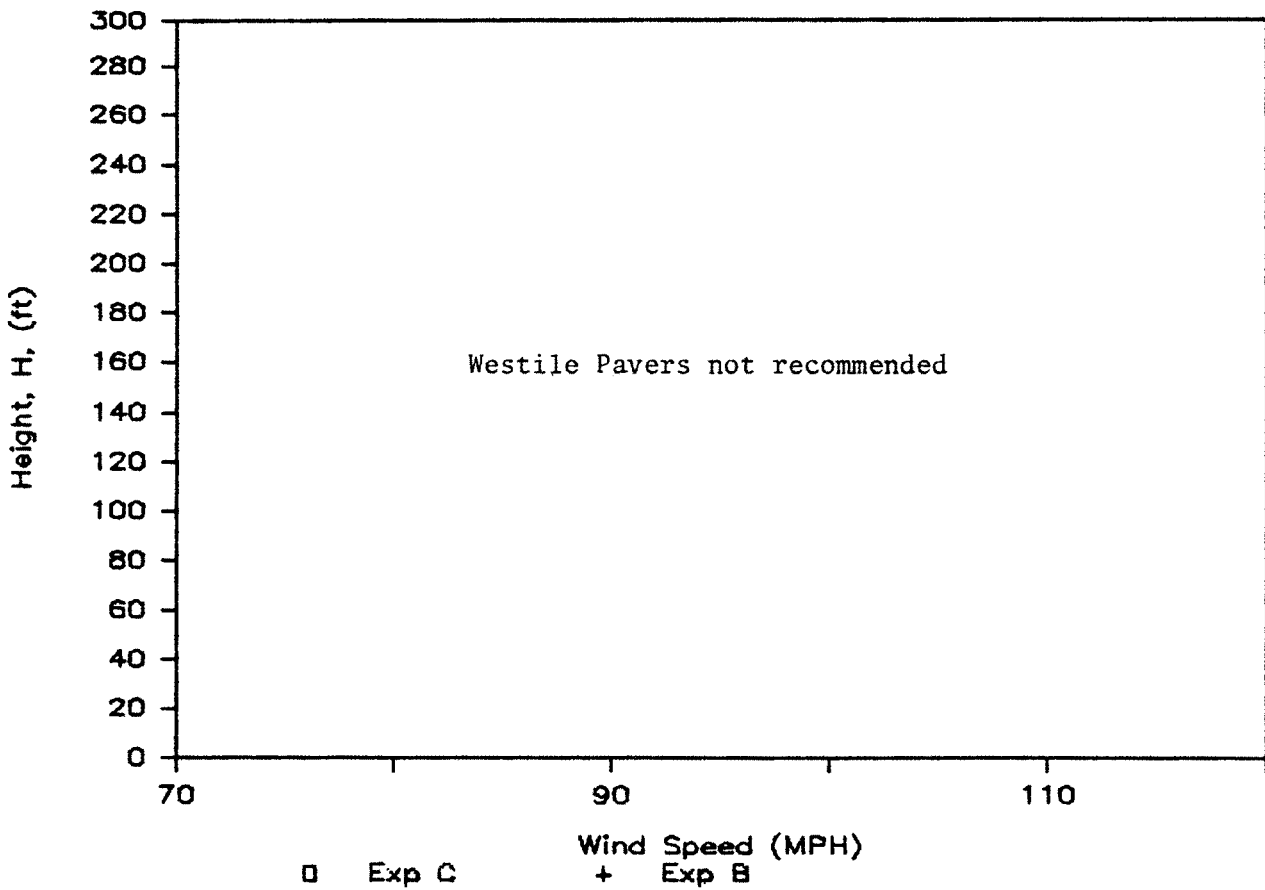


Figure 26. Maximum Building Height Estimated Using UBC -- Original Configuration With 6 in. Parapet, Exposure C and B

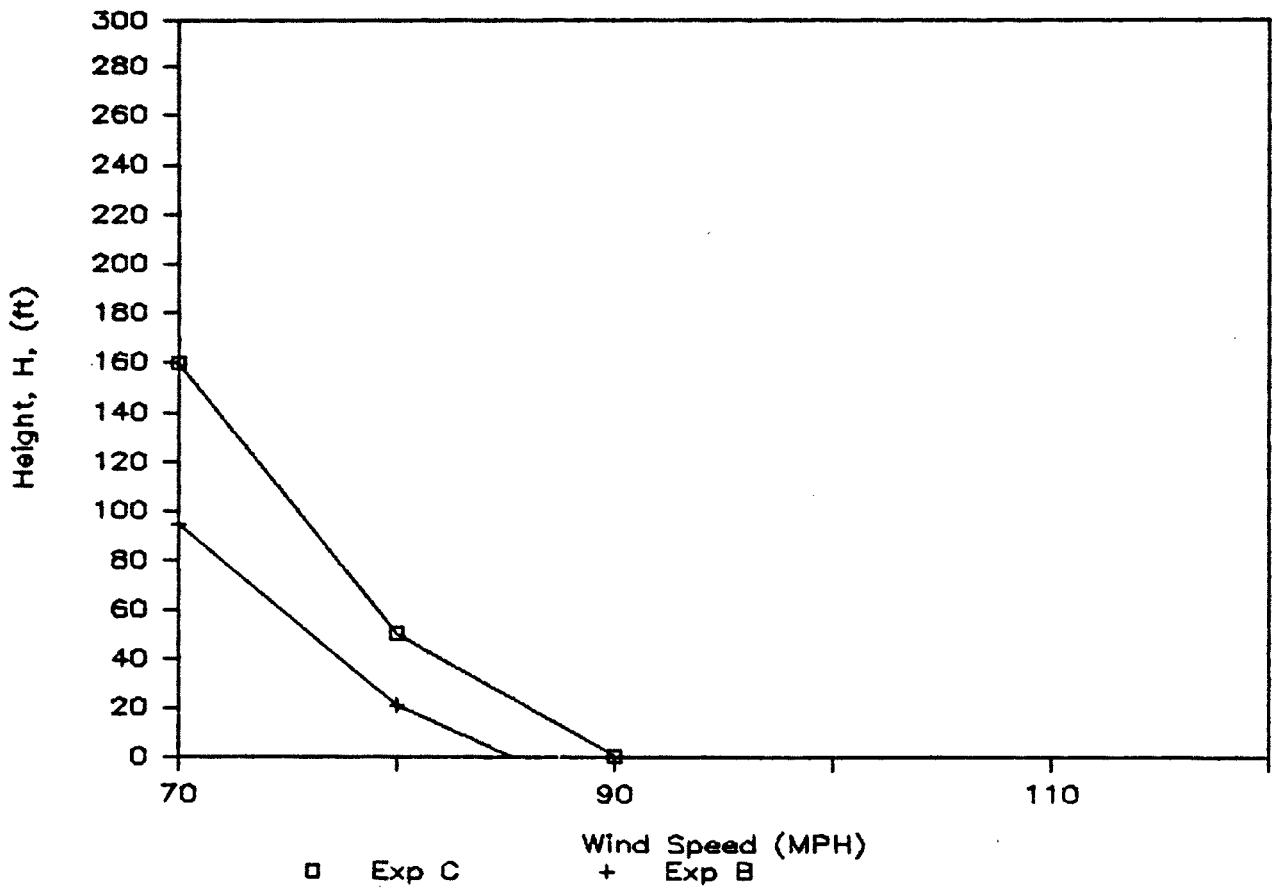


Figure 27. Maximum Building Height Estimated Using UBC -- Original Configuration With 12 in. Parapet, Exposure C and B

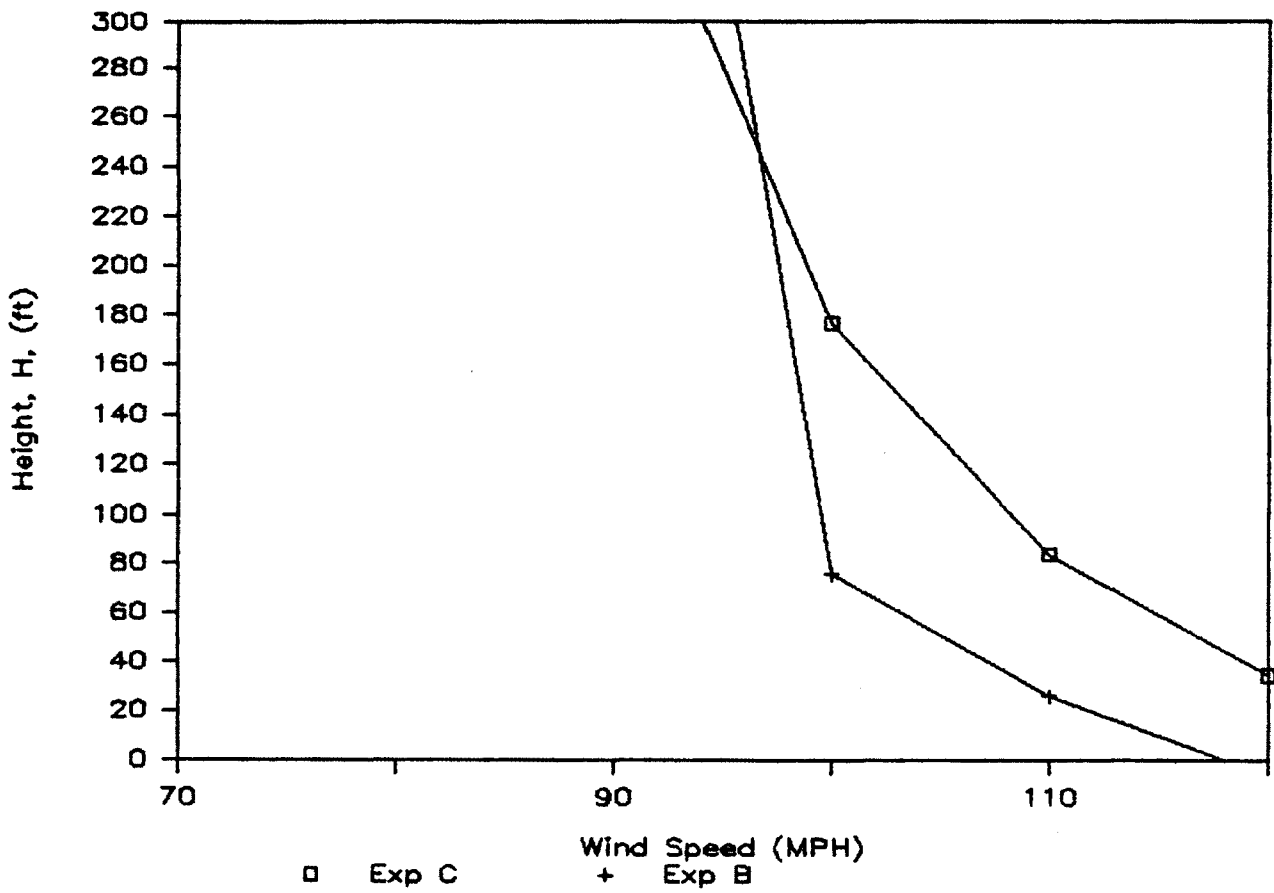


Figure 28. Maximum Building Height Estimated Using UBC -- Original Configuration With 18 in. Parapet, Exposure C and B

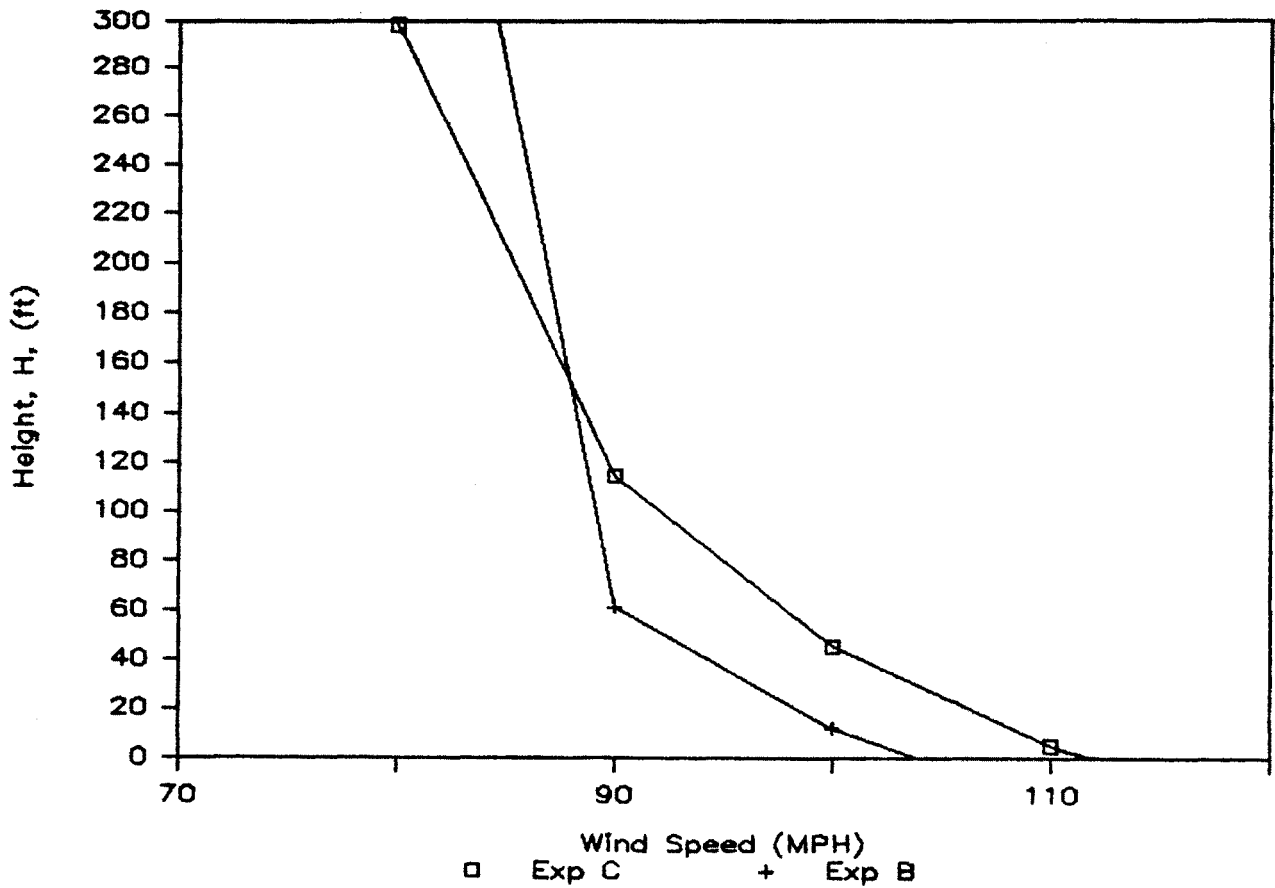


Figure 29. Maximum Building Height Estimated Using UBC -- Modified Configuration With 0 in. Parapet, Exposure C and B

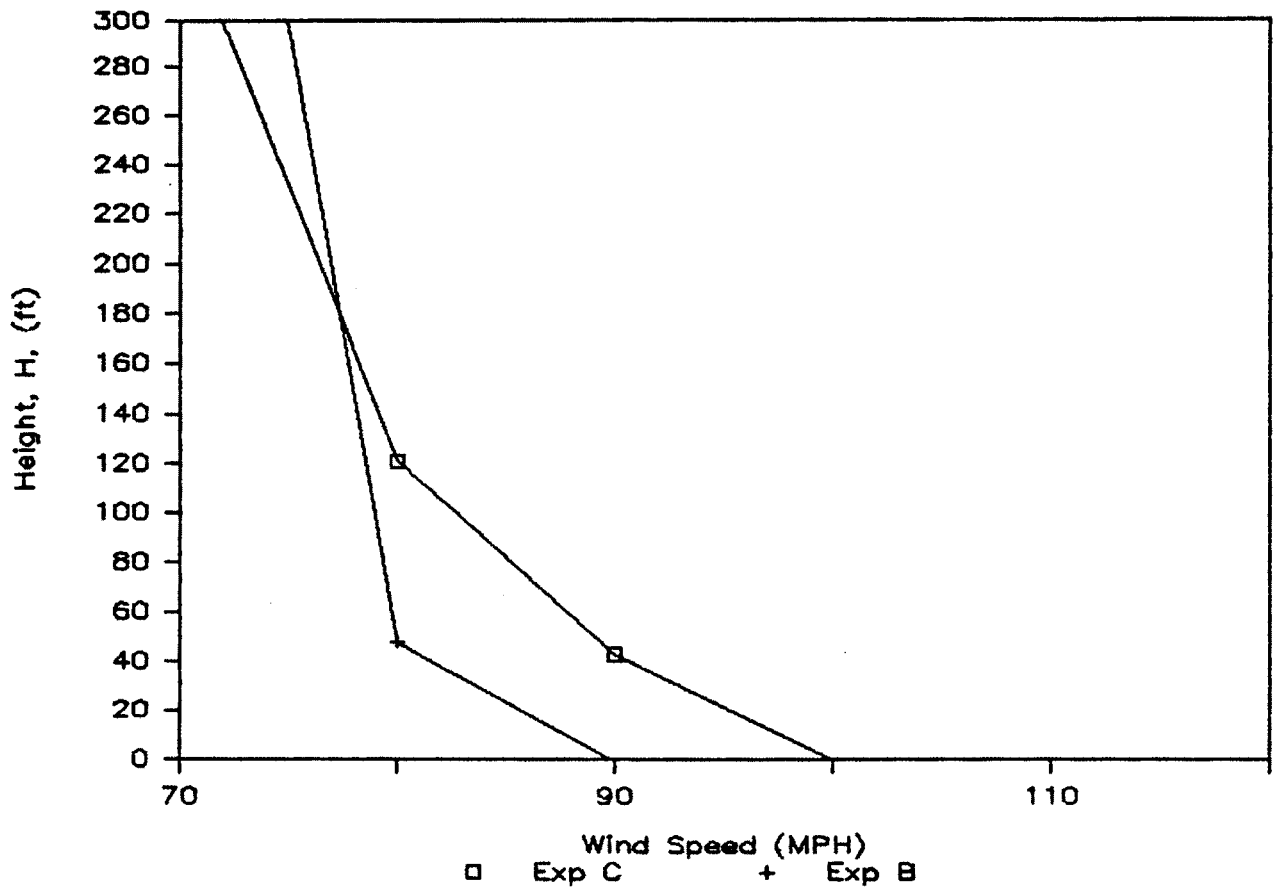


Figure 30. Maximum Building Height Estimated Using UBC -- Modified Configuration With 6 in. Parapet, Exposure C and B

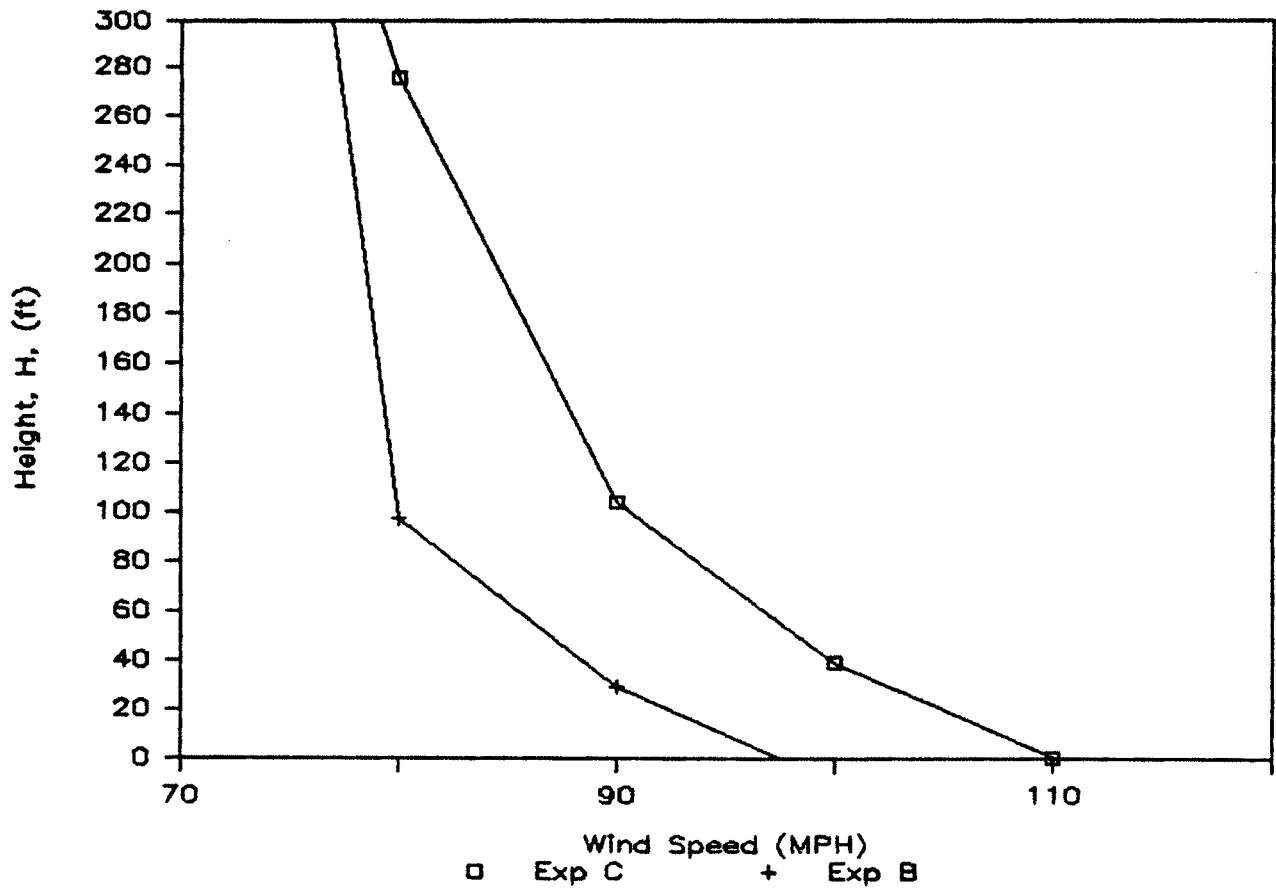


Figure 31. Maximum Building Height Estimated Using UBC -- Modified Configuration With 12 in. Parapet, Exposure C and B

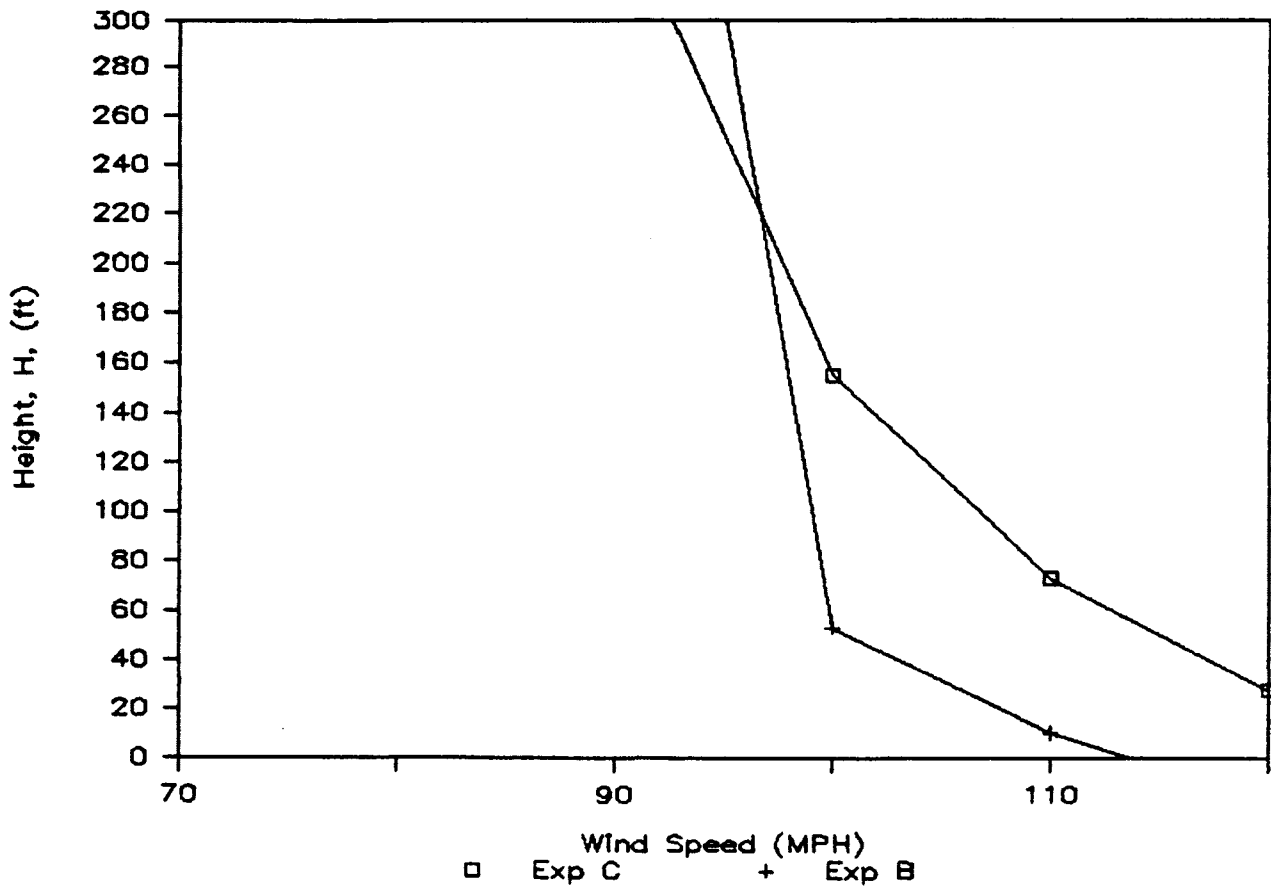


Figure 32. Maximum Building Height Estimated Using UBC -- Modified Configuration With 18 in. Parapet, Exposure C and B

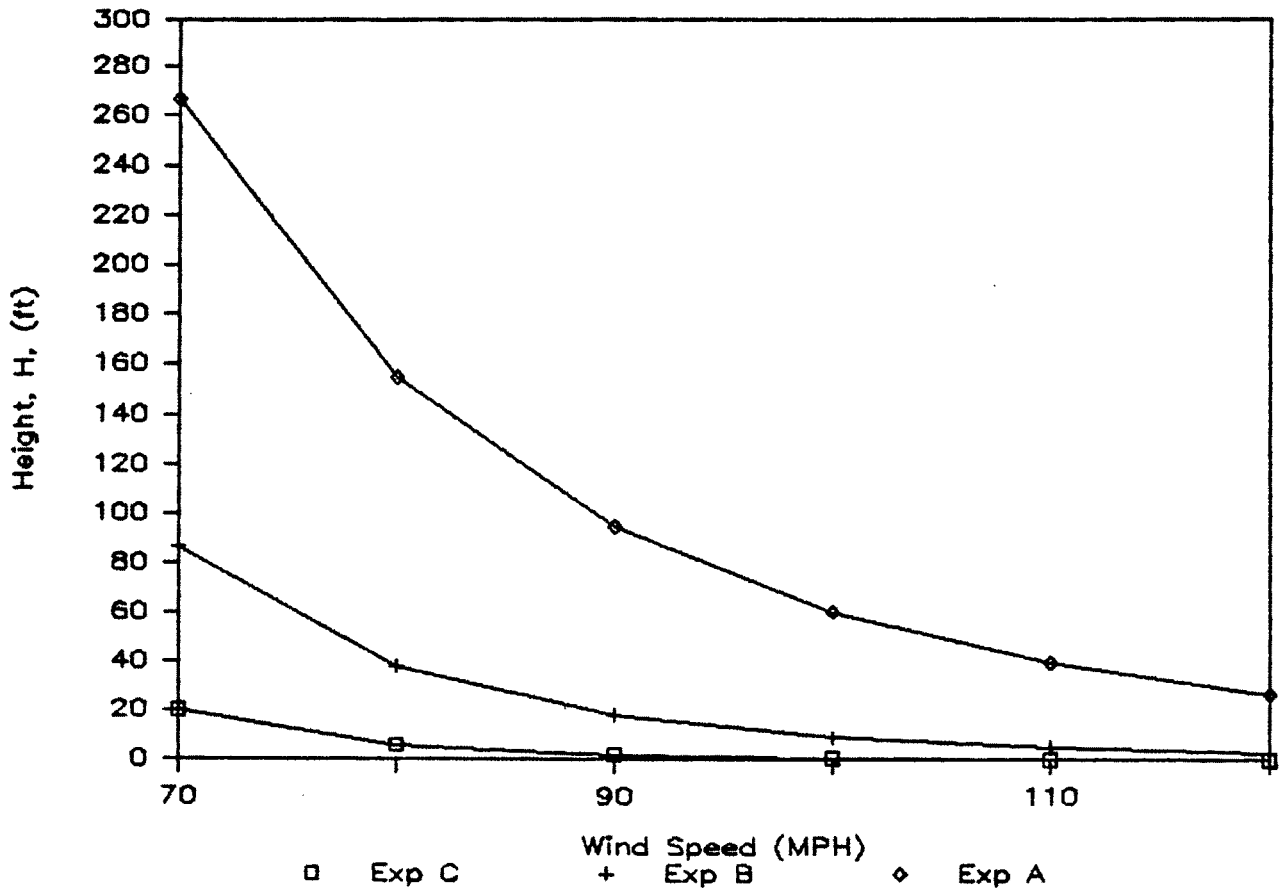


Figure 33. Maximum Building Height Estimated Using ANSI Standard -- Original Configuration With 0 in. Parapet, Exposure A, B and C

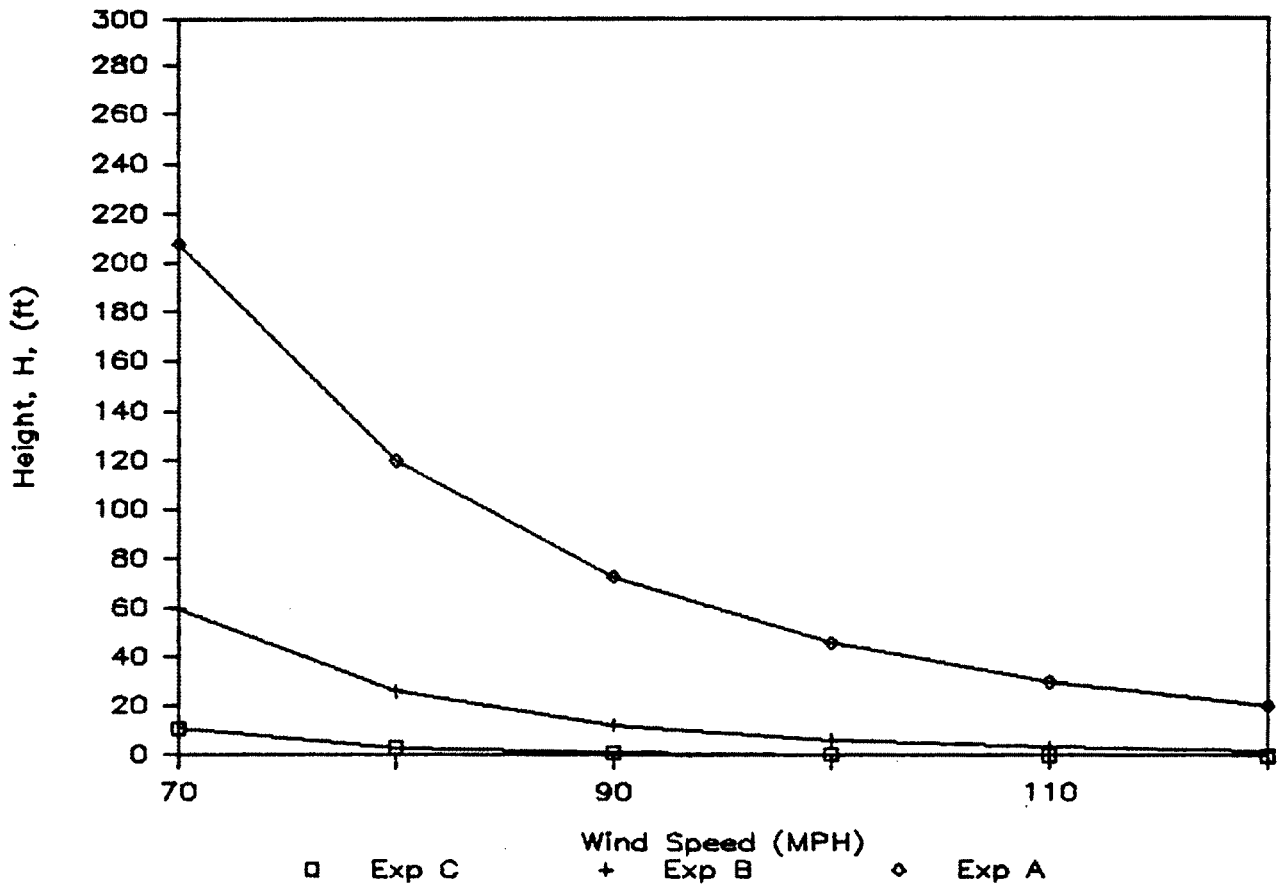


Figure 34. Maximum Building Height Estimated Using ANSI Standard -- Original Configuration With 6 in. Parapet, Exposure A, B and C

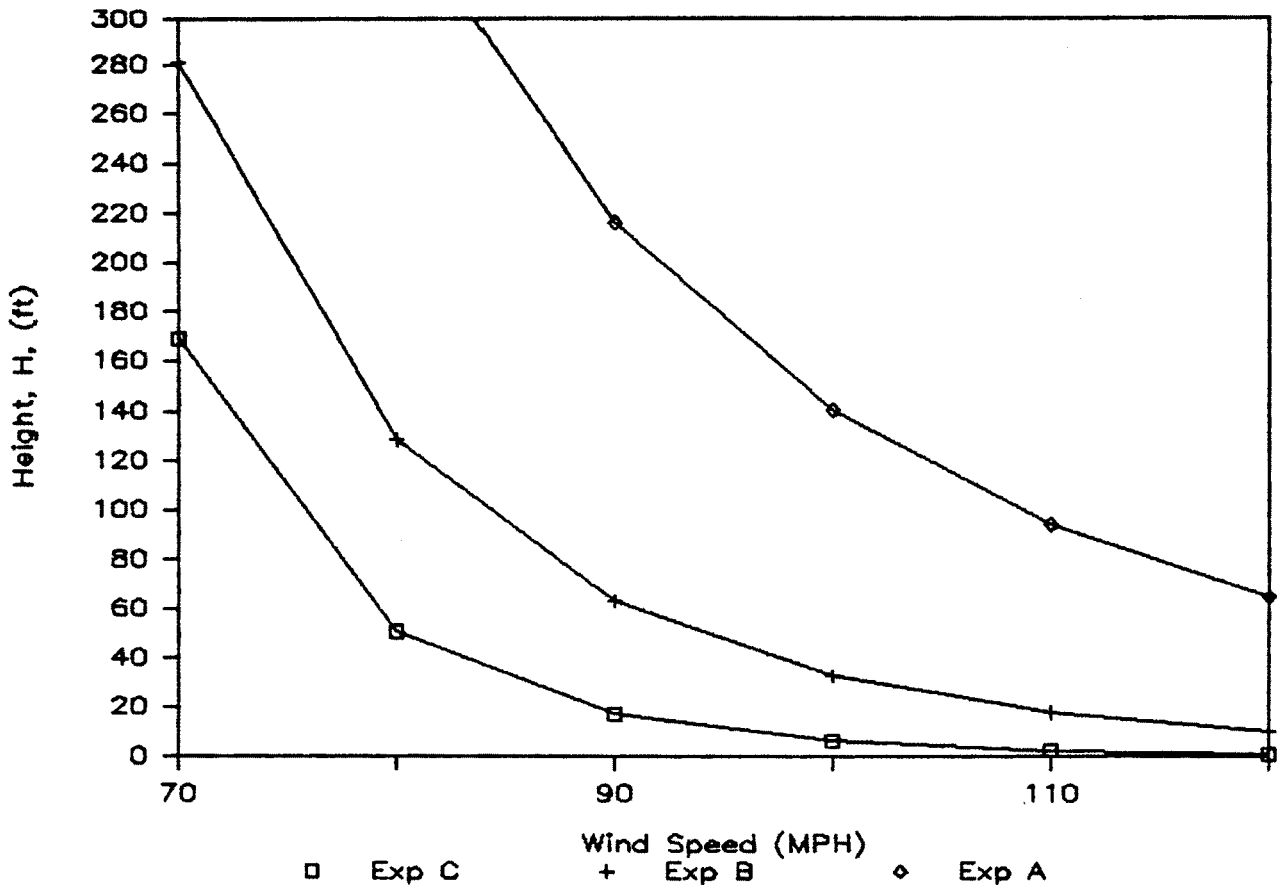


Figure 35. Maximum Building Height Estimated Using ANSI Standard -- Original Configuration With 12 in. Parapet, Exposure A, B and C

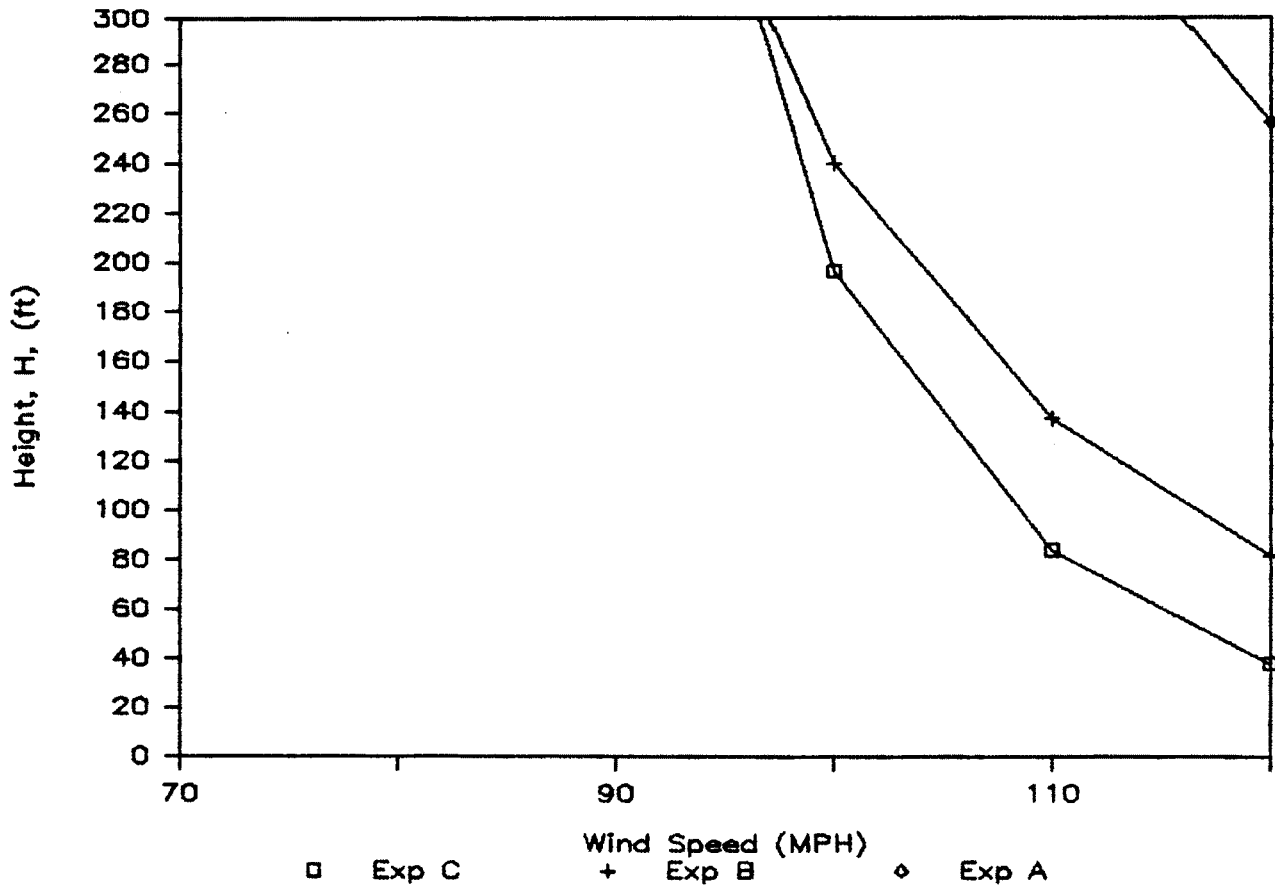


Figure 36. Maximum Building Height Estimated Using ANSI Standard -- Original Configuration With 18 in. Parapet, Exposure A, B and C

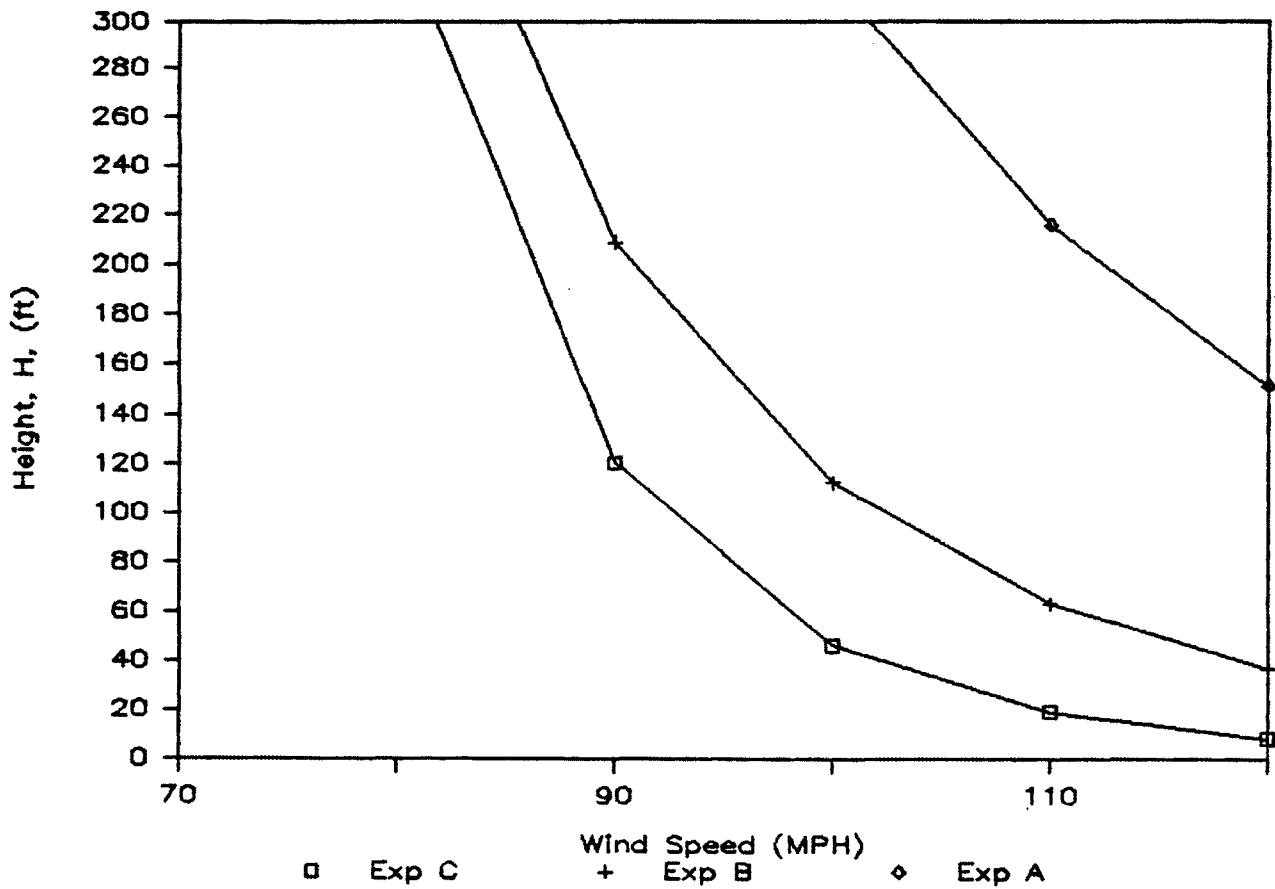


Figure 37. Maximum Building Height Estimated Using ANSI Standard -- Modified Configuration With 0 in. Parapet, Exposure A, B and C

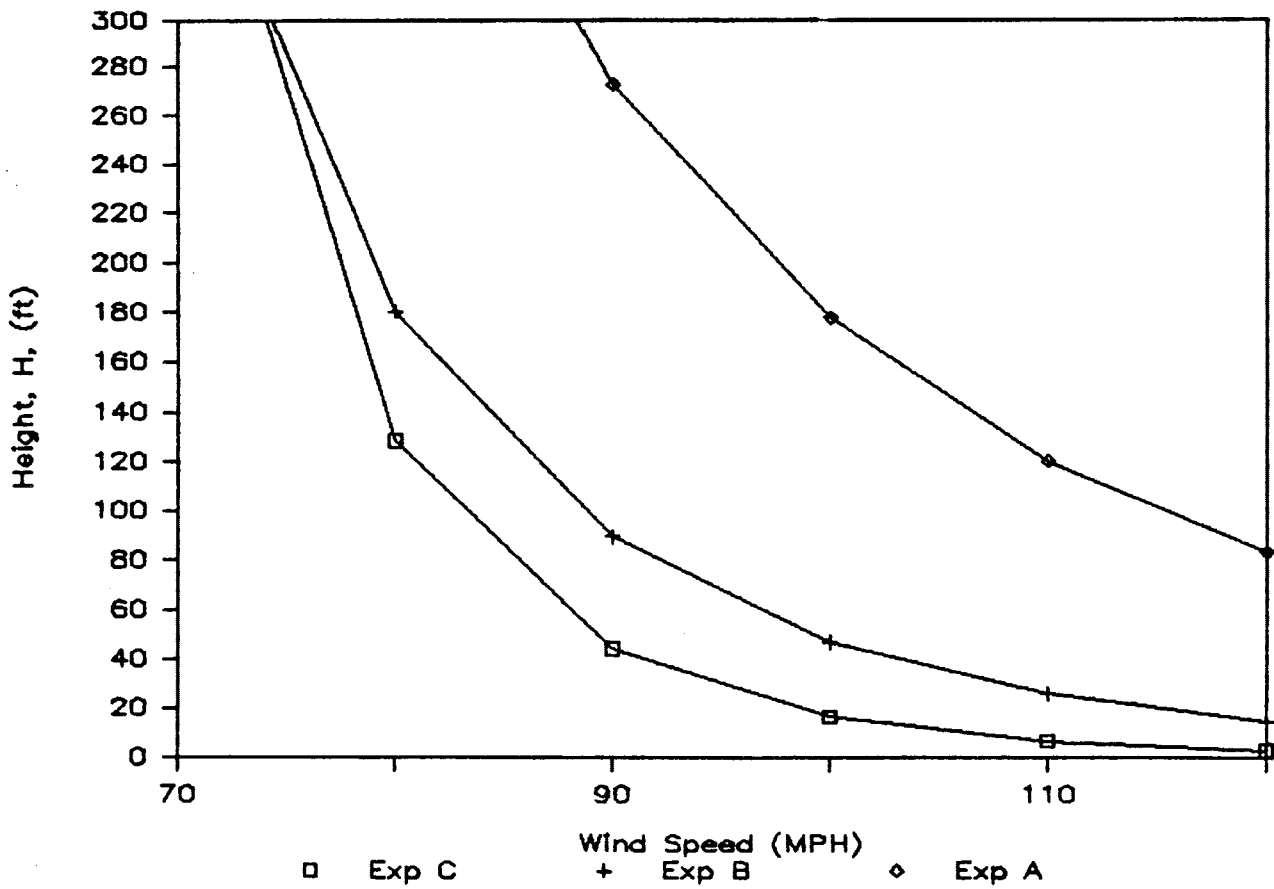


Figure 38. Maximum Building Height Estimated Using ANSI Standard -- Modified Configuration With 6 in. Parapet, Exposure A, B and C

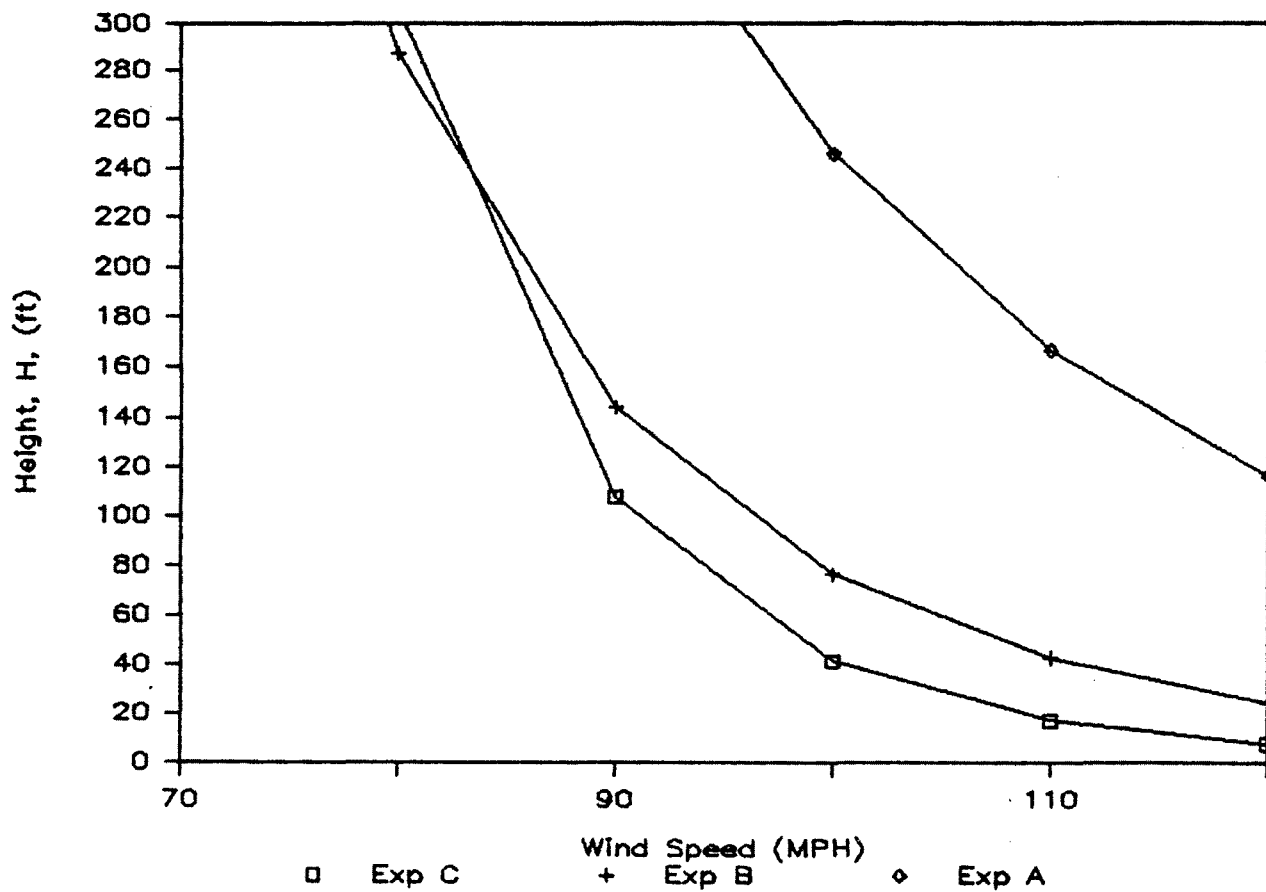


Figure 39. Maximum Building Height Estimated Using ANSI Standard -- Modified Configuration With 12 in. Parapet, Exposure A, B and C

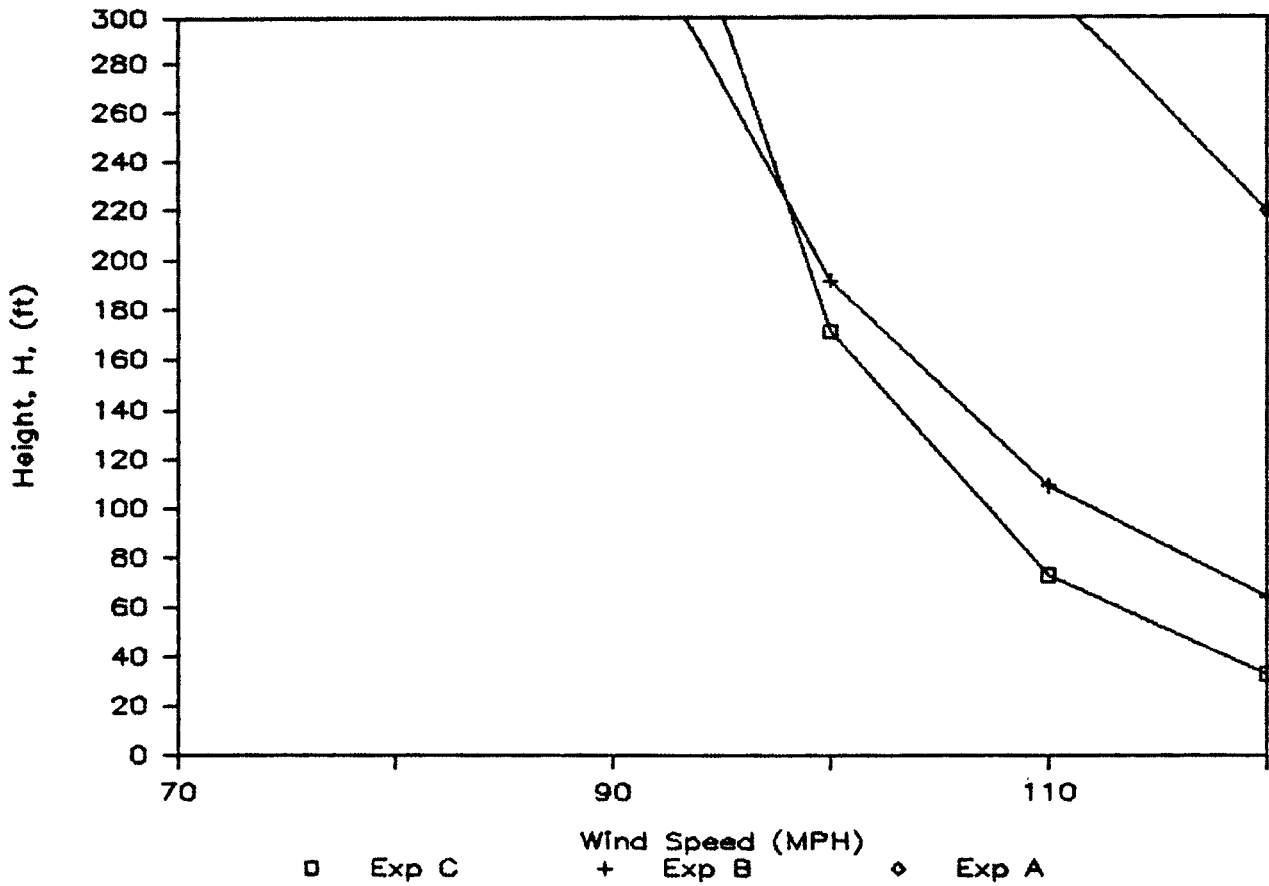


Figure 40. Maximum Building Height Estimated Using ANSI Standard -- Modified Configuration With 18 in. Parapet, Exposure A, B and C

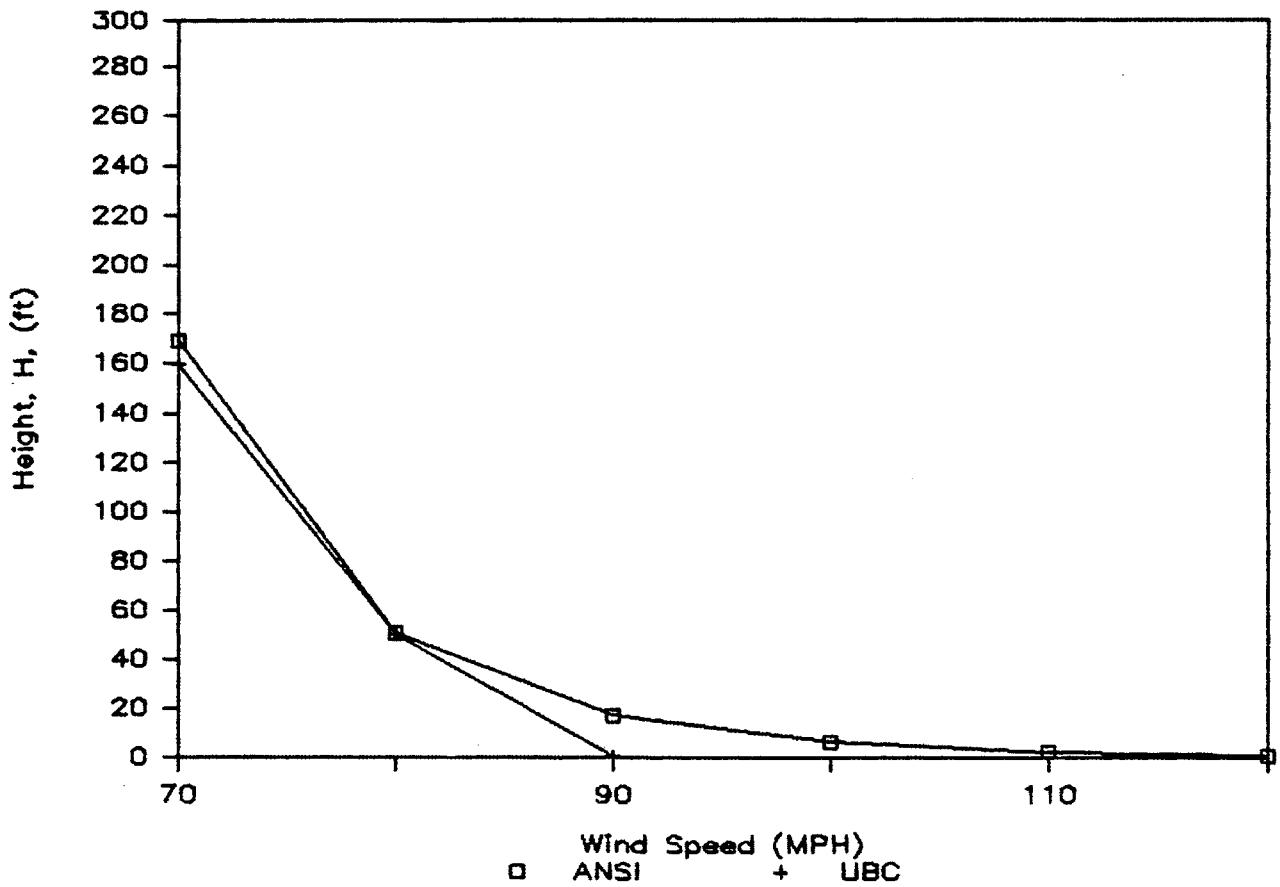


Figure 41. Maximum Building Height Estimated Using UBC and ANSI Standard -- Original Configuration With 12 in. Parapet, Exposure C

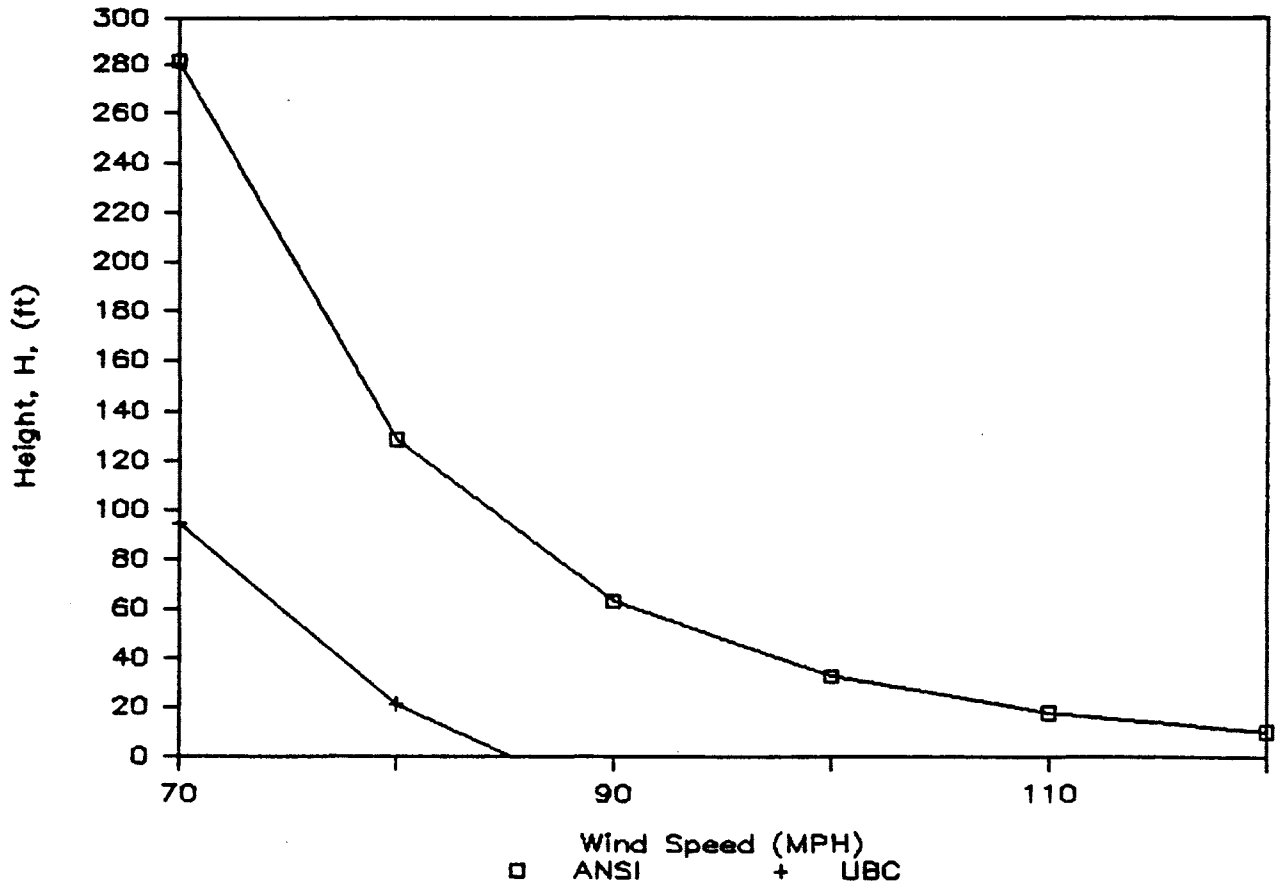


Figure 42. Maximum Building Height Estimated Using UBC and ANSI Standard -- Original Configuration With 12 in. Parapet, Exposure B

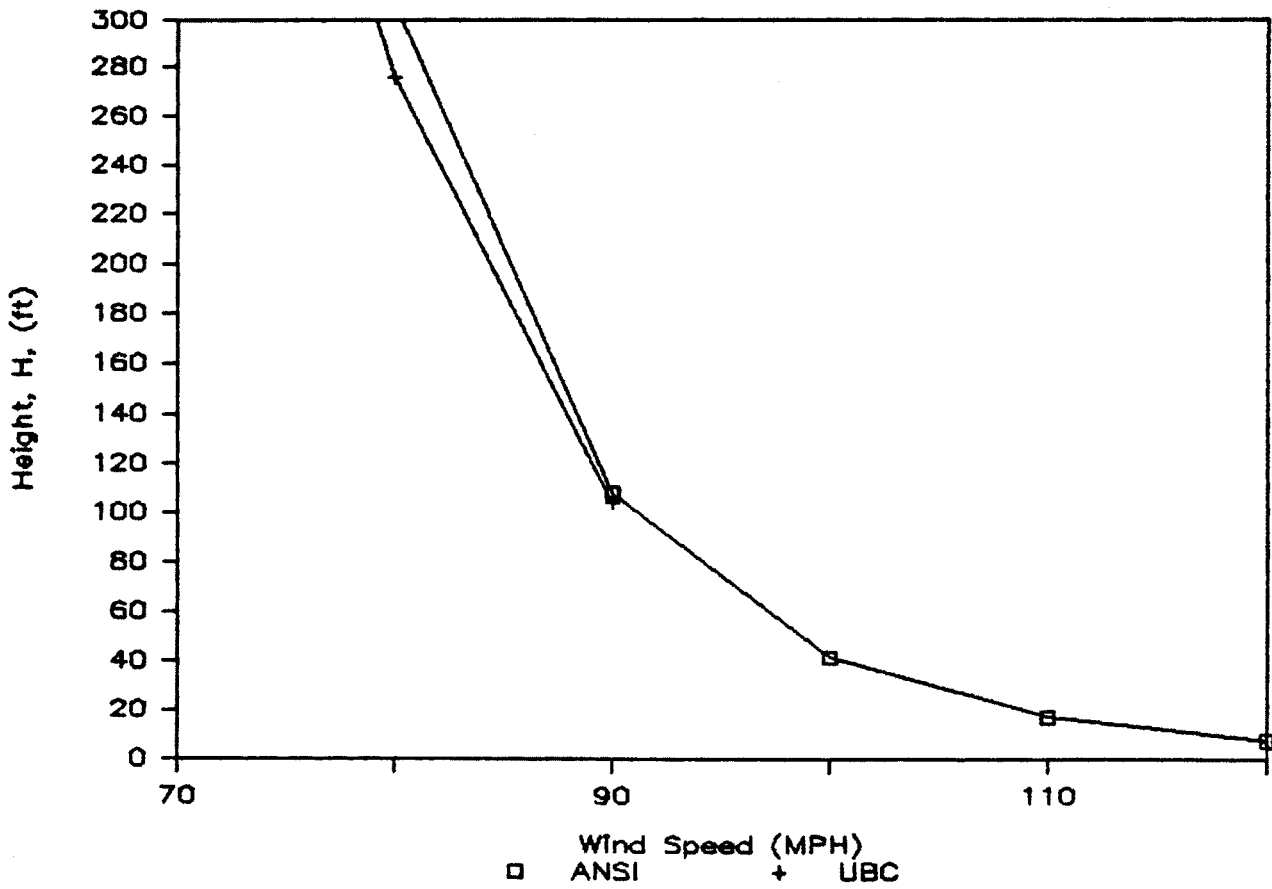


Figure 43. Maximum Building Height Estimated Using UBC and ANSI Standard -- Modified Configuration With 12 in. Parapet, Exposure C

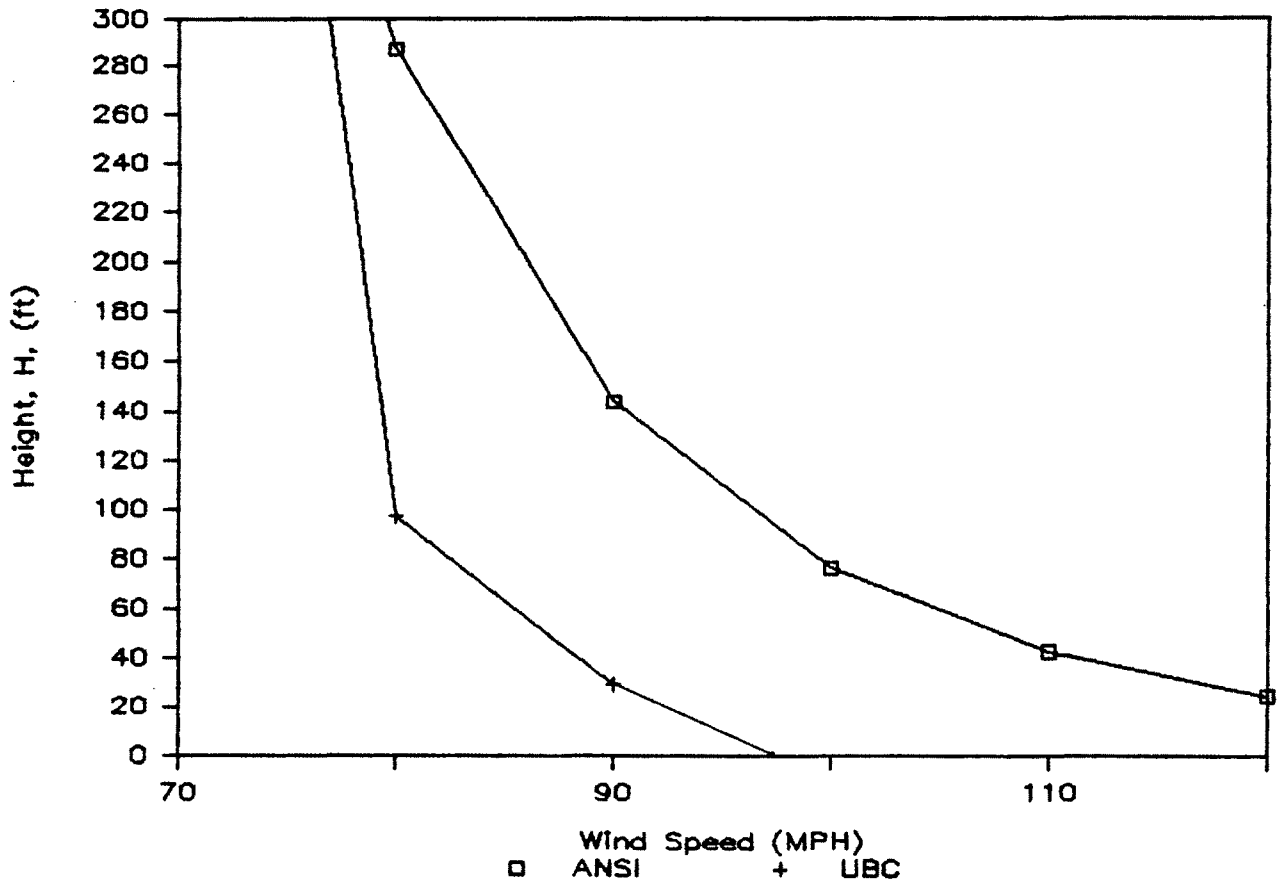


Figure 44. Maximum Building Height Estimated Using UBC and ANSI Standard -- Modified Configuration With 12 in. Parapet, Exposure B

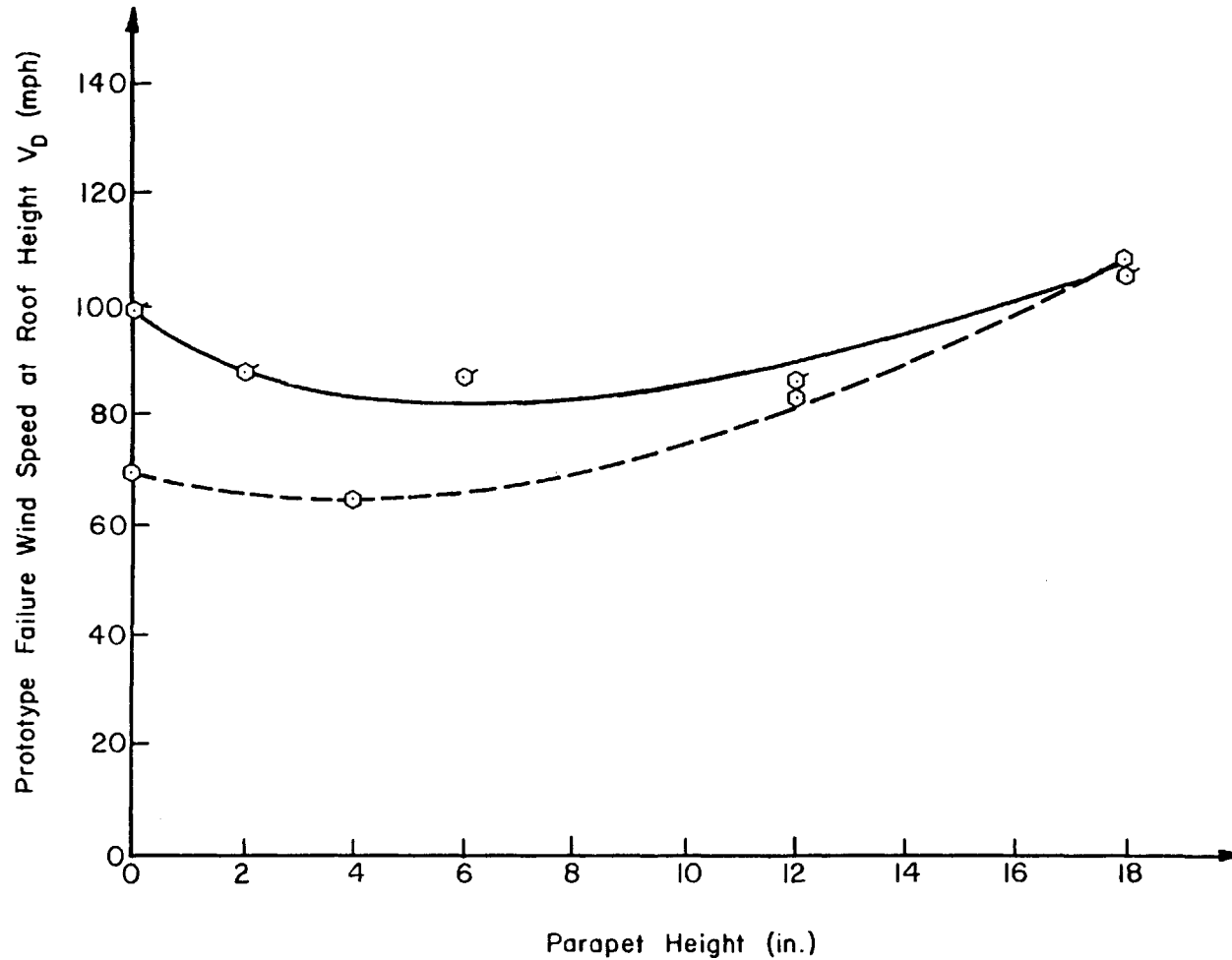


Figure 45. Failure Wind Speed at Roof Height, Exposure A: -- \odot -- Original Configuration, -- \ominus -- Modified Configuration

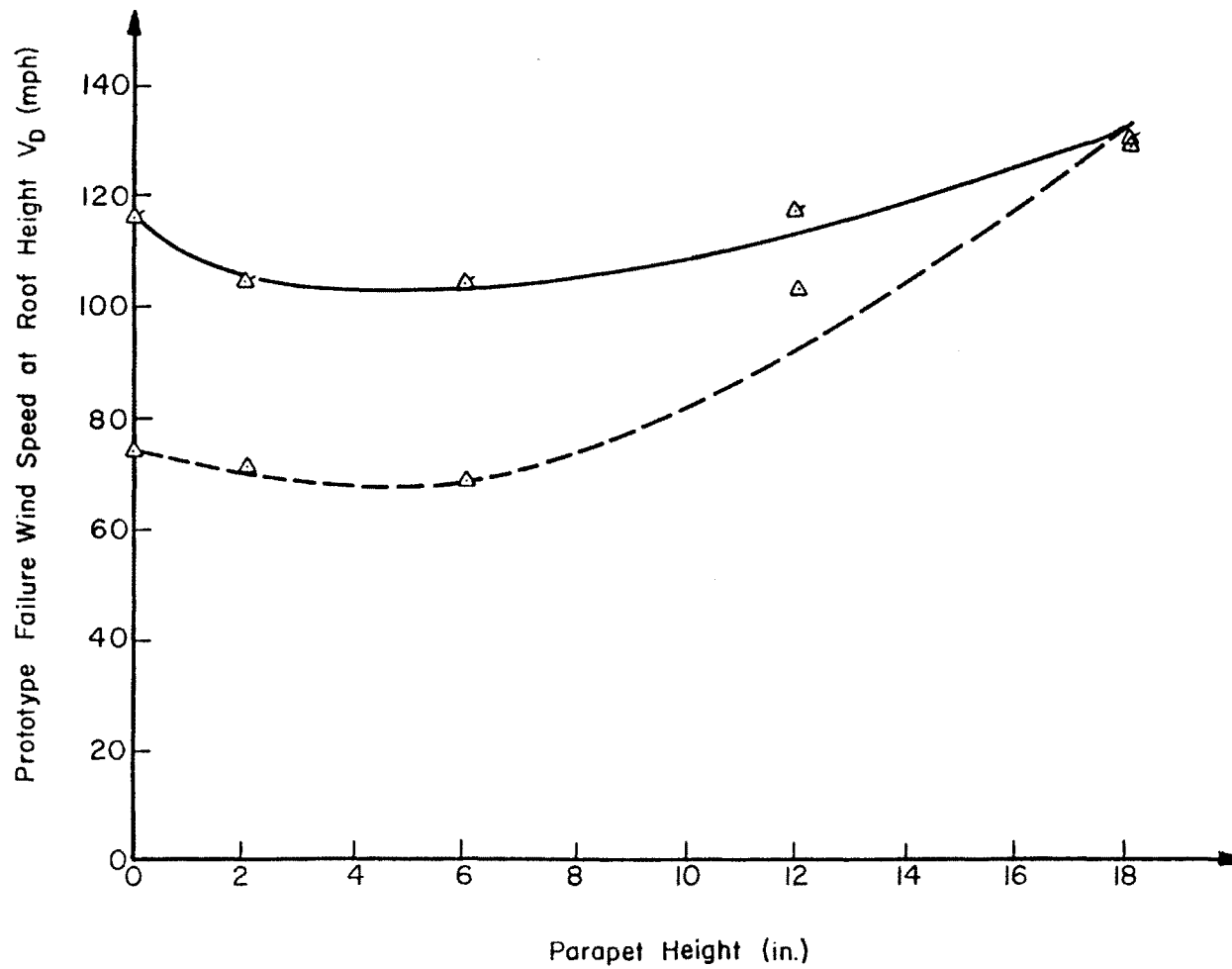


Figure 46. Failure Wind Speed at Roof Height, Exposure C: --- \triangle --- Original Configuration, — \triangle — Modified Configuration

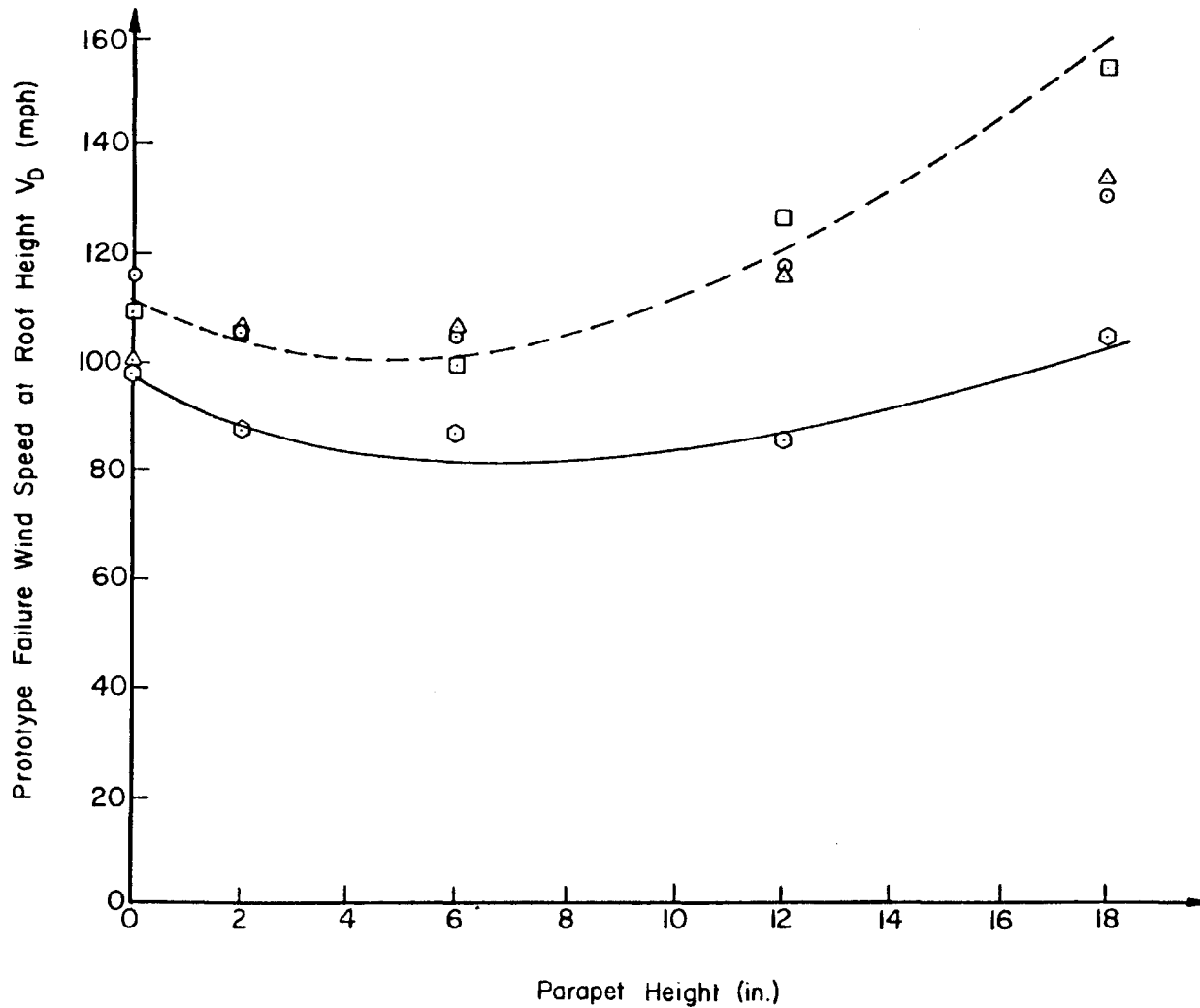


Figure 47. Failure Wind Speed at Roof Height for Different Flow Conditions: --□-- Smooth Flow ($n = 0.10$); Δ Open Country ($n = 0.14$); \odot Suburban Terrain ($n = 0.30$); — \circ — Built-Up Terrain ($n = 0.37$)

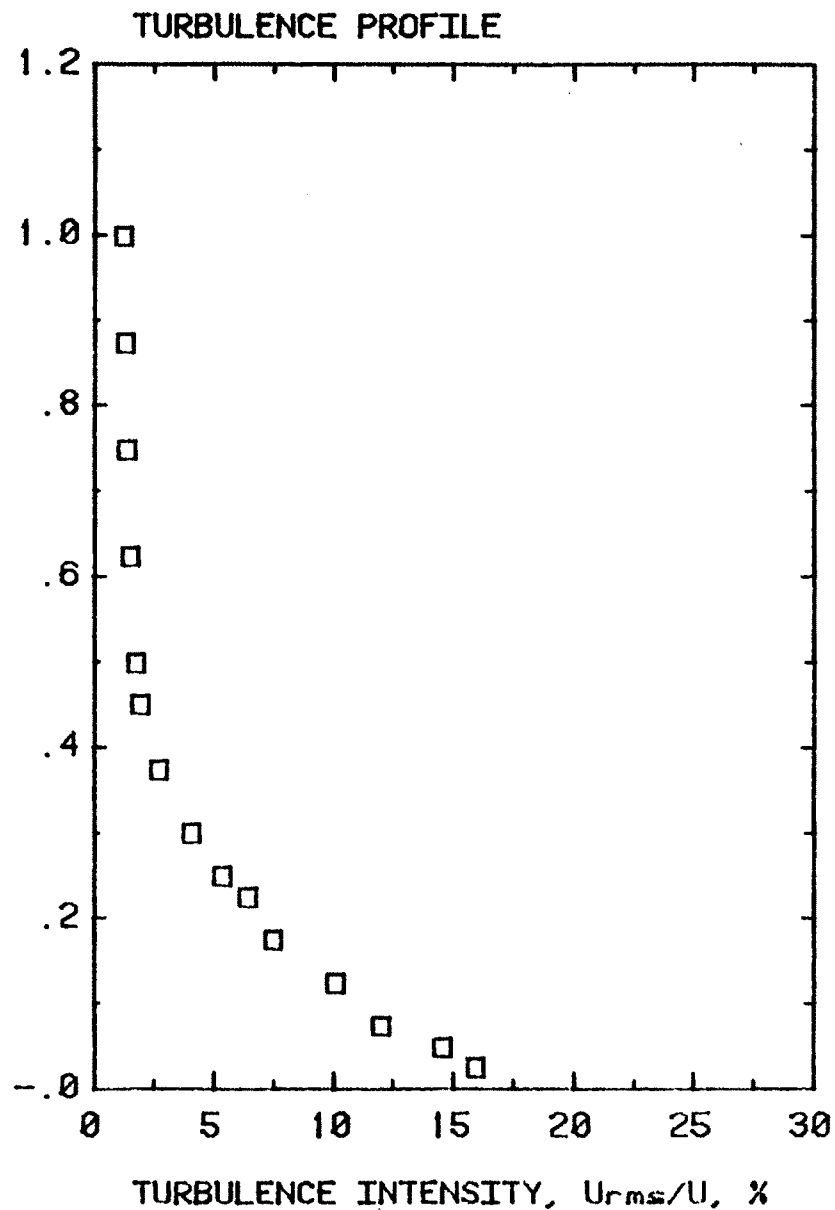
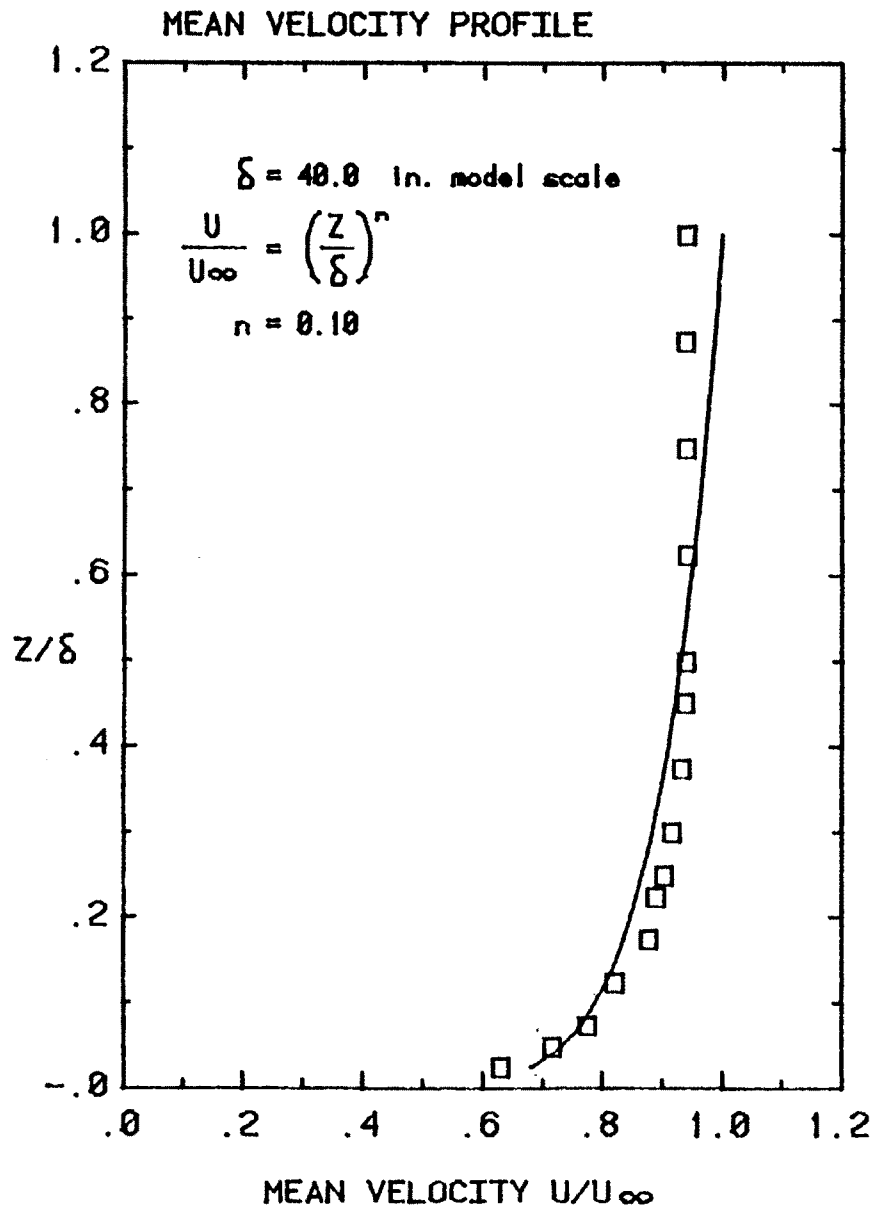


Figure 48. Mean Wind Speed and Turbulence Intensity Profiles -- Smooth Flow

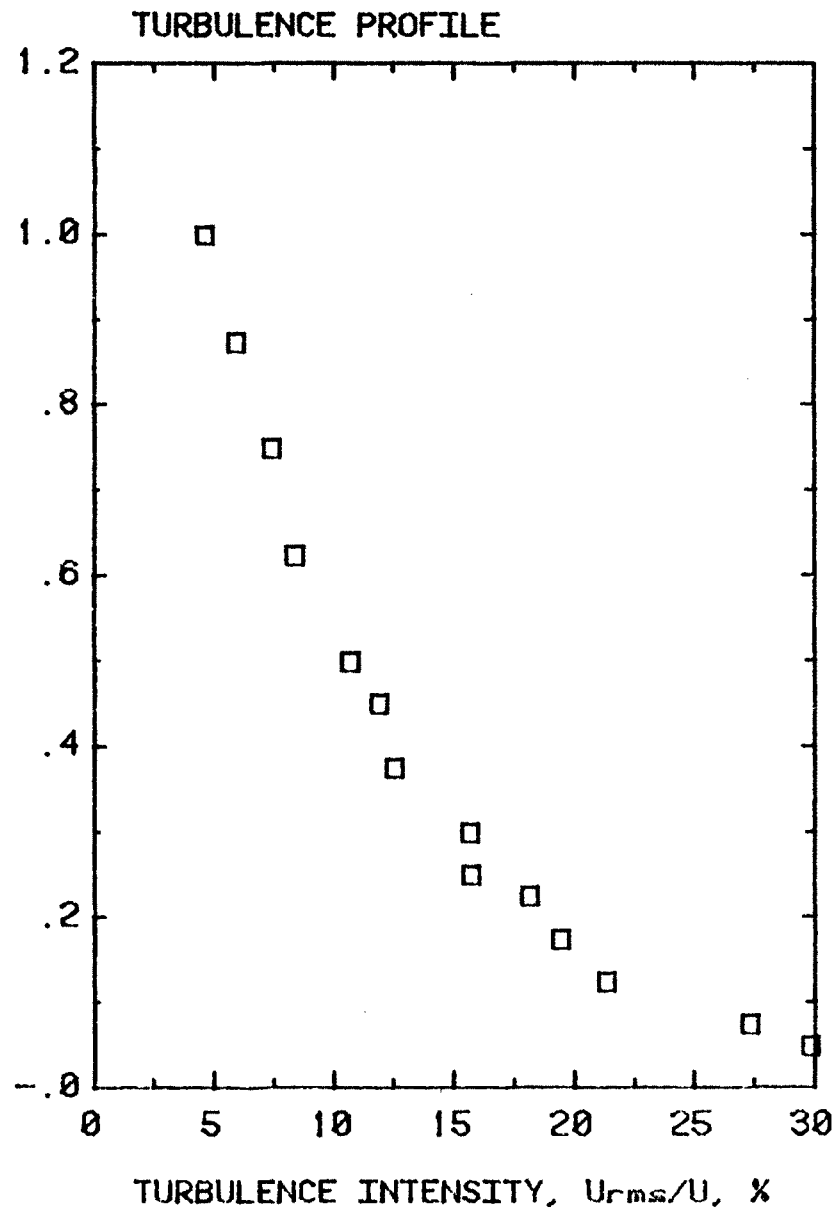
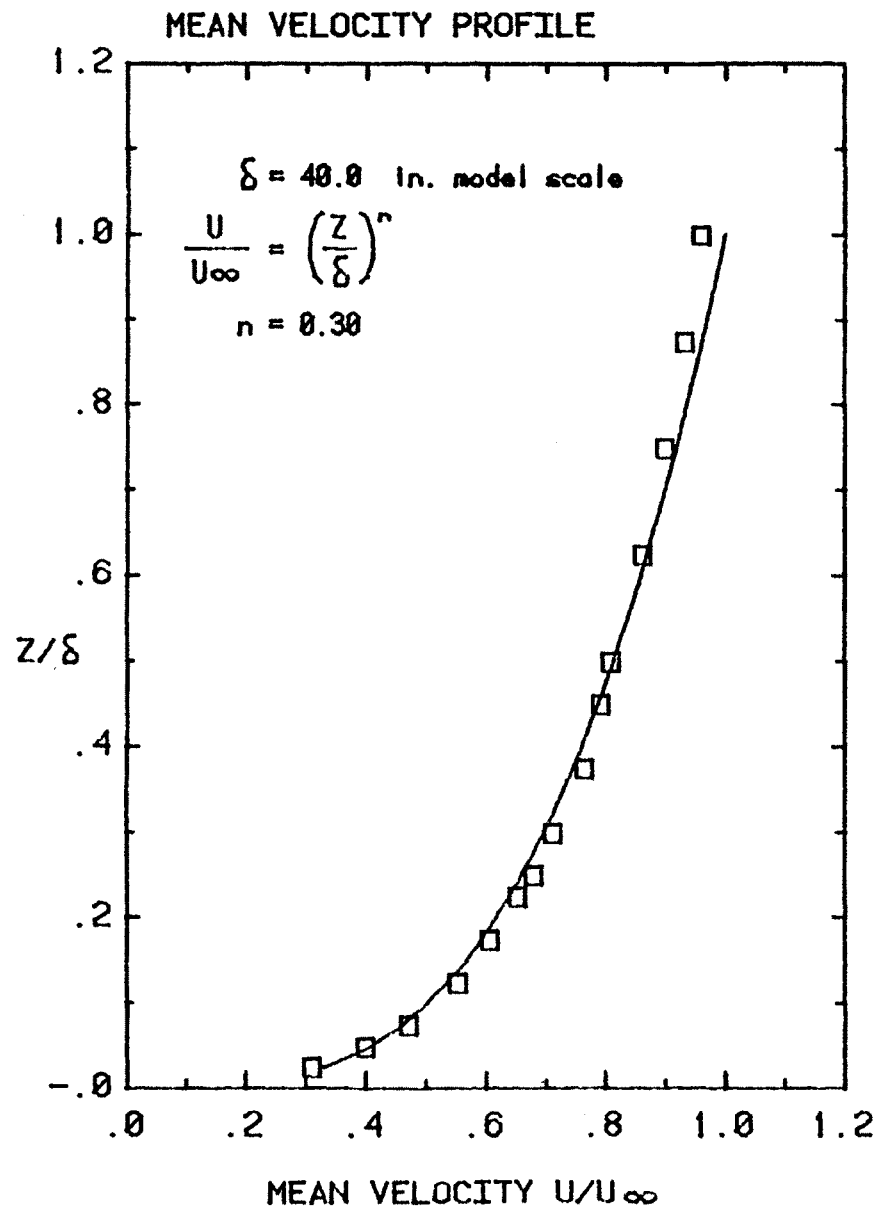


Figure 49. Mean Wind Speed and Turbulence Intensity Profiles -- Suburban Terrain

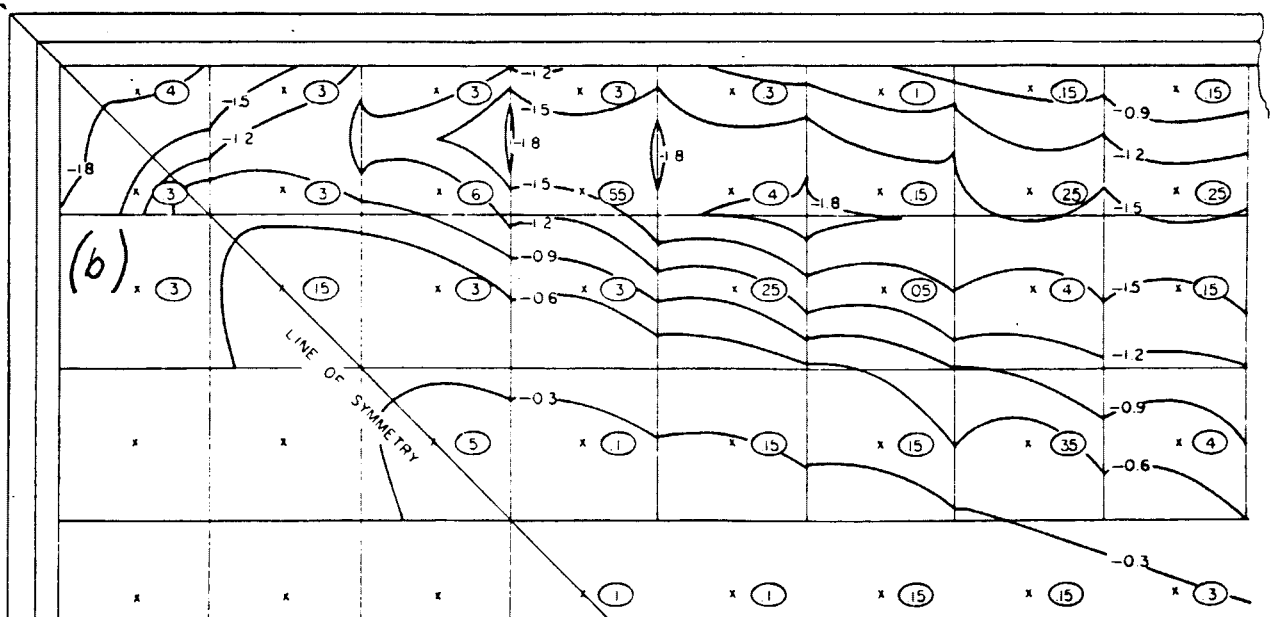
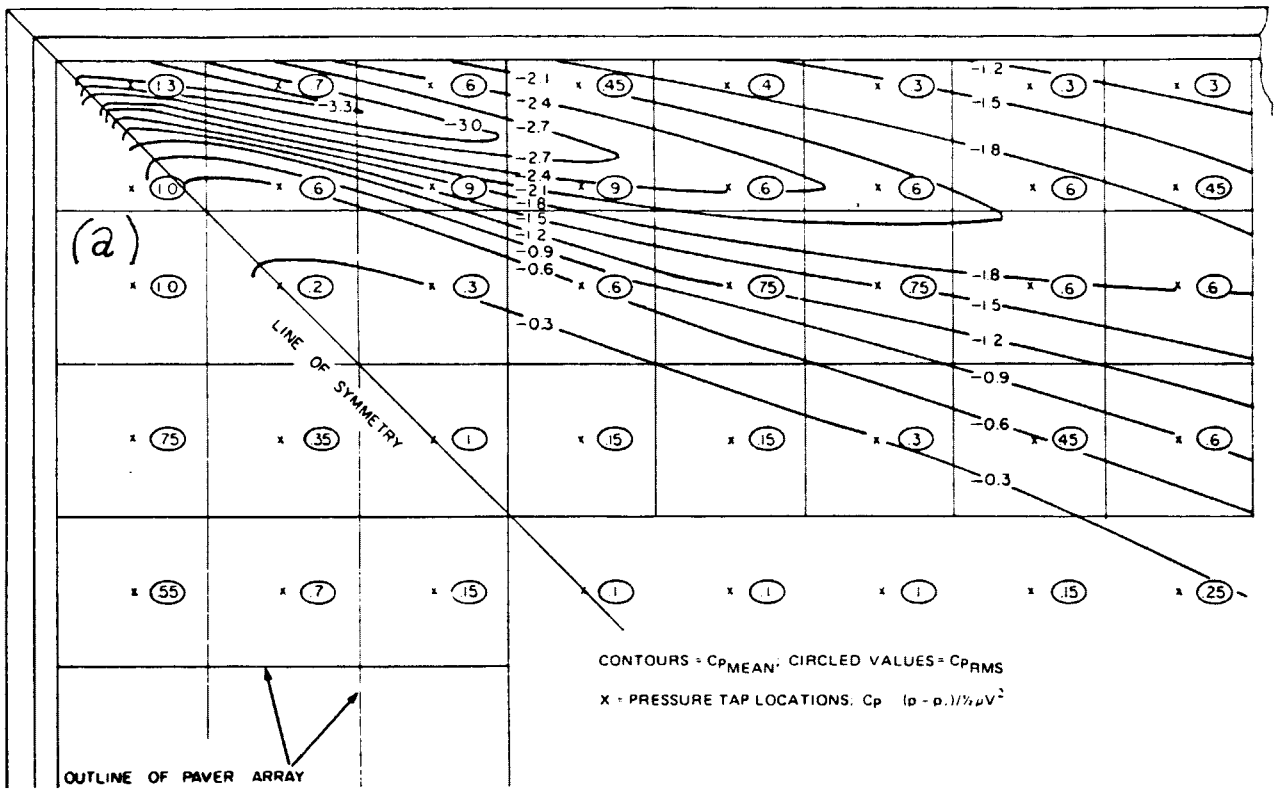


Figure 50. Static-Pressure Coefficient, Parapet Height of 6 in. (Kind and Wardlaw [5]): a) Bare Roof Deck; b) Distribution Under Paver Array

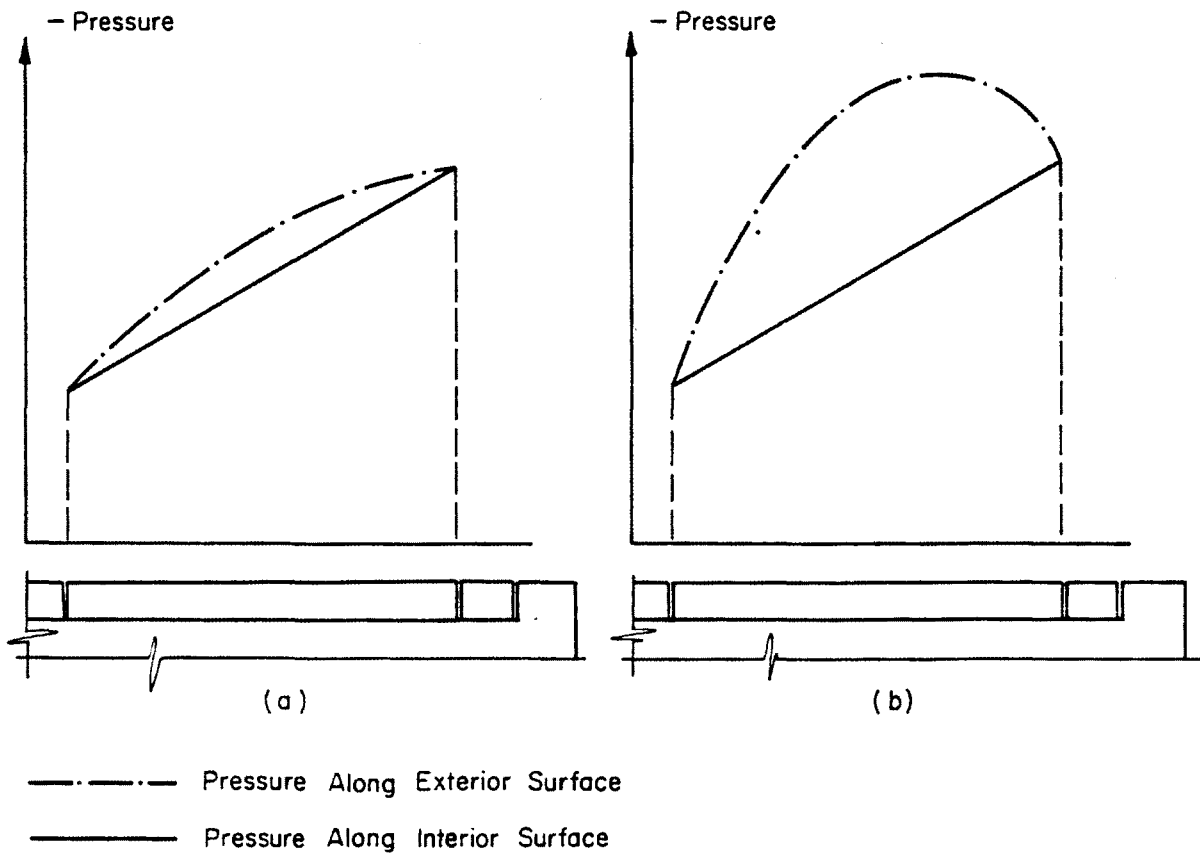


Figure 51. Pressured Distribution Along a Paver (Kind and Wardlaw [4,5]): a) Low Uplift Force; b) High Uplift Force

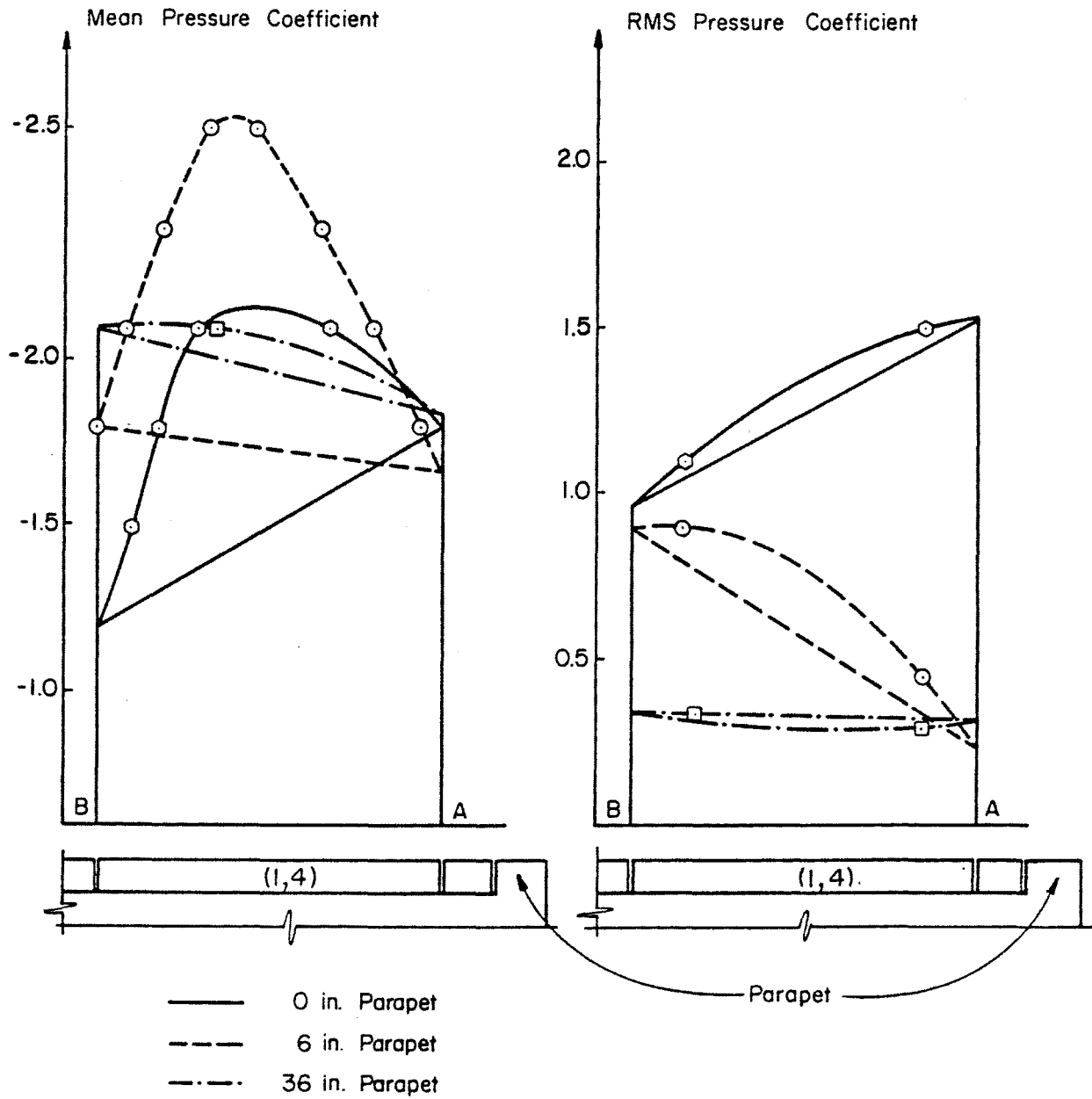


Figure 53. Exterior (nonlinear) and Interior (linear) Static-Pressure Distribution over Paver (1,4)